LIFE Integrated Projects 2016

Optimising the implementation of the 2nd RBMP in the Malta River Basin District

LIFE 16 IPE MT 008

Action A.9:

Development of Groundwater Models to Support Groundwater Management in the Maltese Islands

Deliverable D2.1: Modelling Manual, Part 1: Steady State Models

2019

Development of Groundwater Models to Support Groundwater Management in the Maltese Islands

Deliverable D2.1: Modelling Manual

Part 1: Steady State Models

Contracting Authority	Government of Malta Ministry for Energy and Water Management The Energy & Water Agency
Contractor	TEA SISTEMI SpA (TEA) STEAM Srl. (STEAM) University of Siena-Centre of Geotechnologies (CGT)
Sub-contractor	ADI Associates Environmental Consultants Ltd (ADI)
Contract no.	CT 3068/2018
Project Manager	Iacopo Borsi (TEA)
Title	Development of groundwater models to support groundwater management in the Maltese island, Inception Report
Authors	Iacopo Borsi, Francesca Lotti (TEA) Paolo Basile (STEAM) Enrico Guastaldi, Alessio Barbagli (CGT)
QC check	Riccardo Corsi (STEAM) Adrian Mallia (ADI)
Document history	Version 0, October 2019 – Draft sent to EWA for preliminary approval.

Table of Contents

Acronyms and abbreviations 6
Executive Summary 7
Introduction 10
Part 1: Models for Malta islands 12
Introduction 13
Malta water balance 14
Long period average water balance 14
Soils of Malta 15
Distributed recharge in 1941-1944 19
Geology and slope 21
Land use 22
Dams 23
Sinkholes 25
Results 26
Outflows in 1944-1945 28
Malta MSLA numerical model 32
Domain and discretization 32
Boundary conditions 33
Initial properties 34
Initial heads 36
Model calibration 42
Highly Parametrized Methods 42
Pilot Points and Groundwater-Model Calibration 42
MSLA model steady state calibration 43
Results 45
Sensitivities, linearity test and calibrated parameters 45
Water budget and head distribution 50
Residuals 51
Mizieb and Pwales aquifers 56
Introduction 56
Domain and discretization 56
Boundary condition 58
Initial properties and heads 59
Results 61
Sensitivities, linearity test and adjusted parameters 61

Water budget and head distribution 65
Seawater interface simulation 67
SWI2 Package 67
MSLA Model 68
Mizieb-Pwales Model 70
Part 2: Models for Gozo island 72
Introduction 73
Gozo Mean Sea Level Aquifer 74
Hydrogeologic characterization and conceptual model 74
Model design 74
Model domain and spatial discretization 74
Hydrodynamic parameters and faults 76
Boundary condition 77
Aquifer recharge 78
Abstraction rate 84
Model run (not calibrated) 85
Sensitivity and calibration 86
Observations (calibration targets) 86
Parametrization and Sensitivity 87
Calibration and residual analysis 89
Water balance and head distribution 92
Insights derived from the calibration process 94
Seawater Intrusion 95
Ghajnsielem Perched Aquifer 97
Hydrogeologic characterization and conceptual model 97
Model design 98
Model domain and spatial discretization 98
Hydrodynamic parameters and faults 98
Boundary condition 99
Aquifer recharge 100
Model Run (not calibrated) 100
Sensitivity and calibration 101
Observations (calibration targets) 101
Parametrization and Sensitivity 103
Calibration and residuals analysis 105

Water Balance and head distribution ... 109
Insights derived from the calibration process ... 111
References ... 112
Appendix 1. Modelling journal ... 115
Malta Mean Sea Level Aquifer model ... 115
Mizieb/Pwales Aquifer ... 117
Gozo Mean Sea Level Aquifer model ... 120
Ghajnsielem Perched Aquifer ... 125
Appendix 2. Assumptions register ... 127
Malta MSLA Model ... 127
Mizieb/Pwales model ... 128
Gozo MSLAModel ... 129
Ghajnsielem model ... 130
Appendix 3. Calibration outputs ... 131
Parameter Sensitivities ... 131
Residuals ... 136
Appendix 4: Data Pre-Processing ... 142
1. DTM rectification and geological data spatial adjustment ... 142
1.1 Raster file - DTM and orthophoto ... 143
1.1.1 Step 1 - No-Data reconstruction ... 143
1.1.2 Step - 2 Rectification ... 144
1.2 Vectors - spatial adjustment ... 145
2. Geological formations surfaces interpolation - Input Data ... 146
2.1 Geological map formation boundaries (from geological map and cross-sections) ... 146
2.2 Cross-Sections formation boundaries ... 147
2.3 Well log and borehole data ... 148
2.4 Inconsistencies in the input data ... 148
2.4.1 Geological data ... 148
2.4.2 Borehole data ... 148
3. Geological formations surfaces interpolation - Computing ... 152
3.1 Tested interpolator ... 152
3.2 Interpolation inputs ... 153
4. From the geological surfaces to the model one ... 155
5. New data collection - future implementation ... 156

Acronyms and abbreviations

BC	Blue Clay
EWA	Energy and Water Agency
GUI	Graphical User Interface
GL	Globigerina
LCL	Lower Coralline Limestone
MSLA	Mean Sea Level Aquifer
UCL	Upper Coralline Limestone

Executive Summary

This report describes the work carried out during Activity 2 of the project, namely the definition and implementation of steady state models simulating the groundwater resource for five selected aquifers in Maltese islands.

According to the Inception Report, the calibrated steady state models refer to a time frame representing the pre-exploitation (or non-intensive exploitation) of groundwater resources. According to the data set available and in agreement with the Contracting Authority Energy and Water Agency (EWA in the following), such a time frame has been defined as the years ranging from 1941 to 1944.

The steady state models have the following specific objectives:

1) Assessing the basic assumptions of the conceptual models, namely the values of hydrodynamic parameters, setting of boundary conditions, identification of main terms in the water balance.
2) Identify potential data gaps (in addition to what already assessed during Activity 1), even providing EWA with a list of suggestions and comments for a potential improvement of the data sets currently available, by promoting new measurements campaigns and/or including additional monitoring network on the islands.
3) Use the result of calibrated models as initial condition for the transient models (to be performed during next Activity 4).

This report is organized as follows. Part 1 refers to models developed for Malta island, namely regarding Malta MSLA, Mizieb MSLA and Pwales coastal aquifer. Part 2 refers to models for Gozo island, namely Gozo MSLA and Ghajnsielem perched aquifer. After a first effort of treating all the aquifers together for each island, the decision of splitting the five aquifers was taken. In particular, four (4) separate models describe the 5 aquifers, namely: a model for Malta MSLA, a model including Mizieb MSLA and Pwales coastal aquifer, a model for Gozo MSLA and a model for Ghajnsielem perched aquifer.

The only model that could undergo a proper calibration process was the Malta MSLA model. The information content of the data and prior information could help to constraint a set of parameters, included hydraulic conductivity field and main faults transmissivity. Uncertainty of the possible parameters calibrating the model is still high and several assumptions needed to be formulated in order to simplify the complexity of the system. Still, some aspects emerged that should be double-checked and/or considered carefully:

- Groundwater flow directions and gradients are strongly influenced by the low permeability faults;
- The Maghlaq fault turned out to have a relatively high hydraulic conductivity if compared to other faults;
- Local infiltration through dams could represent a significant term of the water balance that should be better quantified (the present calibrated version of the model includes gross assumptions on this regard);
- Recharge of the perched aquifer was independently re-calculated and compared with BRGM results of a lumped recharge-discharge model. Results are comparable. Leakage from the perched aquifer towards the MSLA was then taken from the BRGM output. It was assumed that the leakage preferentially happens through sinkholes, reallocating the leakage amount accordingly. A detailed potentiometric map of the perched aquifer could help to cross-check and better quantify this important recharge term;

- Water galleries were herein represented as WELL boundary conditions; this was a preliminary strong assumption that does not affect a steady state model in non-intensive exploitation conditions. This assumption won't be applicable to the transient models where an extremely high percentage of the water abstraction derives from galleries. Geometry, exact elevation of tunnels, pumping/draining scheme need to be considered in detail;
- The present version of the model is single-layer; this implies that if local confined/semiconfined condition exists, these cannot be reproduced, as neither vertical aquifer heterogeneity or karst discontinuities;
- The faults represented in the model are the main ones; the rest of the active cells are supposed to be porous-equivalent; further details might be added in the transient model development, if steep hydraulic gradients are noticed with the extended dataset;
- Aquifer bottom is the most sensitive parameter of the model, but it is totally unknown. Little can be done on this regard; even boreholes reaching -150 m asl would provide punctual information hard to generalized.

Mizieb and Pwales aquifers were included in the same numerical model at this stage. Differently from the MSLA, a physical bottom is present and was represented in the numerical model as a smoothed surface to overcome convergence issues. While the Pwales portion of the model was not particularly problematic, the complex geological setting of the Mizieb aquifer required several modelling attempts. The main issues were:

- The aquifer discharge area: wherever a natural recharge exists, a discharge must be present; in this case the only possible natural way out of water is where the lower heads are located, i.e. in the central northern part of the aquifer, where sinkholes are reported nearby a "breccia" fault, as defined in Constain (1957). This geological setting has been simulated including the sinkholes as GHB boundary conditions, and the breccia fault as DRAIN boundary condition;
- The consistent number of dry cells: the dry area in Mizieb aquifer can be reduced in different ways. Rejecting the hypothesis that UCL can locally present very low hydraulic conductivities, and assuming that the private wells are not rainwater cisterns, the existence of an additional fault can be supposed. Available stratigraphic information was analyzed together with land morphology and hydraulic heads, concluding that the presence of an additional fault is "not impossible".

The above points need to be better clarified on the field, being the principal features regulating the Mizieb aquifer behavior. Little can be said about Pwales, since no local information are available.

The calibrated model for Gozo MSLA gives results to be taken only in a qualitative way, due to the following limitations of the data set available:

- There is no information about the conductivity field of the aquifer. Values used through the model have been argued by the Malta MSLA region.
- The number of piezometric observations is very low (only 10 points) on a domain of around 66 km^2 of spatial extension, not uniformly distributed on the domain.
- There is not precise indication on the date of recording, neither on the real stresses present at time of recording (e.g. additional pumping wells). Furthermore, there is only one 1 value for each point, while the model considers an annual average of all the other stresses (e.g. rainfall rate and pumping rate).

Therefore, even if the calibration produces a slight increase of the model performance, the model fit is not satisfactory. However, the statistics computed through the calibration give interesting suggestions:

- Measurements campaigns to get estimate of transmissivity can be done in the zone showed as more influencing in terms of parameter describing the conductivity of LCL.
- Results suggested that a better model fit can be achieved only by setting a more distributed value of conductivity, since the selection of only two conductivity zones (one for Globigerina and one for LCL) seems not promising.
- A part the estimate of parameters, the water budget and the head distribution shows that the model solution is dominated by the sea-side boundary condition. Therefore, it could represent a good initial condition for next transient simulations, since it is a feasible representation of the pre-exploitation age.

Even for the Ghajnsielem model, the calibration procedure increased the model performance but the model fit is not satisfactory. However, also in this case the calibration results need to be evaluated from a qualitative point of view, due to the considerable lack of information, that implies a low conditioning of the model by real world information. In particular, the following findings can be argued from this model stage.

- While the aquifer is clearly defined as isolated from the sea and the MSLA, there is no information of outflow terms for this aquifer, before the exploitation phase. Therefore, the model has to assume the existence of some sink in the aquifer. This is done by defining three different outflows: (i) vertical leakage through the BC, modeled with GHB condition; (ii) springs from the west-side border of the aquifer, discharging to the sea; (iii) spring in the central-east part of the aquifer, where BC outcrops. The last two outflows are represented by DRN package.
- The assumption of considering three types of different outflows distributed on the model domain, seems to be feasible for only 2 of them, namely the central-east drain and the vertical downward leakage through Blue Clay formation. As a matter of fact, the adjusted values of parameters lead to a water budget in which the west-side drain is not active at all. This result, which assumes natural condition, would be hard to confirm or reject even by collecting more information on the west-side part of the aquifer.
- The simplified assumption of considering only one aquifer conductivity (which is the sole feasible assumption due to the lack of prior information) needs to be removed and substituted by a zonation of conductivity, after acquisition of conductivity estimates. The steady state calibration is indeed not so much affected by varying the conductivity, since in the current setting the model is dominated by the geometry (elevation of top and bottom).
- Under these assumptions, the estimated vertical leakage is in line with the values estimated in former modelling studies (e.g. BRGM, 1991). In particular, considering an aquifer area of 2.75 km^2, the obtained leakage flux is equal to 1.07E-04 m/day, which is comparable with the one estimated by (BRGM, 1991), namely 1.70E-04 m/day.
- The water drained by the central-east source amounts at 421.96 m^3/day, which is a feasible value if compared with the geometric mean of the measurements done for some springs in Malta islands (BRGM, 1991), namely 332.41 m^3/day.

Introduction

This report describes the work carried out during Activity 2 of the project, namely the definition and implementation of steady state models simulating the groundwater resource for five selected aquifers in Maltese islands.
According to the Inception report, the calibrated steady state models refer to a time frame representing the pre-exploitation (or non-intensive exploitation) of groundwater resources. According to the data set available and in agreement with the Contracting Authority Energy and Water Agency (EWA in the following), such a time frame has been defined as the years ranging from 1941 to 1944.
The steady state models have the following specific objectives:

4) Assessing the basic assumptions of the conceptual models, namely the values of hydrodynamic parameters, setting of boundary conditions, identification of main terms in the water balance.
5) Identify potential data gaps (in addition to what already assessed during Activity 1), even providing EWA with a list of suggestions and comments for a potential improvement of the data sets currently available, by promoting new measurements campaigns and/or including additional monitoring network on the islands.
6) Use the result of calibrated model as initial condition for the transient models (to be performed during next Activity 4).

The definition of groundwater numerical models is based on conceptual models described in-depth in report Deliverable D1.3. For this reason, aquifer hydrogeological conceptual models are recalled in this report only in a concise form, to underline the main characteristics of each aquifer. The reader is referred to Deliverable D3.1 for further details.

According to standard procedures (e.g. the guidelines reported in Anderson et al. (2015) and ASTM D5447 - 04(2010)), the modelling study started by assuming the simplest setting concerning layers geometry, hydrodynamic parameters and hydrological stresses. The model study proceeded by defining different model stages and versions that correspond to an improved definition of model settings. In this study, a *model stage* corresponds to a specific definition of the model grid. Each stage includes different *model versions* that could change because of variation of boundary conditions, bottom and top of layers, etc. A summary of the variations for each model is reported in the Modelling Journal (Appendix 1).

Models are developed using the MODFLOW-2005 numerical code (Harbaugh, 2005), mainly through the GIS-integrated user interface FREEWAT.

The main features of models describing the principal aquifers of the islands (namely Malta MSLA and Gozo MSLA) have been presented to EWA's Officers during the 1st Interim Meeting held in May 2019. A simplified version of MSLA steady state model has been used to drive the training session held in the same days (Activity 3 of the project).

The final version of the steady state models here presented has experienced a substantial delay compared to the foreseen time schedule: this delay is mainly due to the provision by EWA of new bunches of data, which have been considered very instructive. The activity needed to include such pieces of information in the models, required an additional workload which reflected on the delay of delivering the present report. However, such an activity has been useful also to start defining the transient models, which are objective of next Activity 4: therefore, the delay of delivery could be partially recovered in next phase of the project.

This report is organized as follows. Part 1 refers to models developed for Malta island, namely regarding Malta MSLA, Mizieb MSLA and Pwales perched aquifer. Part 2 refers to models for Gozo island, namely Gozo MSLA and Ghajnsielem perched aquifer. The Modelling Journal (namely the summary of different model versions and sub-versions developed during the study) is reported in Appendix 1. The main assumptions on which models are based are summarized in the Assumption Register, for the reader convenience, reported in Appendix 2. Appendix 3 includes details on the calibration outputs obtained for Malta MSLA. Finally, Appendix 4 reports the elaboration and analysis performed on additional bunches of data which were not documented in Deliverable D3.1.

As requested in the contract's Terms of Reference, the files needed to run the final version of models are attached to this report in form of *.zip archives (one for each model). In particular, the models are shared with EWA such that they can be reproduced with FREEWAT modeling platform, and therefore each archive includes:

i. The SpatiaLite database where all the input data needed to run the model are stored.
ii. The QGIS project (to be opened in QGIS versions ranging from 2.14 to 2.18), where the link to layers within the database are already set up.
iii. A folder containing the native MODFLOW input files, as reference.

Part 1: Models for Malta islands

Introduction

The description of the conceptual models of Malta aquifers (MSLA, Mizieb, Pwales) is reported in Deliverable D1.3, nevertheless, new data and information were made available after the deliver, especially concerning hydrogeological aspects. The conceptual hydrogeological models were then refined, and the new information included into the present version of the models.

The island of Malta was divided into two model domains, the first covering the MSLA, the second the aquifers of Mizieb and Pwales. The two portions of the island present different quality/quantity of data and different hydrogeological settings, mainly linked to the presence of a physical bottom in the aquifer in Mizieb and Pwales (top of the Blue Clay formation), which is not detectable in MSLA.

The domains covered by the two models are shown in Figure 1. The portion of the island at the North of the Mizieb aquifer was not included in any of the two models.

The models are intended to reproduce the pre-development conditions of the Island, and all the efforts have been done to characterize the hydrogeological situation back in time. The first available data allowed to reproduce the conditions of 1941-1944 for the MSLA (BRGM 1991), while only some local information is available for the Mizieb aquifer (Constain 1958). No data is available for Pwales, which has been associated to the Mizieb model, but with no pertinent real observations.

Figure 1. Model domains for the Malta MSLA (green) and Mizieb-Pwales models (red)

Malta water balance

Long period average water balance

The island water balance is crucial to obtain reliable model results. Several different methods were applied. A preliminary approach considered the average rainfall and temperature values over the long available time series. Evapotranspiration was calculated through the classical Thornthwaite and Turc method. The formulation used for Turc (1961) included the temperature correction with rainfall. The simplified natural balance formula expressed in mm/y is:

$$P - AET = I + R$$

where:

P: average annual precipitation.

AET: average annual actual evapotranspiration.

I: infiltration.

R: runoff.

According to Turc, AET is calculated as follows:

$$ETR = \frac{P}{\sqrt{0.9 + \frac{P^2}{L^2}}}$$

where:

P = average annual precipitation in mm.

L = potere evaporante dell’atmosfera = $(300 + 25T_c + 0.05T_c^3)$.

T_c = air average annual temperature, corrected by the precipitation, in °C:

$$\overline{T_c} = \frac{\sum \overline{P_i} \cdot \overline{T_i}}{\sum \overline{P_i}}$$

According to Thornthwaite (Thornthwaite and Mather, 1955), AET is based on average monthly precipitations and temperatures, soils AWC (Available Water Capacity) and thickness.

A summary of results of the natural balance terms expressed as average mm/y is reported in Table 1.

As a comparison, AET calculated by BRGM in 1991 for the Rabat-Dingli Plateau, considering rainfall time series from 1840 to 1991, was 320 mm/y with an average rainfall of 506 mm/y. The AET percentage over precipitation (63%, cfr. Table 10), is similar to the Thornthwaite annual average result (62.5%).

Balance Term	**Station**	**Available Period**	**Value**
T (°C)	Luqa	1940-2017	18.9
P (mm/y)	Luqa	1941-2018	554.6
AET (mm/y) Thornthwaite with U = 46 mm			346.9 (62.5% of P)
I + R (mm/y) Thornthwaite with U = 46 mm			155.2
AET (mm/y) Turc with Tc			498 (89.8% of P)
I + R (mm/y) Turc with Tc			56.6

Table 1. Terms of the average water balance

Given the high variability of the water balance terms from one year to another, data pertaining to the specific modelled periods were considered. Average monthly values of P and T are reported in Table 2.

Period		Gen	Feb	Mar	Apr	Mag	Giu	Lug	Ago	Set	Ott	Nov	Dic	Year
1941 - 1944	**P**	68.4	72.2	67.1	18.4	17.2	2.9	0.0	19.3	21.6	54.5	94.9	142.3	578.8
	T	12.2	12.4	13.5	15.8	19.1	22.4	25.5	25.9	24.4	21.1	17.3	14.3	18.7
1955 - 1957	**P**	71.4	35.5	32.5	36.1	8.3	0.1	0.0	3.7	39.9	157.6	104.9	64.0	554.0
	T	13.6	12.8	13.2	15.1	18.8	23.1	25.9	26.4	24.2	20.3	16.7	13.3	18.6

Table 2. Average monthly values of P and T referred to 1941-1945 period

Soils of Malta

An in-depth description of the Maltese soils is reported in (Lang, 1960). Distribution of soils is shown in Figure 2 and their main characteristics are summarized in Table 3. The different soils were analyzed in order to figure out information such as the approximate thickness (intended as the depth reached by the roots) and grain size.

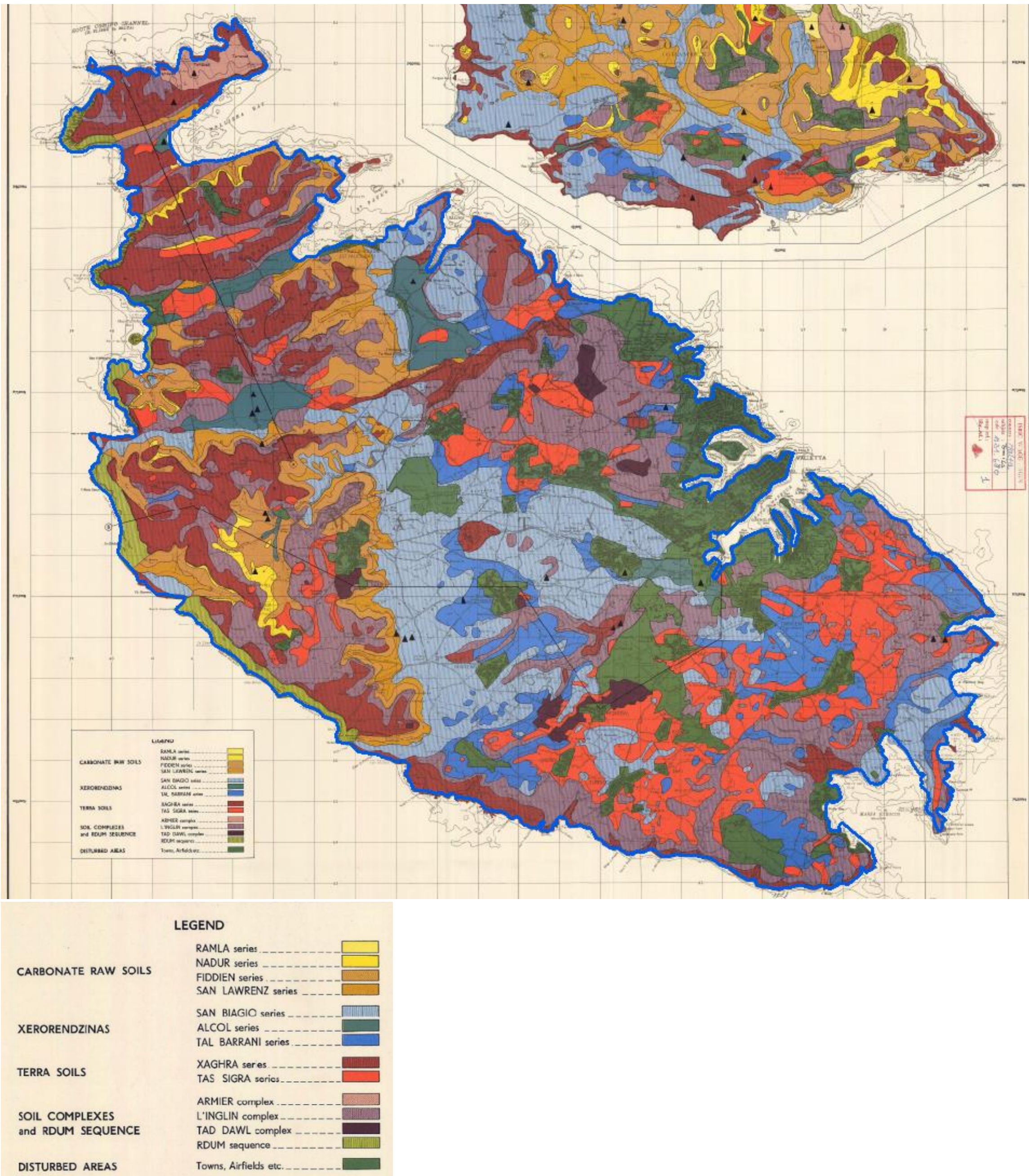

Figure 2. Soil map of Malta from Lang, 1960

Carbonate raw soils	
Nadur: from greensand, lower part of UCL and Quaternary conglomerates; reddish brown gravelly, gritty loamy sand; main roots 0-12 inches	
Ramla: develops on sandy dunes, main roots 0-7 inches	

<table>
<tr><td>Fiddien and San Lawrenz:

dominated by blue clay content; Olive clay; saline soil (Na 10%); main roots 0-10, 0-30</td><td>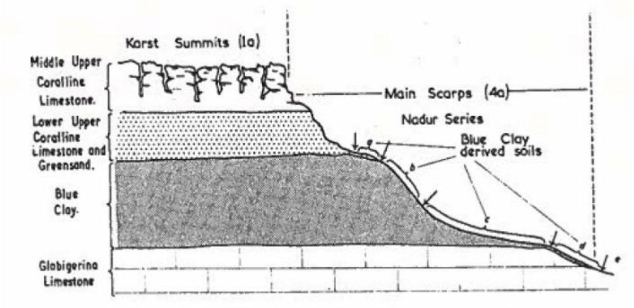

Fig.7. Location of soils of Blue Clay derivation on a main scarp.

Example of San Lawrenz soil profile</td></tr>
<tr><td colspan="2">Rdum sequence</td></tr>
<tr><td colspan="2">Steep coastal slopes where a rapid sequence of parent rocks is exposed (i.e. Dingli cliff)</td></tr>
<tr><td colspan="2">Xerorendzinas</td></tr>
<tr><td>San Biagio:

observed only cultivated; very pale brown silt loam, sandy loam; main roots 0-10, 0-28 inches</td><td rowspan="2">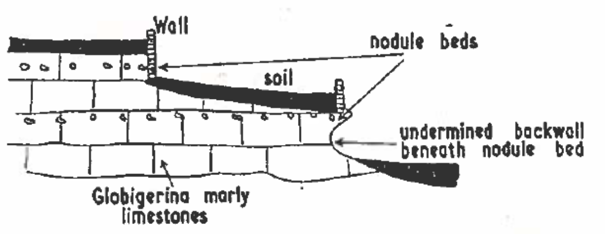

Fig. 9. Terracing in the nodular Globigerina soft limestone.

Example of san Biagio soil profile</td></tr>
<tr><td>Alcol:

from valley loams composed by fine sandy/silty clay loam; main roots 0-21 inches,

Tal Barrani: from GL, brown gravelly silt loam; main roots 0-18 inches, strongly terraced</td></tr>
<tr><td colspan="2">Terra soils</td></tr>
<tr><td>Xagra series:

reddish brown clay loam</td><td rowspan="3">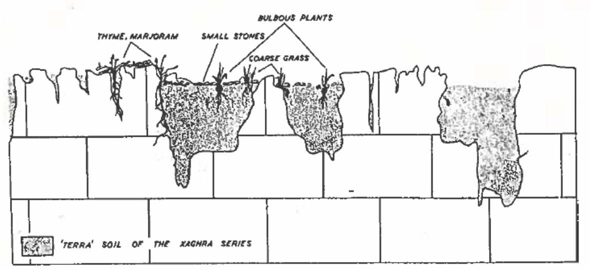

Fig.10. Section through karst lapiés illustrating Xaghra series.

Example of Xagra soils</td></tr>
<tr><td>Tas Sigra series:

flat, valleys and dolines, dark yellowish red clay loam or clay</td></tr>
<tr><td>Armier complex:

mostly sandy</td></tr>
<tr><td colspan="2">Soil complex</td></tr>
<tr><td colspan="2">Inglin complex: high terrace walls, cultivated, varied soils</td></tr>
<tr><td colspan="2">Tad Dawl complex: high variability</td></tr>
</table>

Table 3 Soil descriptions available in Lang, 1960

The soils as described by Lang (1960) were grouped according to the prevailing textural composition and associated to the pertinent AWC (Table 4), according to the USDA procedure (USDA, 1999). The summary of the soil analysis is reported in Table 5.

Available Water Capacities in Centimeters per Centimeter of Soil [1] [2]

Soil Texture Classes	Greater than or equal to 3 percent OM	0.5 to 3 percent OM	Less than 0.5 percent OM
Coarse sand and gravel	0.04-0.06	0.03-0.05	0.02-0.04
Sands	0.07-0.09	0.06-0.08	0.05-0.07
Loamy sands	0.10-0.12	0.09-0.11	0.08-0.10
Sandy loams	0.13-0.15	0.12-0.14	0.11-0.13
Fine sandy loams	0.16-0.18	0.15-0.17	0.14-0.16
Loams and very fine sandy loams	0.20-0.22	0.17-0.19	0.17-0.19
Silt loams	0.22-0.24	0.20-0.22	0.20-0.22
Silty clay loams	0.21-0.23	0.18-0.20	0.18-0.20
Sandy clay loams	0.18-0.20	0.16-0.18	0.15-0.17
Clay loams	0.17-0.19	0.15-0.19	0.14-0.16
Silty clays	0.12-0.14	0.11-0.13	0.10-0.12
Clays	0.11-0.13	0.09-0.11	0.08-0.10
Sapric horizons	0.35-0.45		
Hemic horizons	0.45-0.55		
Fibric horizons	0.55-0.65		

Table 4. Available Water Capacities according to different soil texture classes, from USDA

SOIL	Texture (LANG)	Inches	Thickness cm (LANG or assumption)	AWC/cm USDA, assuming less 0.5% organic matter	AWC/cm USDA (average)	AWC in mm USDA
RAMLA	sandy	14	36	0.05-0.07	0.06	21
NADUR	gravelly loamy sand	10	25	0.08-0.10	0.09	23
ARMIER	sandy	12	30	0.05-0.07	0.06	18
FIDDIEN	clay	30	76	0.08-0.10	0.09	68
SAN LAWRENZ	silt loam, sandy loam	13	33	0.20-0.22	0.21	69
ALCOL (2 profiles)	sandy silty clay loam	17	43	0.15-0.17	0.16	69

SAN BIAGIO (eroded and alluvial phase average)	silt loam, sandy loam	19	48	0.11-0.22	0.17	82
TAL SIGRA	clay loam	36	91	0.08-0.10	0.09	82
TAL BARRANI	gravelly silt loam	18	46	0.20-0.22	0.21	97
XAGHRA	clay loam	1	3	0.14-0.16	0.15	4
INGLIN (assumed as average)	mix	17	43		0.13	56
TAD DAWL (assumed as average)	mix	17	43		0.13	56
Disturbed (assumed as average)	mix	17	43		0.13	56
RDUM	no		0	0		0
TOWN	no		0	0		0

Table 5. Summary of soils characteristics used in the Thornthwait-Mather method.

Distributed recharge in 1941-1944

In order to define the amount of direct aquifer recharge, the terms I and R (Table 1) need to be separated. The water balance was re-calculated focusing on the period of interest (1941-44). The Thornthwaite-Mather method was applied on a monthly basis using the ACW associated to the different soils. Table 6 reports the results. This first step provided the *soil surplus* distributed over the island, as well as the *water deficit*. This last term can be used as an indirect check of the crops water need, which is likely to be covered by irrigation. The spatial distribution of the soils grouped in texture classes is shown in Figure 3.

Soil defined by Lang, 1960	**PET**	**AWC (mm)**	**AET (mm/year)**	**Surplus**	**Deficit**
Disturbed	847.6	56	351	219	497
Tal Barrani	847.6	97	391	178	457
San Biagio	847.6	82	377	193	471
Tas Sigra	847.6	82	377	193	471
Xagra	847.6	4	298	271	549

Inglin, Tad Dawl (soil complex)	847.6	56	351	219	497
Urban	847.6	0	0	0	0
Fiddien, San Lawrenz	847.6	69	364	206	484
Alcol	847.6	69	364	206	484
Rdum	847.6	0	0	0	0
Armier complex	847.6	18	313	257	535
Ramla, Nadur	847.6	18	313	257	535

Table 6. Results of the Thornthwait-Mather method. PET = Potential Evapotraspiration, AWC = Availbla Soil Capacity; AET = Actual Evapotranspiration

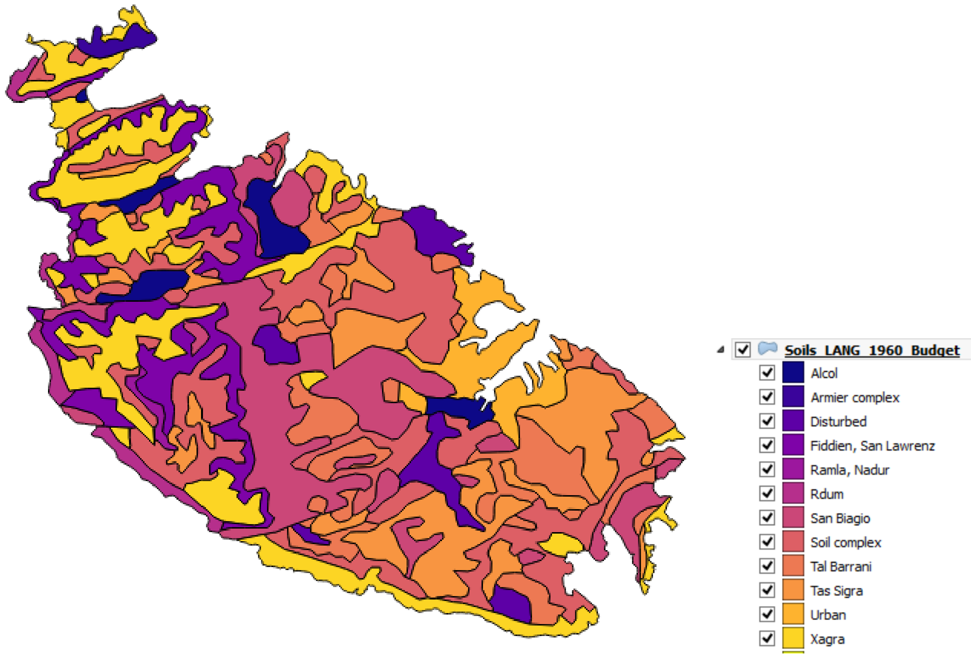

Figure 3. Spatial distribution of the soil groups cited in Table 6

Besides soils characteristics, other aspects were included in the recharge calculation.

1. Geology and slope: an infiltration coefficient corrected by the slope was associated to each lithology;
2. Land use: the first available map is dated 1957; it is assumed that in 1944 the land use was not too different;
3. Dams: the presence of several dams have been considered as areas were infiltration of a portion of runoff is enhanced, i.e., as an additional recharge;
4. Sinkholes: the presence of sinkholes crossing the Blue Clay under the Rabat plateau has been considered as a leakage towards the MSLA, i.e., as an additional recharge.

The assumptions and methods applied to include the above features in the recharge calculation are detailed hereafter.

Geology and slope

The Island geology is widely described in Deliverable D1.3 and reported for convenience herein (Figure 4). An Infiltration coefficient (CIP) was associated to each formation on the basis of the available information in literature (Civita, 2005; Celico, 1986), as detailed in Table 7.

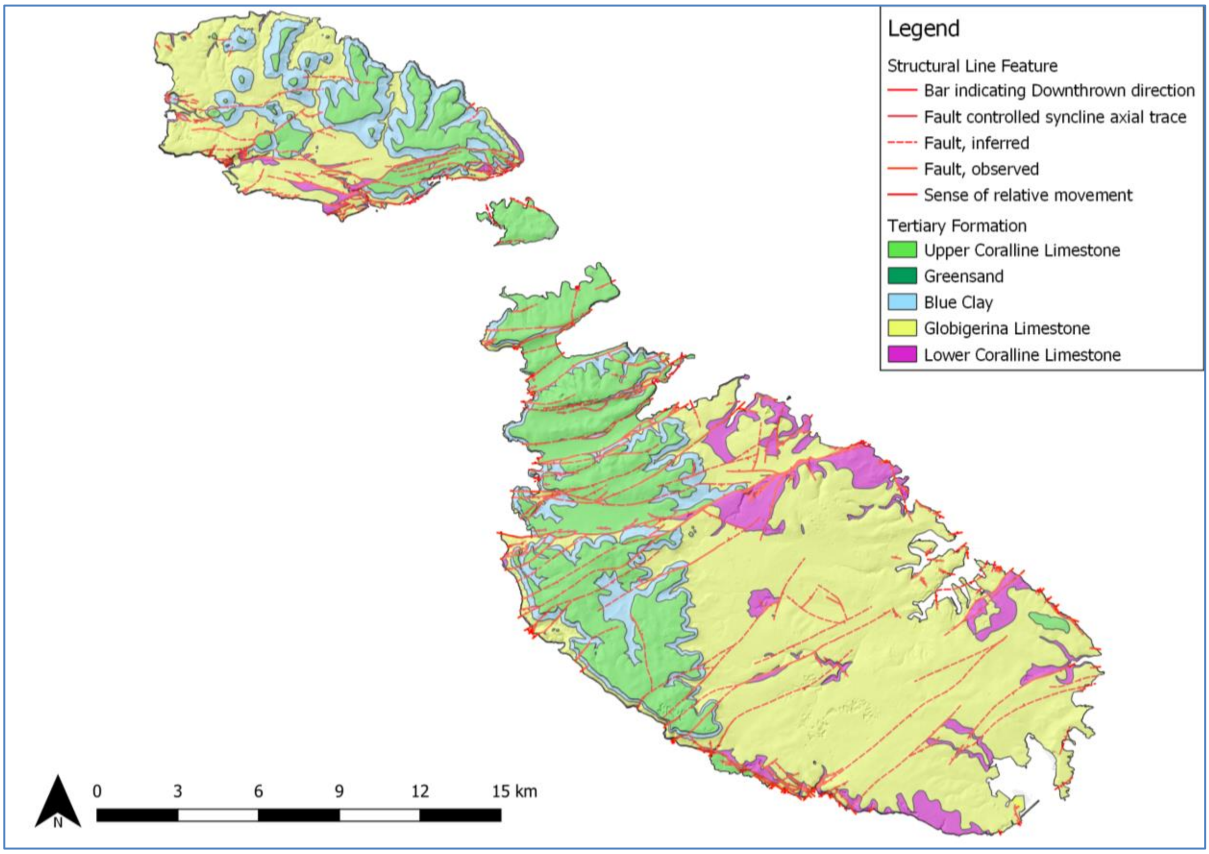

Figure 4. Geology of Maltese archipelago

Formation	Infiltration coefficient (CIP)
Upper Coralline Limestone	100%
Greensand	100%
Blue Clay	10%
Globigerina Limestone	80%
Lower Coralline Limestone	90%

Table 7. Infiltration coefficients

Though the Island morphology is predominantly flat, the slope correction to the infiltration coefficient was applied, obtaining the CIPS values (Viaroli et al. 2018). To include the effect of the morphology on infiltration, the raster map of C.I.P. distribution was multiplied by the slope map (S, in %, Figure 5) calculated from the digital elevation model map. The CIPS were calculated cell by cell according to the following relationship:

$$CIPS = CIP \times \left(1 - \frac{S}{100}\right)$$

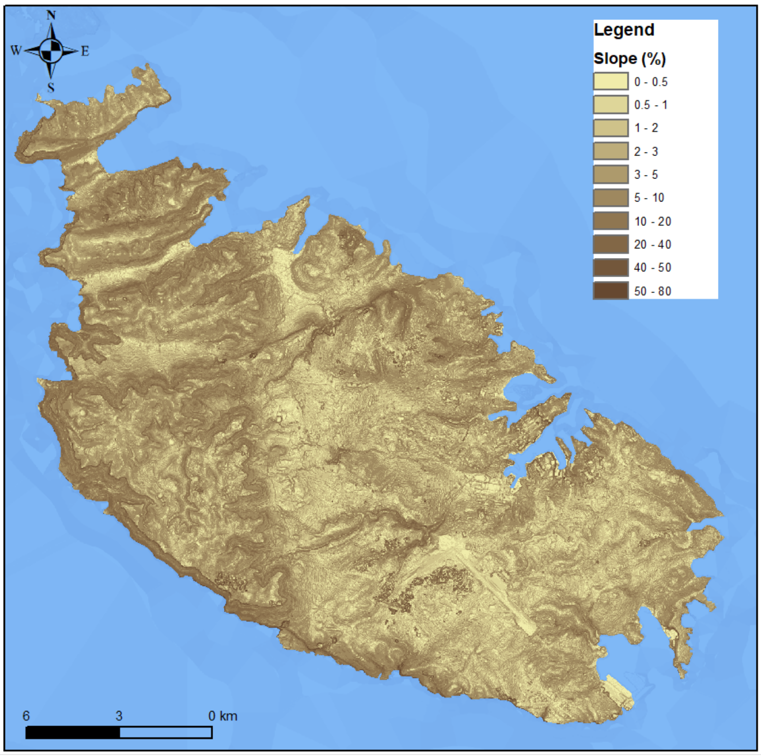

Figure 5. Slope map

Land use

The first available land use map is dated 1957, as shown in Figure 6. It is assumed that the situation was similar during the period of reference, with the majority of the surface covered by cultivated areas.

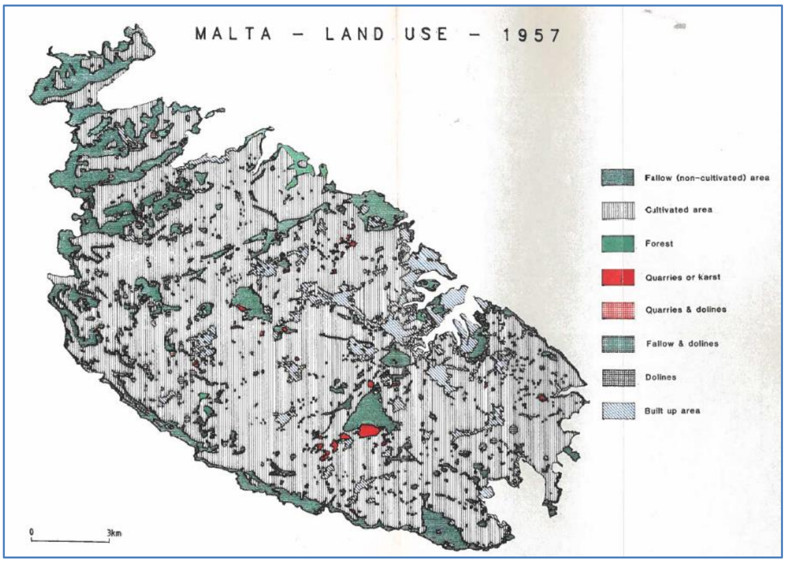

Figure 6. Land use map (1957)

Dams

Available data include the position of 75 dams (Table 8); for 54 dams capacities are declared, from 200 to 9000 m^3, with an average of 2800 m^3. The average value of capacity was assigned to the dams with no information. The frequency distribution of capacities and associated statistics are shown in Table 9.

The estimated dataset of capacities (75 dams) has been used to make a guess about the total annual replenishment, assuming that the dams are "full" about 5 times per year. Additional recharge generated by the dams is local; a buffer around each dam is then assumed of about 200x200 m, giving a total surface of 3000000 m^2 (Figure 7). The total yearly volume (assuming 5 replenishments) is about 1000000 m^3/y, which corresponds to about 300 mm/y over the considered area which are added to the previously calculated recharge (as additional "recollected" runoff).

Station_id	Name	Eastings	Northings	Capacity (m^3)
25001	WIED IS-SEWDA	49645	71635	5389
25002	WIED IL-HMAR/GNEJNA	40970	75090	2539
25003	WIED L-GNEJNA	41145	75410	234
25004	WIED L-KALKARA/MISTRA	44075	79015	1472
25005	WIED MUSA 1	40410	82600	2565
25006	WIED MUSA 2	40362	81905	1869
25007	WIED RANDA	41730	79410	n.a.
25008	WIED L-IMGIEBAH	43968	79920	1404
25009	WIED IL-KBIR	41100	82140	2247
25010	WIED GHAJN RIHANA 1	46960	75450	7580
25011	WIED GHAJN RIHANA 2	47130	75550	5227
25012	WIED GHAJN RIHANA 3	47215	75750	3858
25013	WIED GHAJN RIHANA 4	47280	75810	3409
25014	WIED IL-GHASEL/SANTA KATARINA	48820	75745	4315
25015	WIED IL-GHASEL/BURMARRAD	47720	76820	3142
25016	WIED KANNOTTA/BURMARRAD	46505	77275	n.a.
25017	WIED SILLANI/GHAJR HANZIR	51900	68590	2028
25018	WIED BAKKJA 1	47750	69460	1790
25019	WIED BAKKJA 2	47835	69400	1730
25020	WIED SAN BLAS	47510	69550	1253
25021	WIED IT-TUTI/CIRKEWWA	39870	82170	2048
25022	WIED L-ISPERANZA	47950	74695	5779
25023	WIED KANNOTTA 1	45505	76915	1770
25024	WIED KANNOTTA 2	45695	77030	3878
25025	WIED HESRI 1	48430	68470	3401
25026	WIED HESRI 2	48790	68620	3619
25027	WIED HESRI 3	49080	68810	682
25028	WIED HESRI 4	49170	68810	n.a.
25029	WIED GHOMOR	52940	75015	2503
25030	WIED IL-FRANCIS	52990	74945	1353
25031	WIED GHAR DALAM	57350	66610	1830
25032	WIED SAN NIKLAW	41845	79560	935
25033	WIED IL-QOTTON	56960	64780	3818
25034	GHAJN IL-KBIRA/GIRGENTI	46545	67950	2565
25035	WIED HAL DWIEL	49450	69550	1352
25036	CHADWICK LAKES 1	44390	72160	1412
25037	CHADWICK LAKES 2	44660	72295	3480

Station_id	Name	Eastings	Northings	Capacity (m^3)
25038	CHADWICK LAKES 3	45085	72385	9068
25039	CHADWICK LAKES 4	45315	72650	6006
25040	GNIEN INGRAW	42200	79865	1243
25041	WIED IL-FAHAM	51010	76590	n.a.
25042	MIGRA FERHA	41200	70610	3409
25043	WIED BLANDUN	56140	70470	1364
25044	WIED HESRI 5	49410	68920	2045
25045	WIED QIRDA 1	50240	69550	1818
25046	WIED QIRDA 2	50820	69660	1591
25047	WIED QIRDA 3	50970	69670	1364
25048	WIED QIRDA 4	51050	69630	4545
25049	BAHRIJA	40705	73715	455
25050	WIED QLIEGHA 1	46390	73415	4545
25051	WIED QLIEGHA 2	46460	73555	2273
25052	WIED QLIEGHA 3	46685	73565	4091
25053	WIED QLIEGHA 4	46790	73665	3409
25054	M'SCALA VALLEY	60115	69875	1364
25055	MARSA COURSE 1	53390	70640	1818
25056	MARSA COURSE 2	53580	70640	n.a.
25057	MARSA COURSE 3	53880	70600	n.a.
25058	MARSA COURSE 4	54118	70575	n.a.
25059	MARSA COURSE 5	54275	70575	n.a.
25060	MARSA COURSE 6	54402	70540	n.a.
25061	MARSA RUN OFF	54525	70612	n.a.
25062	WIED BAKKJA I	48650	69020	n.a.
25063	WIED BAKKJA II	48690	69055	n.a.
25064	WIED BAKKJA III	48710	69150	n.a.
25065	WIED BAKKJA IV	48810	69335	n.a.
25066	WIED BAKKJA V	49045	69355	n.a.
25067	TAS-SALIB 1	44145	72060	n.a.
25068	TAS-SALIB 2	44230	72150	n.a.
25069	QASSAM BARRANI	41745	79655	n.a.
25070	WIED RANDA	41620	79480	n.a.
25071	WIED RANDA	41540	79505	n.a.
25072	BAHRIJA VALLEY	40705	73715	n.a.
25073	WIED HZEJJEN 1	46430	75245	2273
25074	WIED HZEJJEN 2	46550	75200	2727
25075	WIED HZEJJEN 3	46700	75250	3409

Table 8. Dams information

Descriptor	Value	Frequency distribution
N	54	
Min	234	
Max	9068	
Sum	151293	
Mean	2802	
Std. error	238	
Variance	3066345	
Stand. dev	1751	
Median	2273	

25°percentile	1457	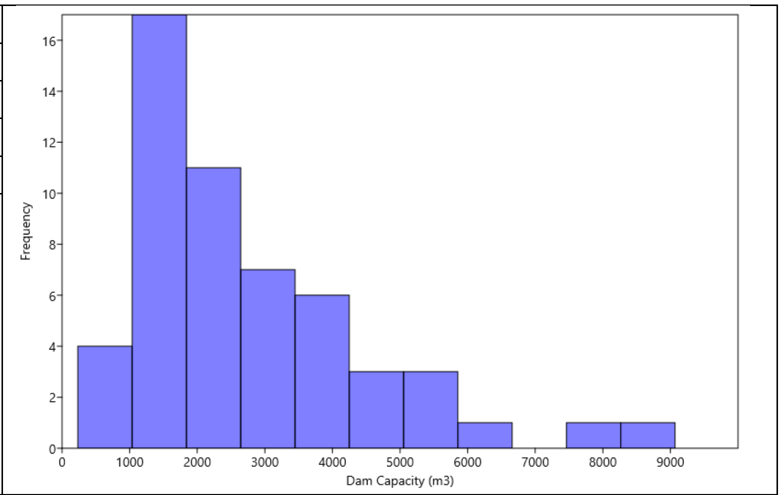
75°percentile	3669	
Skewness	1.390026	
Kurtosis	2.48241	
Geom. mean	2307	
Coeff. var	62.5	

Table 9. Dams statistics

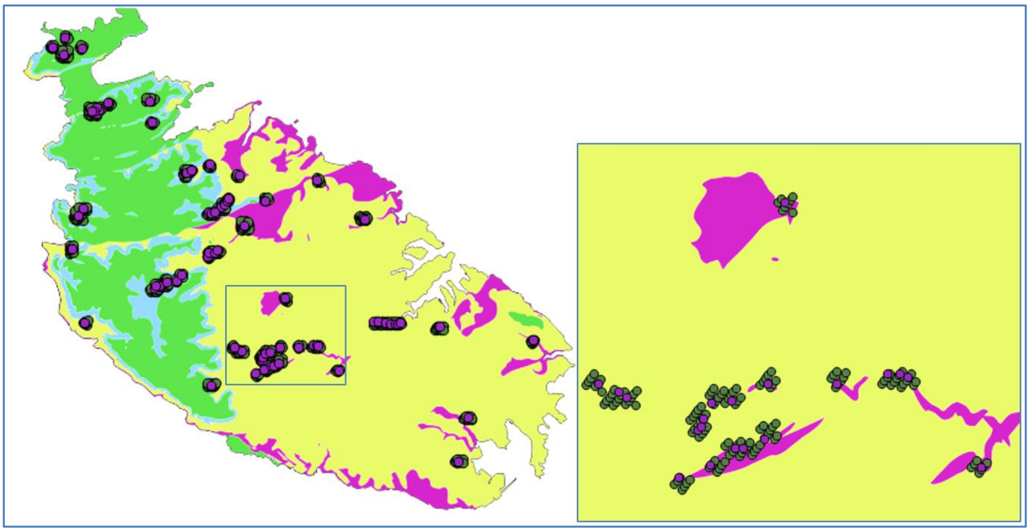

Figure 7. Dams location

Sinkholes

A further term of recharge that needs to be counted is the leakage from the Rabat-Dingli Plateau towards the MSLA. The detailed work of BRGM "*Lumped hydrological model simulation of the Wignacourt springs discharge*" (May 1991) was considered. The objective of the lumped rainfall-discharge model *Gardenia* was to determine the aquifer recharge of the perched aquifer. This enabled an estimation of the overall water resources of the Rabat-Dingli Plateau aquifer, from which it was possible to evaluate the leakage towards the underlying MSLA across the Blue Clay formation. The water balance is reported in Table 10, where the estimated leakage is 12% of rainfall, i.e. 63 mm/y in the period considered in the BRGM report (1840-1991), that would be about 69 mm/y if the period 1941-1944 is considered.

Hydraulic balance component	From lumped modeling of Wignacourt Springs		Whole perched aquifer Rabat Dingli plateau - 22.3 km²	
	Water depth (mm)	Variation coeff. (%)	Discharge (l/s)	Yearly volume 10^6 m³
Rainfall	506 (100%)	27	358	11,28
Actual Evapotranspiration	320 (63%)		227	7,14
Effective rainfall	186 (37%)	58	131	4,14
Perched Aquifer Spring Discharge	123 (22,7 l/s) (25%)	33	87	2,74
Vertical leakage through the Blue Clay	63 (12%)	23	44	1,40

Table 10 Assessment of the components of the hydrological balance for the perched aquifer of the Rabat-Dingli Plateau under conditions of little or no influence (BRGM, 1991)

Given the extremely low hydraulic conductivity of the Blue Clay, it is assumed that the estimated leakage takes preferentially place through the structural discontinuities of the clayey thickness, i.e, mostly through sinkholes. Starting from the island recharge distribution, the recharge over the Rabat-Dingli plateau is subtracted, multiplied by 12% and reallocated in coincidence of the known sinkholes. The yearly volume derived by 69 mm/y over the whole Plateau surface (22.3 km^2, BRGM 1991) equals 1.5 Mm3/y. If a buffer is applied to each sinkhole, the area where the yearly volume is likely to leak would be approximately 3.7 km^2 (Figure 8), leading to an equivalent height of 375 mm/y. The remaining surface of Rabat-Dingli Plateau is considered almost impermeable.

Information about the portion of the island at the North of the Victoria Fault are not sufficient to clearly characterized the area. It is preliminarily assumed that the perched aquifer hosted in UCL has little or no influence over the MSLA because of the lack of evidence of solution structures.

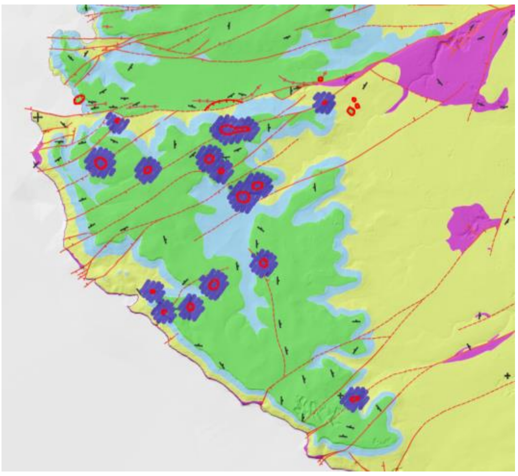

Figure 8. Sinkholes of the Rabat-Dingli Plateau

Results

The raster maps of the above elements have been combined via map algebraic operations to spatially distribute the recharge over the model domain. Weights were assigned and adjusted iteratively in order to approximate the 37% of the mean annual rainfall is taken as reference (BRGM, 1991). The final map equation can be conceptually written as:

$$NatRCH = Surplus\text{*CIPS x } U - \text{UCL} + \text{SH} + \text{D}$$

Where:
Surplus = Soil surplus map, computed using Thornthwaite method and the soil classification obtained from Lang (1960),
CIPS = Infiltration coefficient map, taking into account the lithologies types corrected with slope,
U = urbanized area, from the land use map (1957),
UCL = recharge infiltrating over UCL,
SH = recharge due to sinkholes,
D = recharge due to dams.

The resulting maps obtained at different stage of the calculation are reported in the following figures.

If only the area of Rabat plateau is considered for comparison with the BRGM report (Table 10), the local recharge over UCL is 218 mm/y (Figure 9), equal to the 37.7% of recharge in 1941-44, comparable with results obtained by Gardenia (BRGM), i.e. 37%.

The final average recharge over the MSLA extension (216.6 km^2) included the inflows from dams and sinkholes is 116 mm/y (Figure 11).

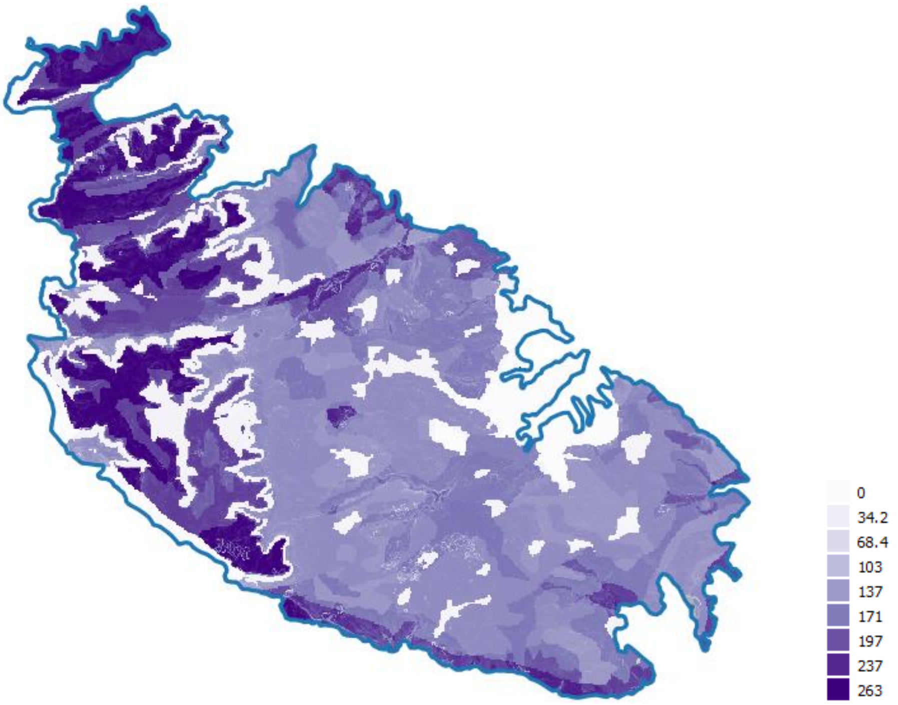

Figure 9. Recharge obtained from Thornthwaite surplus x CIPS x Landcover Mean 149, SD 72, Median 153 mm/y

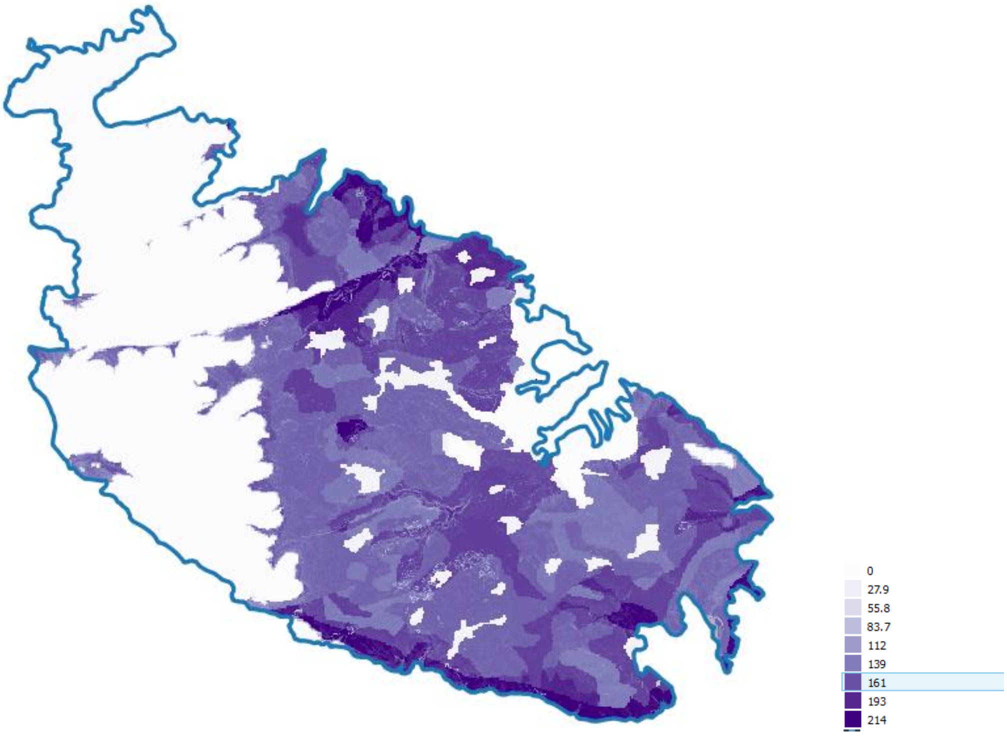

Figure 10. Recharge obtained from Thornthwaite surplus x CIPS x Landcover - Blue Clay_UCL zones (mm/year).

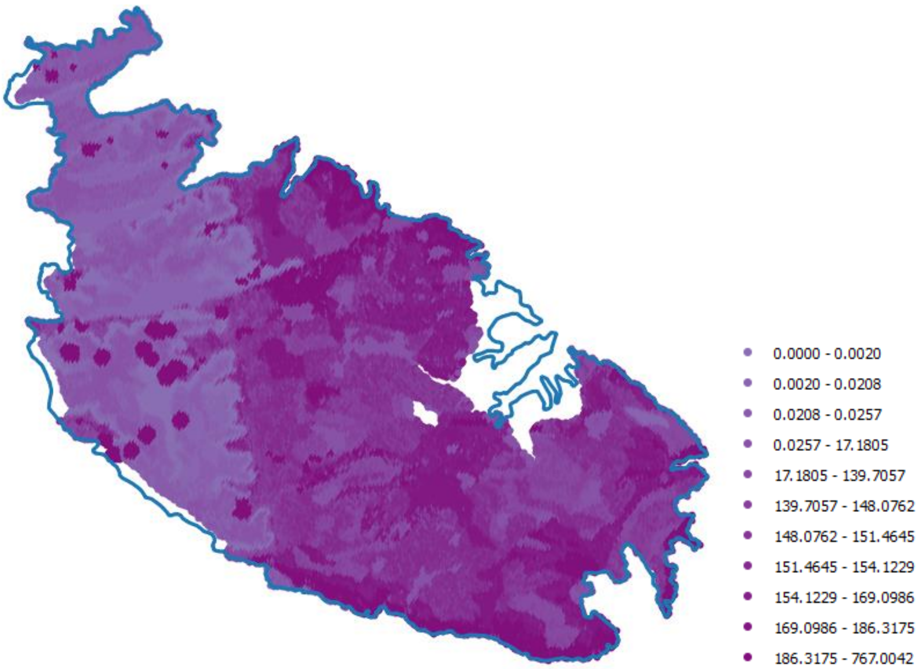

Figure 11. Final recharge distribution (mm/year).

Outflows in 1944-1945

During the period of reference, several private and public pumping over the whole island were already active. Available information includes the position of water production points, the cumulative volume pumped from 10 public boreholes and 5 pumping stations (Table 11) and qualitative/incomplete information about 366 private abstraction wells. Table 12 reports the private wells with information about the volume tapped in 1945 (66 over 366 records). The position of all points is shown in Figure 12.

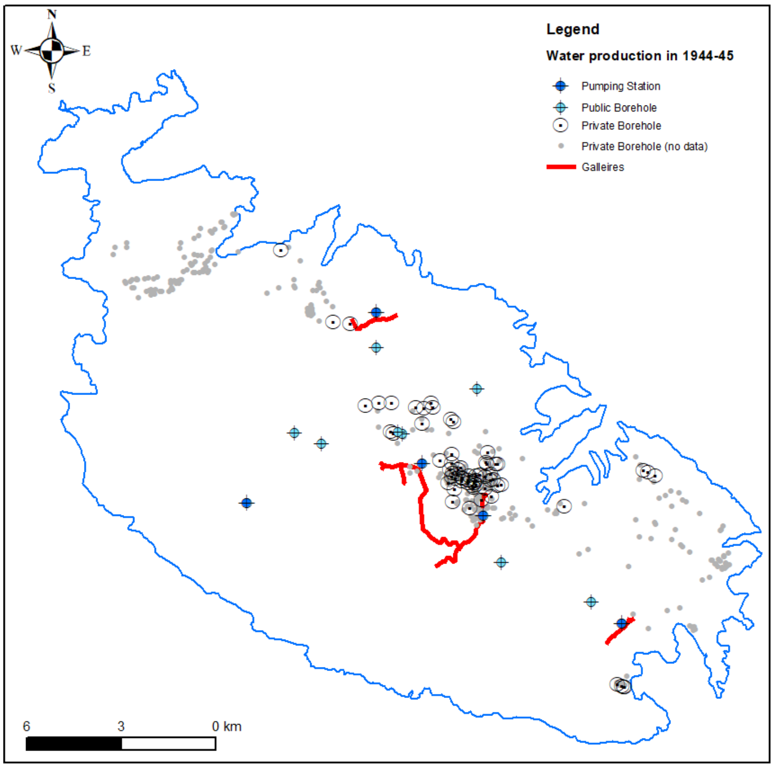

Figure 12. Water production in 1944-1945.

ID	Type	Pumped volume (m^3/y)	Average pumping discharge (m^3/s)	Year
10012	Borehole	69966	0.002219	1944
10017	Borehole	39393	0.001249	1944
10031	Borehole	19803	0.000628	1944
10037	Borehole	44470	0.00141	1944
10051	Borehole	3283	0.000104	1944
10055	Borehole	23477	0.000744	1944
10056	Borehole	27571	0.000874	1944
10069	Borehole	17854	0.000566	1944
10071	Borehole	69349	0.002199	1944
10308	Borehole	54303	0.001722	1944
11002	Pumping Station	79058	0.002507	1944
11003	Pumping Station	1725149	0.054704	1944
11005	Pumping Station	1877560	0.059537	1944
11006	Pumping Station	97228	0.003083	1944
11008	Pumping Station	960221	0.030448	1944
Tot public		**5108685**	**0.16**	**1944**

Table 11. Public boreholes and pumping station active in the reference period.

ID	Water Production (Gallons/year)	Pumped volume (m^3/y)	Average pumping discharge (m^3/s)	Year
902	232500	1057	3.35E-05	1945
906	1947000	8851	2.81E-04	1945
177	594980	2705	8.58E-05	1945
159	194370	884	2.80E-05	1945
161	76000	346	1.10E-05	1945
160	76000	346	1.10E-05	1945
158	76000	346	1.10E-05	1945
154	8422368	38289	1.21E-03	1945
129	4055424	18436	5.85E-04	1945
126	3903456	17745	5.63E-04	1945
38	4526480	20578	6.53E-04	1945
114	4312192	19604	6.22E-04	1945
197	7608168	34587	1.10E-03	1945
52	21900	100	3.16E-06	1945
27	2920136	13275	4.21E-04	1945
29	1557600	7081	2.25E-04	1945
17	1869120	8497	2.69E-04	1945
95	21900	100	3.16E-06	1945
19	2102760	9559	3.03E-04	1945
16	2358348	10721	3.40E-04	1945
14	5534672	25161	7.98E-04	1945
12	3234144	14703	4.66E-04	1945
77	623040	2832	8.98E-05	1945
3017	623040	2832	8.98E-05	1945
80	337952	1536	4.87E-05	1945
35	39900	181	5.75E-06	1945
32	88892	404	1.28E-05	1945
55	4873220	22154	7.03E-04	1945
57	88202	401	1.27E-05	1945
6	21900	100	3.16E-06	1945
33	21900	100	3.16E-06	1945
7	3460704	15733	4.99E-04	1945
9	1347717	6127	1.94E-04	1945
4	5811264	26419	8.38E-04	1945
5	8085360	36757	1.17E-03	1945
1	16500	75	2.38E-06	1945
205	3593808	16338	5.18E-04	1945
61	1154984	5251	1.66E-04	1945
198	6288928	28590	9.07E-04	1945
79	1067664	4854	1.54E-04	1945
26	2695120	12252	3.89E-04	1945
78	15840	72	2.28E-06	1945
24	2299584	10454	3.31E-04	1945
25	846758	3849	1.22E-04	1945
18	933380	4243	1.35E-04	1945
23	4732272	21513	6.82E-04	1945
15	1661440	7553	2.40E-04	1945
90	2920136	13275	4.21E-04	1945
91	6756680	30716	9.74E-04	1945
93	1577424	7171	2.27E-04	1945
92	18250	83	2.63E-06	1945

ID	Water Production (Gallons/year)	Pumped volume (m^3/y)	Average pumping discharge (m^3/s)	Year
62	2118336	9630	3.05E-04	1945
193	882168	4010	1.27E-04	1945
107	2554464	11613	3.68E-04	1945
87	343220	1560	4.95E-05	1945
103	3943560	17928	5.68E-04	1945
104	1081824	4918	1.56E-04	1945
121	843024	3832	1.22E-04	1945
120	2020160	9184	2.91E-04	1945
3	1683860	7655	2.43E-04	1945
82	4099200	18635	5.91E-04	1945
108	5192000	23603	7.48E-04	1945
3	1683860	7655	2.43E-04	1945
106	2596000	11802	3.74E-04	1945
4	5811264	26419	8.38E-04	1945
1888	208000	946	3.00E-05	1945

Table 12. Private abstraction well with estimates of average discharges.

Concerning private wells, a fictitious pumping rate was assigned to the points with no data (Figure 12). The average pumping volume is approximately 10000 m^3/y; this value was assigned to the wells without information about the pumped volume, obtaining a total estimated amount of 3694225 m^3/y for private abstraction. If this volume is assumed to be the same of the previous year and is added to the public water production, an overall abstraction of 8802910 m^3/y can be supposed in 1944 over the entire Island of Malta (included the northern sector). The estimated amount of water tapped from MSLA is given by public abstraction (5108685 m^3/y) plus 2827917 m^3/y given by the private abstractions pertinent to the MSLA (286 over 366 private wells).

Descriptor	Value	Frequency distribution
N	66	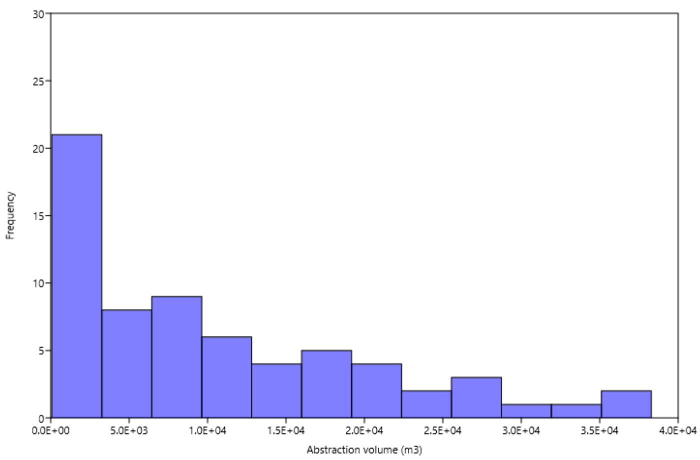
Min	72	
Max	38289	
Sum	694226	
Mean	10519	
Std. error	1257	
Variance	1.04E08	
Stand. dev	10211	
Median	7655	
25° percentile	1416	
75° percentile	17791	
Skewness	0.98852 2	
Kurtosis	0.19892 6	
Geom. mean	4109	
Coeff. var	97	

Table 13. Statistics of private wells discharges

Malta MSLA numerical model

Domain and discretization

The Malta MSLA model grid covers an area of about 500 km^2, divided into 105536 cells with dimension 50x100 m, rotated by 53 degree (Figure 13). The aquifer surface (216.6 km^2) occupies 43318 cells, the sea 59068 cells, while the northern area of the island was excluded assigning the no-flow condition to 3150 cells. The model is single-layer, with a thickness assumed to be 150 m or higher. The bottom elevation was set as top elevation (ground surface and bathymetry) – 150 m. In case of absolute bottom elevations higher than -150 m a.s.l., the bottom was rectified equal to -150 m a.s.l. elevation (Figure 13).

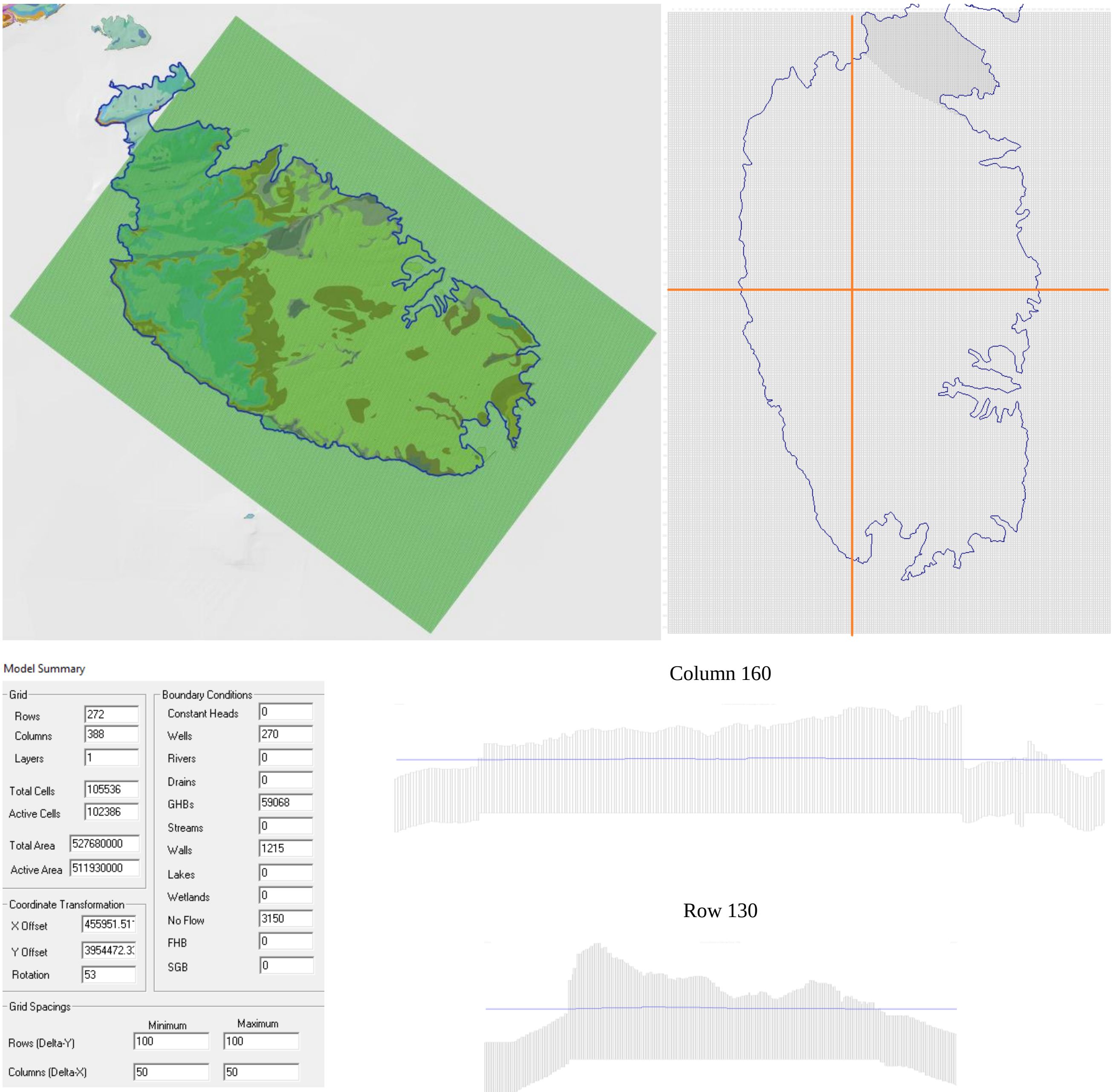

Figure 13. Model grid for Malta MSLA.

Boundary conditions

The model structure, defined by geometry of the aquifer and boundary conditions, is the principal factor regulating groundwater flow in the case of Malta. Different settings where tried, leading to a preliminary configuration which presently includes (Figure 14):

1. General head boundary (GHB) to represent the sea, characterized by head elevation = 0 m a.s.l. and conductance = 5 m^3/s, derived by the assigned hydraulic conductivity of 0.001 m/s times the cell area;
2. Hydraulic flow barrier (HFB) to represent the main faults discontinuities with an initial low hydraulic conductivity (1.0E-8 m/s);
3. Wells (WELL) to represent pumping wells and galleries that were active during the period of reference (1944).

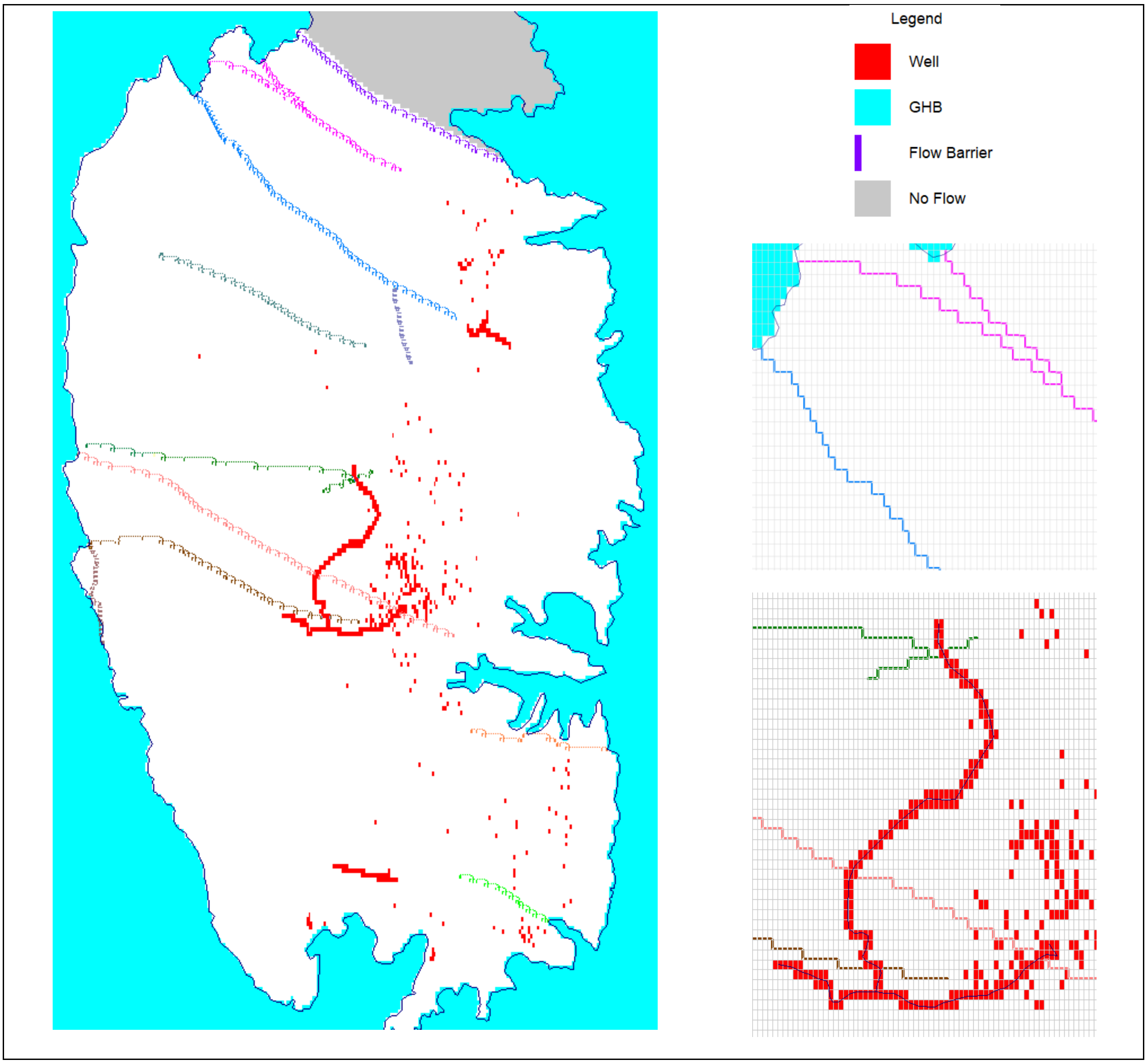

Figure 14. Model boundary conditions.

Concerning the water galleries active in 1944, the discharge of the relative pumping stations are available (Table 11). The annual water production of each pumping station was assigned to the closer shaft of the gallery or to the whole gallery if only one pumping station is present. The annual volume was “spread” over the gallery extension, dividing the discharge by the number of cells intercepted by the gallery, as specified in Table 14.

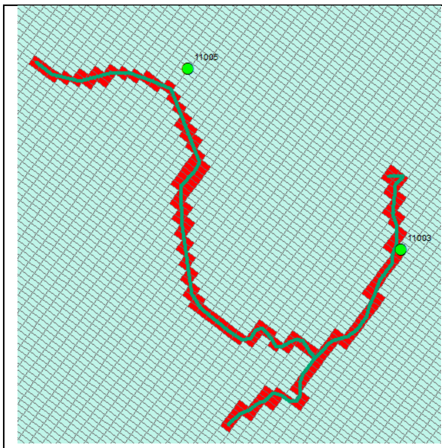	**Tal-Hlas – Wied Il-Kbir** Pumping station: 11003, 11005 Total discharge of 11005: 0.0595 m^3/s in 110 cells Total discharge of 11003: 0.0547 m^3/s in 79 cells
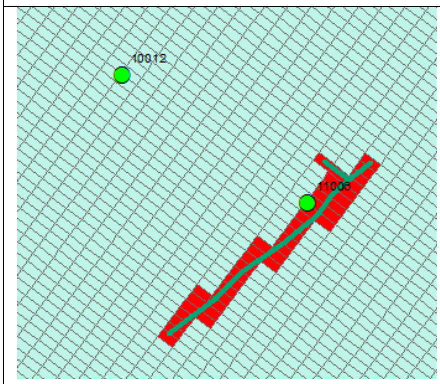	**Wied-Dalam** Pumping station: 11006 Total discharge of 11006: 0.0031 m^3/s in 41 cells
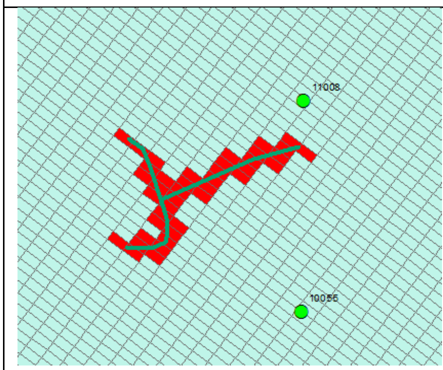	**Wied-Il-Ghasel** Pumping station: 11008 Total discharge of 11008: 0.0304 m^3/s in 40 cells

Table 14. Model representation of water galleries.

Initial properties

The transmissivity distribution was described in paragraph “3.2 Hydrogeological Conceptual Model” of Deliverable D1.3 (Figure 15), and was based on the pumping and tide tests described in BRGM report (1991). If an aquifer thickness of about 150 m is assumed, hydraulic conductivity values are reported in Table 15. Supposing a similar hydrogeological behavior of similar lithologies, supposing spatial continuity of the parameter and extending the available information to the whole island, the preliminary rough spatial distribution of hydraulic conductivity can be assumed as an initial parameter guess to be entered in the numerical model (Figure 16).

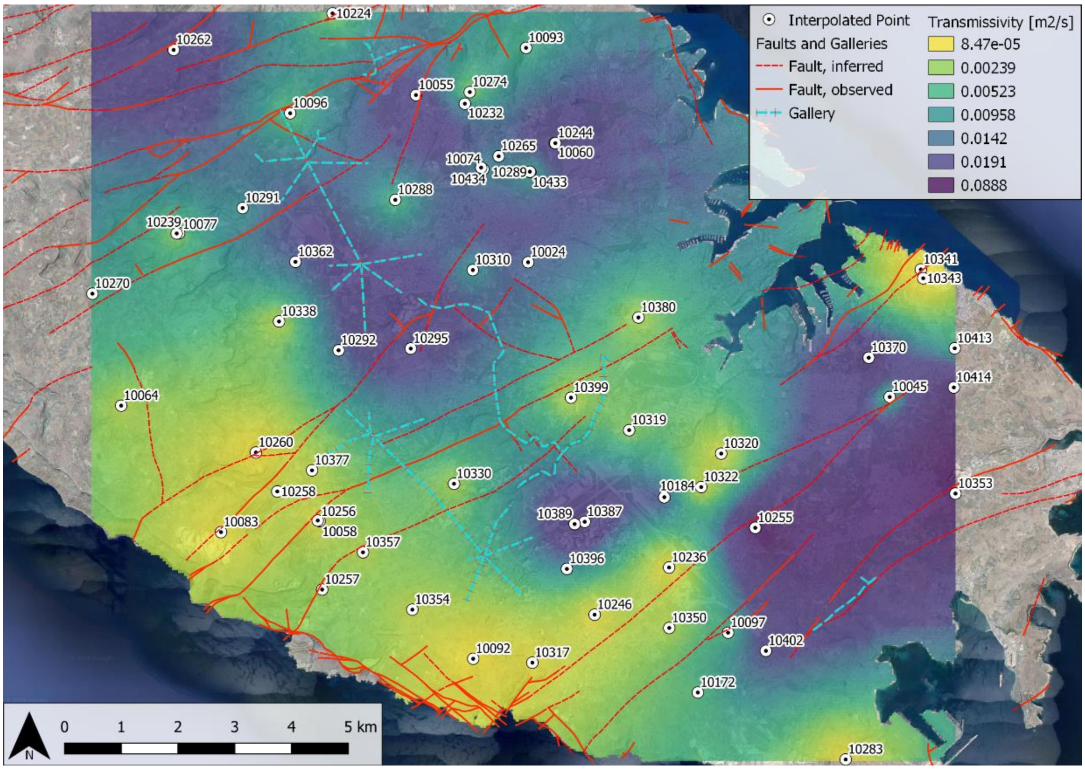

Figure 15. Ordinary Kriging representing the distribution of T in m^2/s.

Statistical descriptor	Units	Value	Hydraulic conductivity (150m of thickness), in m/s
Number of data	-	62	62
Minimum value	m^2/s	7E-5	4.67E-07
Maximum value	m^2/s	0.1	0.000667
Mean	m^2/s	0.01038	6.92E-05
Standard error	m^2/s	0.00224	1.49E-05
Variance	$(m^2/s)^2$	0.00031	2.07E-06
Standard deviation	m^2/s	0.0178	0.000119
Median	m^2/s	0.0038	2.53E-05
25th percentile	m^2/s	0.001	6.67E-06

Statistical descriptor	Units	Value	Hydraulic conductivity (150m of thickness), in m/s
75th percentile	m^2/s	0.013	8.67E-05
Skewness	-	3.2	
Kurtosis	-	12.1	
Geometric mean	m^2/s	0.003	0.00002
Coefficient of Variation	-	170	

Table 15. Descriptive statistics of the transmissivity datasets and Hydraulic conductivity for a supposed aquifer thickness of 150 m.

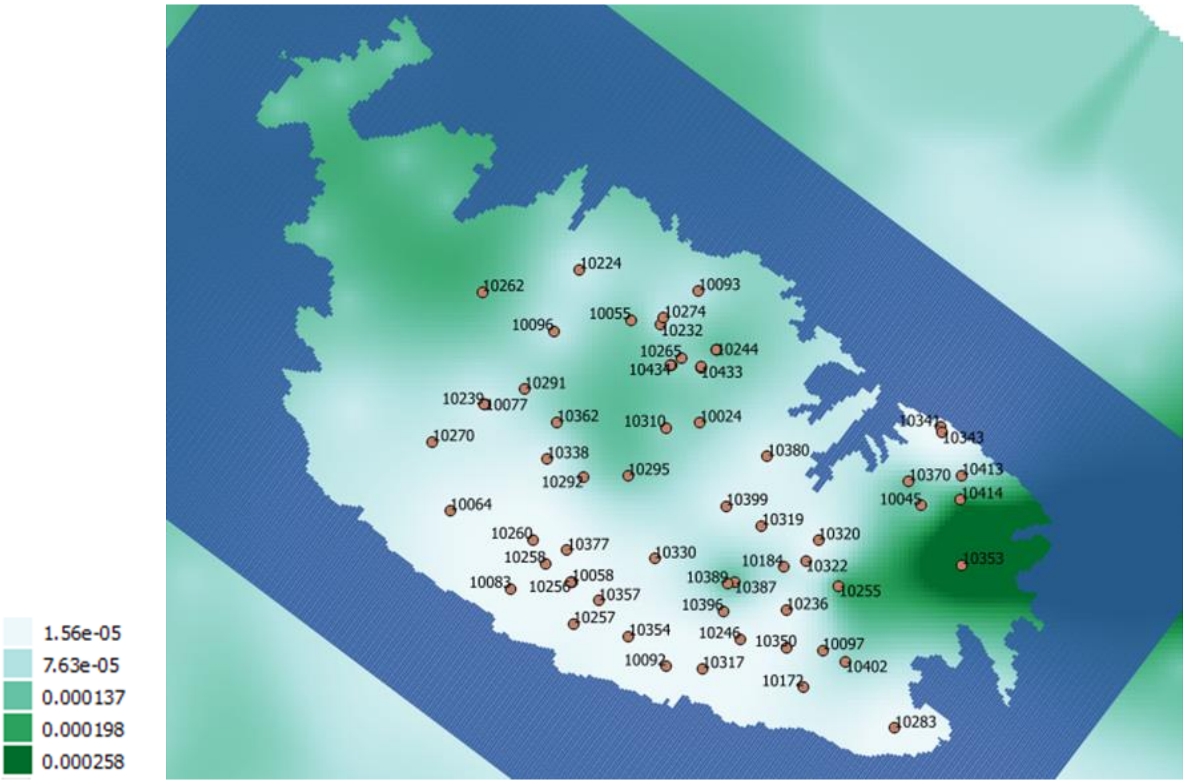

Figure 16. Reconstructed hydraulic conductivity distribution, given by the interpolation of available data plus fictitious points to cover the whole model domain.

Initial heads

The first available measurements of hydraulic heads from 1944 (Table 16) were used to build a preliminary potentiometric surface; the same points were also used as observations ("targets") in the model calibration process. In order to connect groundwater levels to the seawater surface, the borehole dataset was integrated with fictitious points along the coast and offshore with water elevation equal to 0 m a.s.l.

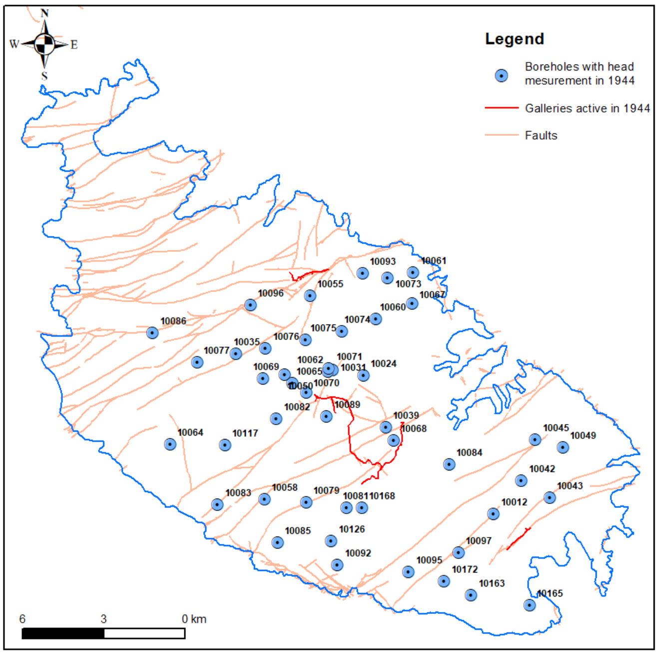

Figure 17. Available points with head measurements in 1944.

OBSID	H_1944 m asl	OBSID	H_1944 m asl	OBSID	H_1944 m asl
10086	1.4	10055	2.9	10077	3.2
10035	4.6	10126	3.3	10067	0.9
10069	3.1	10031	3	10045	1
10012	1.8	10071	2.6	10042	2.3
10083	3.6	10082	4.1	10043	1.3
10092	2.7	10079	2.6	10039	2
10172	0.4	10095	1.2	10050	3.4
10084	1.5	10064	3.2	10061	0.1
10074	2.8	10081	3.9	10062	2.1
10097	1.4	10089	3.6	10065	3.3
10085	2.1	10058	3.3	10068	1.7
10049	1.9	10117	4.3	10070	2.7
10093	1.9	10060	2.2	10073	1.8
10075	2.5	10096	3.2	10163	0.2
10024	2.9	10076	2.4	10165	0.4
				10168	3.4

Table 16. Available points with head measurements in 1944.

The point data were processed before being interpolated. Data present a slight trend which can be described by a second order exponential trend surface. The recognized trend has been removed to guarantee stationarity of the data sets in order to be processed with the kriging technique.

The omnidirectional semivariogram producing the lower error of the cross-validation (CV) is the gaussian model (even if other theoretical models give similar errors and results); since the semivariogram map highlights the presence of anisotropy with major axis direction NW-SE, this parameter has been introduced as well, giving a further lowering of the CV error. The main direction followed by the semivariogram map has been slightly adjusted to make the minor axis follow the principal directions of the island SW-NE faults, resulting in a 1.4 anisotropy ratio with direction shown in Figure 18.

Results of cross-validation gave a standardized RMSE of almost 2 m. This is an overall indication of the quality of data and of their degree of spatial correlation, which will be taken into account as a term of reference during the calibration process.

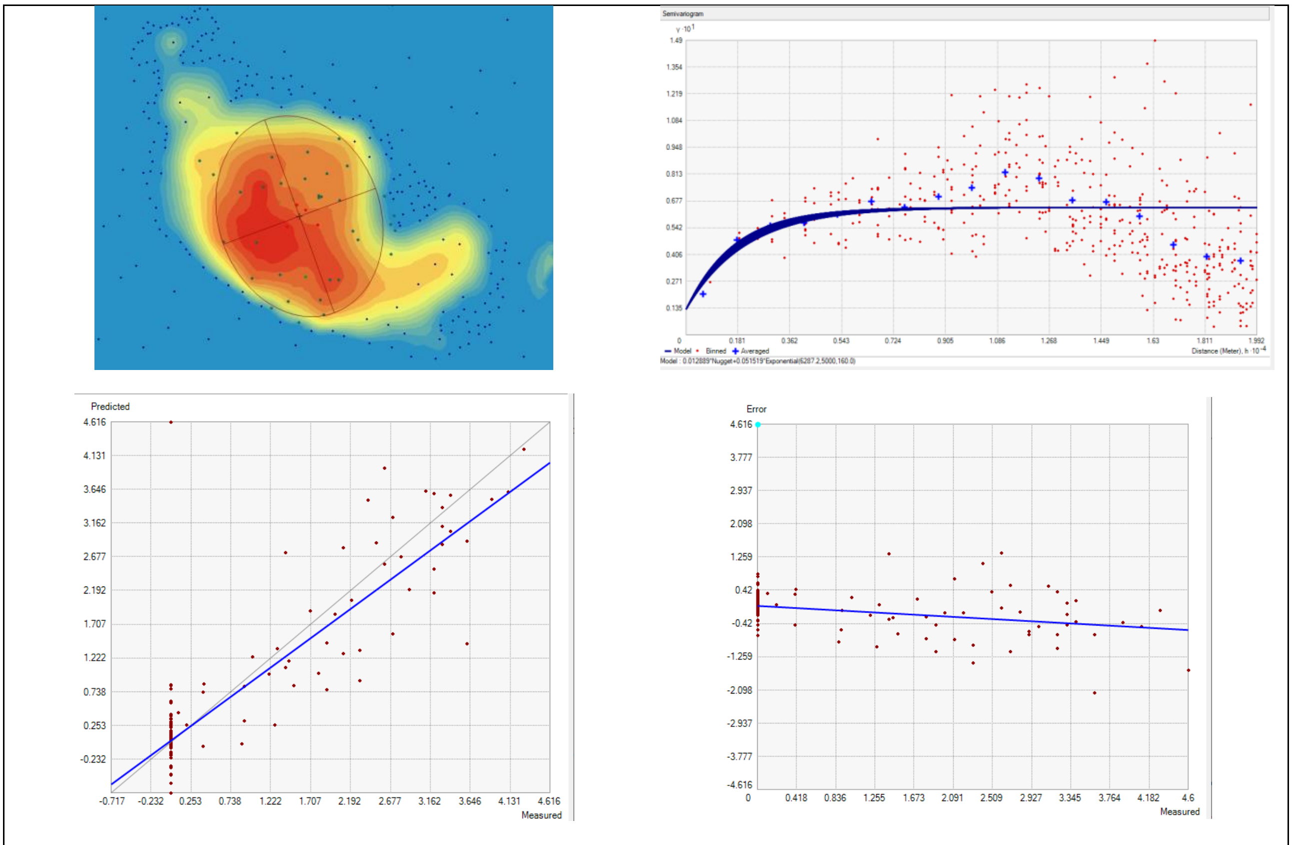

N (included seawater levels)	294
Mean error	-0.0065 m
RMSE	0.43 m
RMSE standardized	1.96 m

Figure 18 Geostatistical analysis of head data, which included trend removal, semivariogram analysis and cross-validation

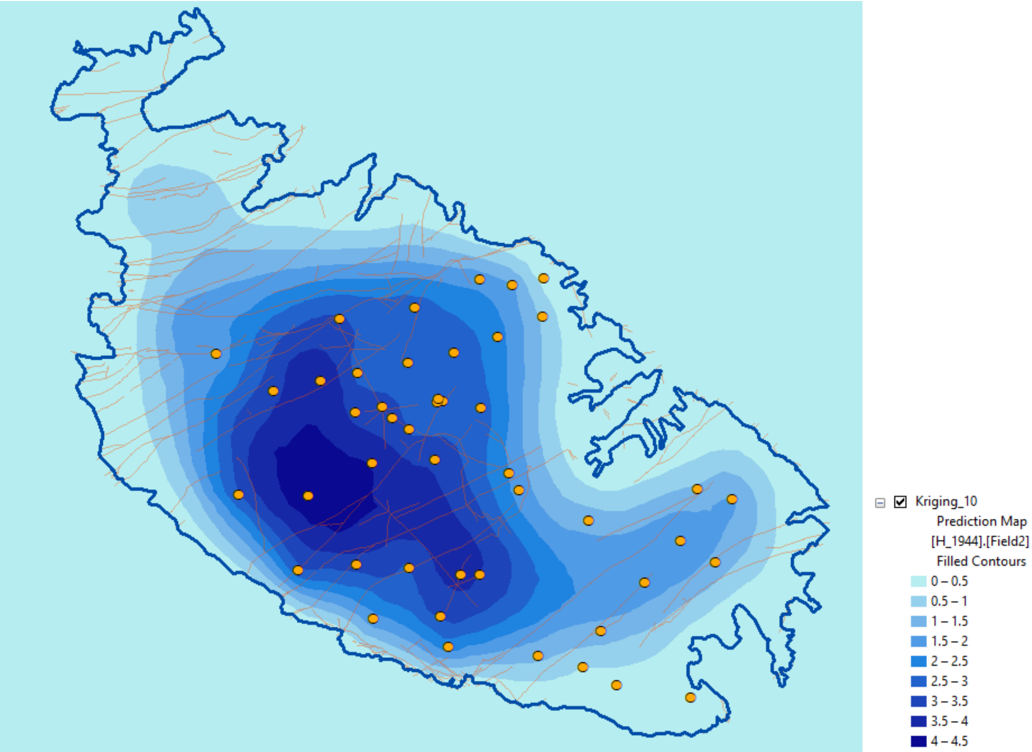

Figure 19 Simplified head interpolation used to assigned the initial heads to the model

The above interpolation assumes spatial continuity of the potentiometric surface. Given the geological structure of the island, this is just a rough approximation used to assign the initial heads to the model. It surely has no bearing on reality, nevertheless it can be used to do preliminary water budget calculations.

The natural groundwater discharge towards the sea can be estimated with the Darcy law, as:

$$Q = TLi$$

where:
Q = aquifer discharge,
T = aquifer transmissivity,
L = considered length of the discharge section,
i = hydraulic gradient.

The island can be divided into sectors according to the hydraulic gradient variation. For each sector it is possible to calculate the length of the section L, the hydraulic gradient *i* according to the reconstructed piezometry (Figure 19), the transmissivity T according to the available pumping tests results shown in Figure 15 (considering the average value of the points upgradient of the closing section).

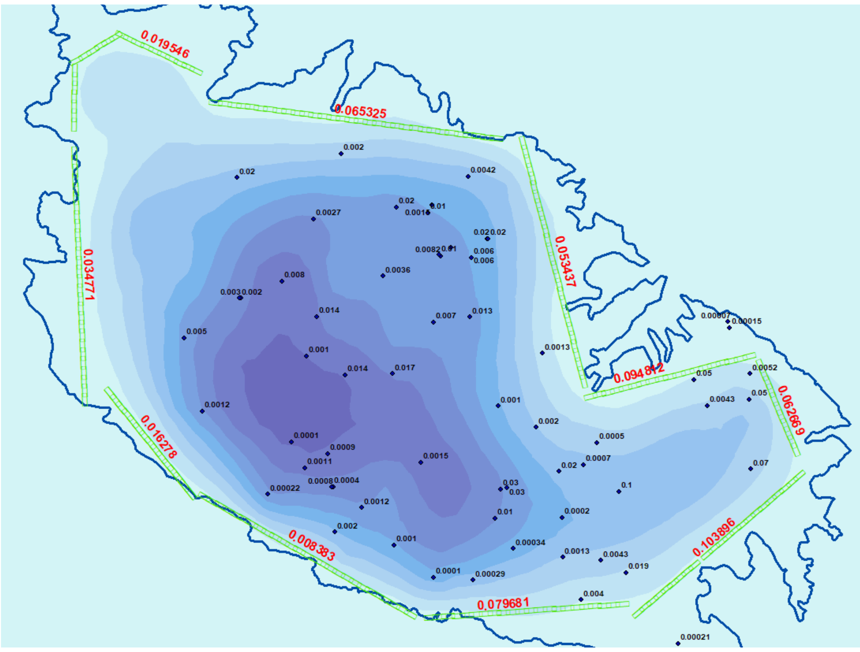

Figure 20 Closing sections of different sectors of the island, with values of transmissivity in m2/s for each point and estimated outflows in m3/s.

This preliminary estimate of the natural freshwater outflow towards the sea is based on hydrogeological data (hydraulic gradients and transmissivities), and it is independent by the amount of recharge. Table 17 reports the outflows for each sector, with a total aquifer discharge of 0.54 m^3/s.

ID	Section Length [m]	Hydraulic gradient	Average transmissivity [m^2/s]	Aquifer discharge [m^3/s]
1	7764	0.000975	0.008629	0.0653
2	6831	0.000833	0.00938	0.0534
3	4616	0.000800	0.02567	0.0948
4	2627	0.000929	0.025674	0.0627
5	5935	0.000682	0.02567	0.1039
6	5462	0.001045	0.013953	0.0797
7	6577	0.0013823	0.000922	0.0084
8	6862	0.0006667	0.0076	0.0348
9	3675	0.0014286	0.0031	0.0163
10	5692	0.0001716	0.0200	0.0196
			Total estimated aquifer discharge toward the sea	0.5389
			m^3/y	16994750

Table 17 Indirect estimate of the aquifer discharge towards the sea, based on the 1944 heads interpolation.

This outflow can be compared to the inflows of the aquifer (Table 18). The inflows taken as reference are those calculated by Thornthwaite, similar to the BRGM results but independently obtained with a different approach, where the recharge obtained was 116 mm/y.

Balance term over the MSLA surface (216.6 km^2)	m^3/s	mm/y
Infiltration (aquifer recharge)	0.797	116
Natural outflow towards the seaside (calculated as in-out terms, no abstractions are present)	0.797	116
1944 Outflow towards the seaside (calculated according to Darcy and based on the average available values of transmissivity)	0.540	79
Natural outflow – 1944 outflow	**0.257**	**37**

Table 18. Natural inflow and outflow calculated for Malta MSLA.

Even if the above calculation presents consistent margins of error, it is evident from the potentiometric map that pumping from MSLA should be present in the reference period. A rough estimate might be the difference from the natural average outflow and the one calculated according to the potentiometric surface, giving a volume equal to 0.257 m^3/s. This amount is comparable with the declared water abstraction over the MSLA (0.252 m^3/s).

Model calibration

Highly Parametrized Methods

Highly parameterized (HP) groundwater models are characterized by having more parameters than those that can be estimated uniquely on the basis of a given calibration dataset, having more parameters than observations. Such models are commonly referred to as "ill posed." Ill-posed models require an approach to model calibration and uncertainty different from the traditional methods typically used with well-posed models (Hill and Tiedeman, 2007). Regularized inversion has been suggested as one means of obtaining a unique calibration from the fundamentally nonunique, highly parameterized family of calibrated models. "Regularization" simply refers to approaches that make ill-posed problems mathematically tractable; "inversion" refers to the automated parameter-estimation operations that use measurements to constrain model input parameters (Hunt et al., 2007).

Regularized inversion problems are most commonly addressed by use of the Parameter ESTimation code PEST (Doherty, 2015). PEST is an open-source, public-domain software suite that allows model-independent parameter estimation and parameter/predictive-uncertainty analysis, accompanied by two supplementary software suites for calibration of groundwater and surface-water models (Doherty, 2007, 2008).

The optimal number of parameters needed for a representative model is often not clear, and in many ways model complexity is ultimately determined by the objectives that the model is asked to achieve. However, benefits of regularized inversion include greater parameter flexibility than the parameter-simplification strategies of zonation. This flexibility helps the modeler extract information contained in a calibration dataset during the calibration process, whereas regularization algorithms allow the modeler to control the degree of parameter variation. Indeed, high numbers of parameters used in calibration can collapse to relatively homogeneous optimal parameter fields (as described by, for example, Muffels, 2008). Thus, the twin ideals of parsimony—simple as possible but not simpler—are fully met.

Pilot Points and Groundwater-Model Calibration

The use of pilot points as a spatial parameterization device in groundwater-model calibration is becoming commonplace. Pilot points can be useful for any model parameter or boundary condition, but are most commonly applied to aquifer hydraulic conductivity. Early uses include those of de Marsily and others (1984), Certes and de Marsily (1991), and LaVenue and Pickens (1992) and were extended by RamaRao and others (1995), LaVenue and others (1995), and LaVenue and de Marsily (2001). The latter authors combined the use of pilot points with a methodology for optimal selection of pilot-point locations. They also developed a methodology for using pilot points in conjunction with stochastic fields to derive multiple hydraulic-property distributions that on one hand calibrate a model, while on the other hand respect the geostatistical characterization of a study area. Use of multiple field realizations in making model predictions allows the exploration of estimates of the uncertainty associated with these predictions.

Doherty (2003) used pilot points in the context of highly parametrized model calibration. In such problems, uniqueness in solution of the inverse problem is achieved through the use of mathematical regularization. Regularization is a general class of methods that provides stability and uniqueness to calibrating underdetermined models by adding constraints of structure or a preferred condition to the parameters being estimated (see, for example, Hunt and others 2007). While regularization is a necessary component of this extension of pilot points to underdetermined problems, regularization has been used in many other contexts for a much longer time (see, for example, Tikhonov and Arsenin, 1977 and Tarantola, 2005). For general information about regularization, Menke (1984) and Aster et al. (2005) provide introductory discussions.

The use of pilot points in highly parametrized context marked a departure from conventional pilot-point usage, allowing pilot points to be distributed throughout a model domain. Parsimony is achieved by restricting the infinite possible number of solutions in an underdetermined problem only to include solutions:

(1) Which respect the information provided by the data (hard knowledge),
(2) that are consistent with the general (soft) knowledge of the site.

The use of many pilot points in regularized inversion contexts has led to the development of new methodologies for exploration of calibration-constrained model predictive uncertainty analysis. Not only can the uncertainty of key model predictions be estimated through such an analysis, but contributions to that uncertainty by different parameter groups also can be determined. The efficacy of different observation types in reducing that uncertainty also can be established, constituting a valid support in monitoring planning.

MSLA model steady state calibration

The MSLA model underwent a long process of calibration which included several major revisions of the model structure and extension, besides variation of parameters and boundary conditions. The different versions tested, the relative main assumptions and settings are detailed in Appendix 1 and 2.

After a first calibration through zones of hydraulic conductivity, the HP approach was applied in the last model versions. The properties and boundary conditions which were included in the calibration as *parameters* were:

1. Aquifer hydraulic conductivity, varied in pilot points whose interpolation is spatially delimited by faults;
2. Hydraulic conductivity of faults, uniform along each fault;
3. Model bottom, varied by hand as a constant thickness of the saturated aquifer.

Recharge was not modified at this stage, though quite uncertain.

The measurements taken in 1944 and used as calibration dataset of the steady state model are reported in Table 16, being the same heads used to build the starting head distribution (Figure 19). The observation points in the model are shown in Figure 21. Besides the head observations, prior parameter information was introduced in order to make the inverse model mathematically tractable. *Prior information* equations were defined for each pilot point, for example, as follows:

$$\text{i1k}_i \qquad 1.0 * log(\text{Kppp}_i) = x \qquad 1.0 \qquad \text{regul\_kp1}$$

where:

- ilk_i = name of the i^{th} equation;
- Kppp_i = name of the i^{th} PP;
- x = preferred value of PP
- 1.0 = weight;

- regul_kp1 = observation group name.

The preferred value of hydraulic conductivity associated to each PP was taken from the log-transformation of the initial parameter distribution shown in Figure 16, according to the PP position (Figure 22). The preferred value is respected only if in agreement with the weighted head observations. If the quality of data is low (small weights), the parameter will tend to respect the preferred value; if the quality of data is good, the preferred value will be considered only in portions of the model domain where observations are not available.

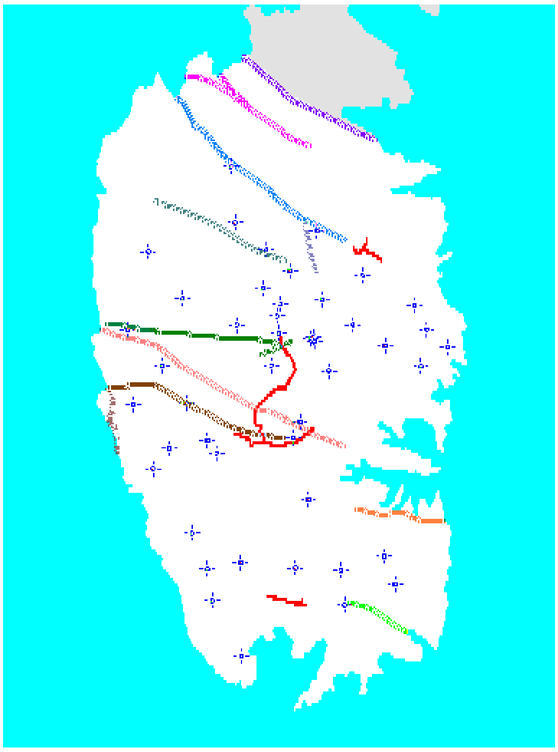

Figure 21 Observation points of head in 1944.

The different colours of the HBF BC (Figure 21) used to reproduce the aquifer discontinuities generated by the faults, define the length in which uniform properties are assumed along the 11 main faults. The northern Pwales fault was assigned a hydraulic conductivity of 1E-8 m/s which was not varied; the other 10 were calibrated starting from the same value, assuming that all the faults have a low permeability. The position of the 185 pilot points used as prior information and as parameters to calibrate the aquifer hydraulic conductivity are shown in Figure 22, together with the spatial barriers of their interpolation (zones with different colours).

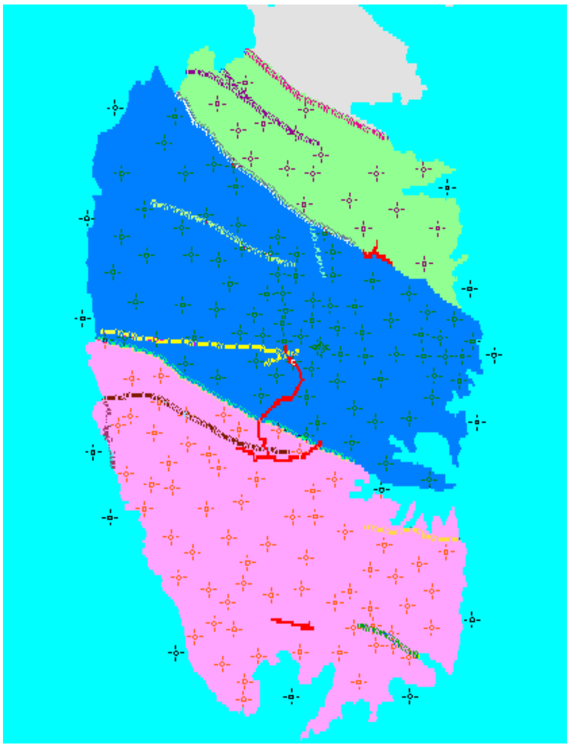

Figure 22 Position of the hydraulic conductivity PP

Results

Calibration results are reported for one version of the model (v40, Appendix 1), specifically the one which will be used as a starting point for the transient calibration. Results are given in terms of parameter sensitivities, water budget, hydraulic conductivity distribution, observed-simulated heads residuals statistics and the obtained hydraulic head distribution. The calibrated model was then used in conjunction with SWI2 (Bakker et al., 2013) to reproduce a preliminary seawater interface, as described in hereafter.

Sensitivities, linearity test and calibrated parameters

Sensitivity analysis considered the same parameters included in calibration, i.e. hydraulic conductivity of 185 pilot points and 10 main faults (HFB BC). Composite sensitivities of K pilot points are reported in Figure 23. The position of PP with higher sensitivities are located along the Victoria fault and Maghlaq fault (Figure 24). This might indicate areas with important control over groundwater outflows, which can be limited or helped according to variations of K. The spatial distribution of the hydraulic conductivity field obtained in the steady state calibration is shown in Figure 25. All PP calibrated values and their composite sensitivities are detailed in Annex 3.

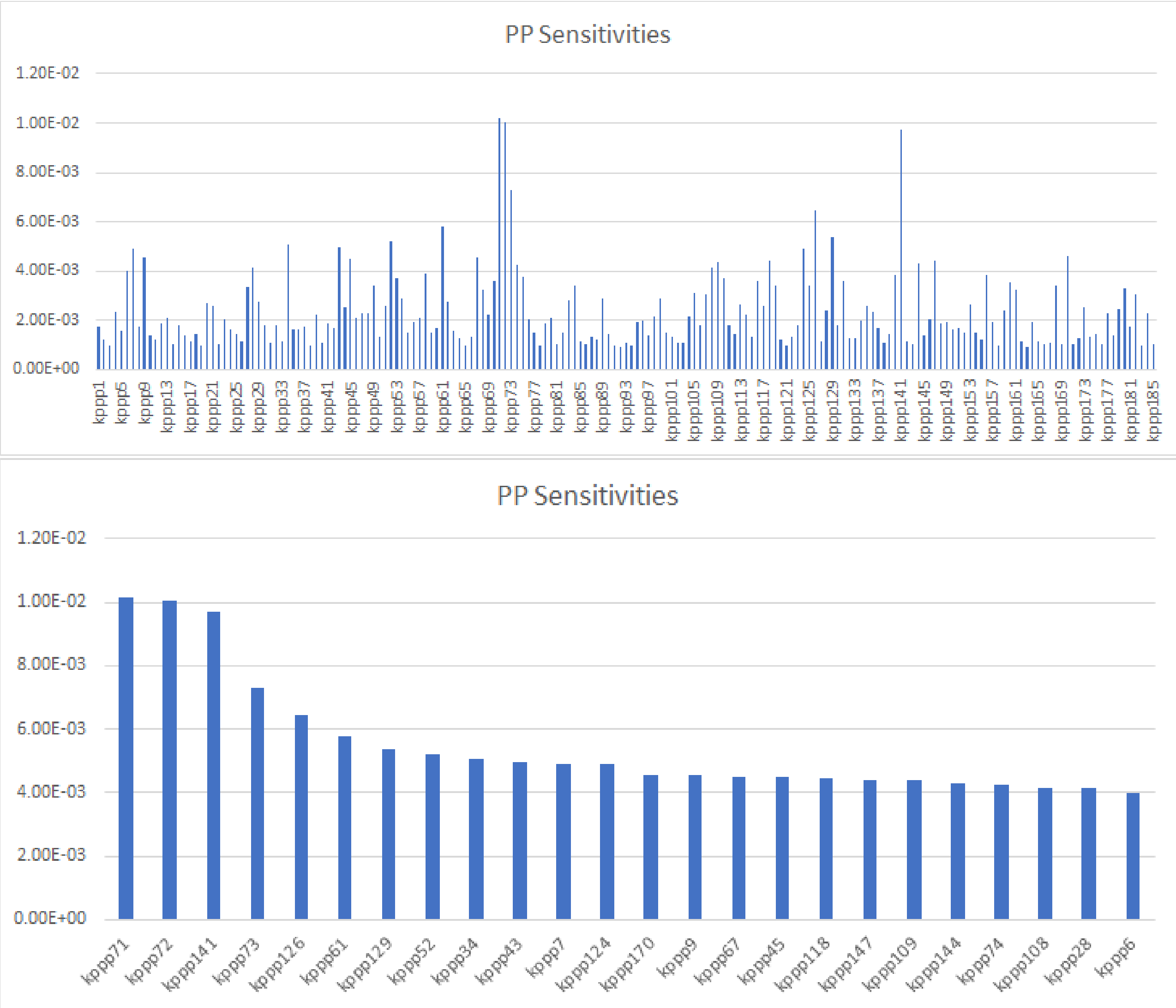

Figure 23. Pilot points composite sensitivities.

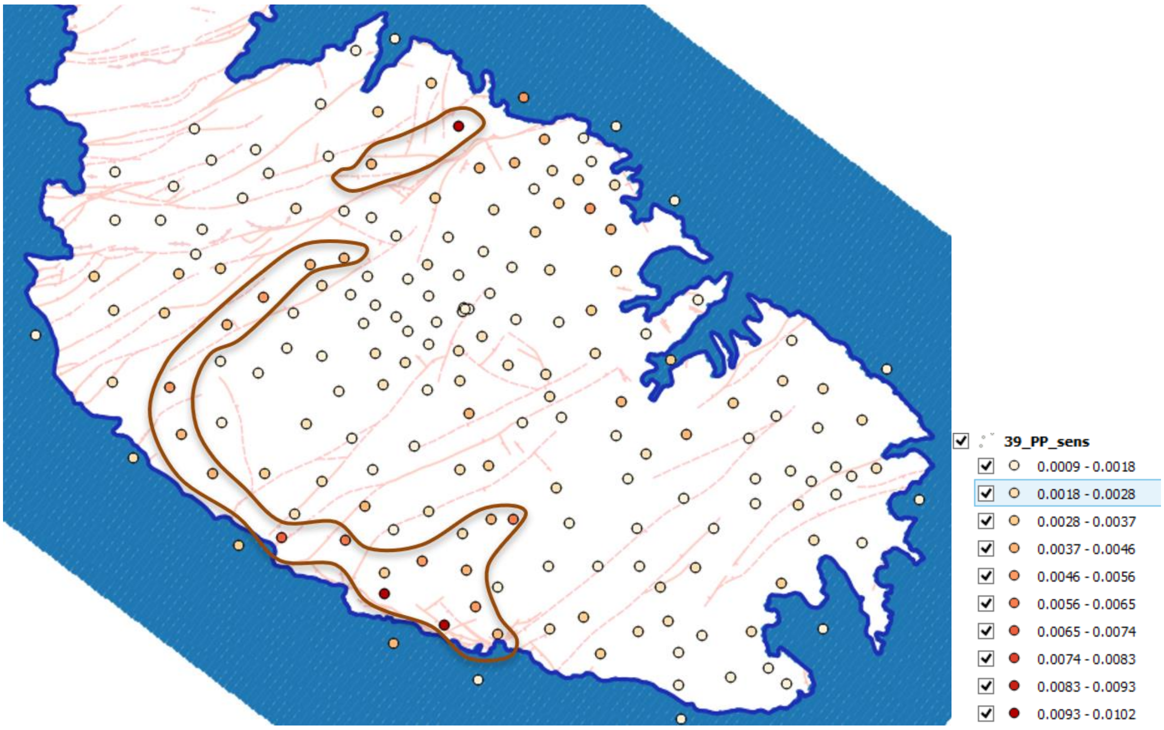

Figure 24. Map of pilot point sensitivities; higher values are highlighted.

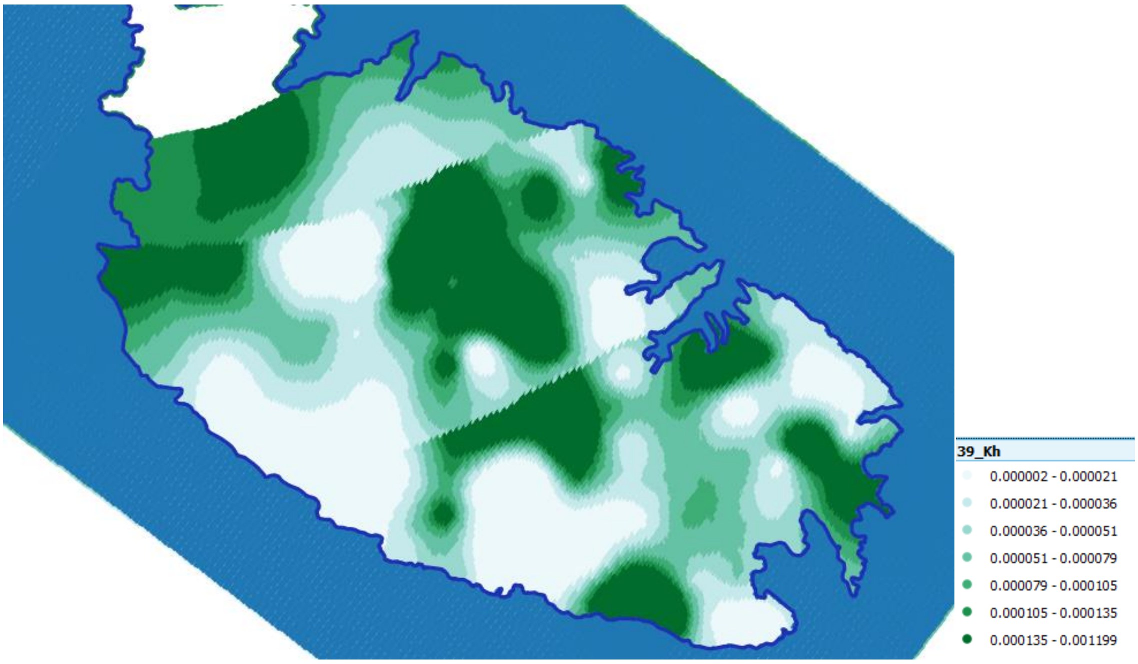

Figure 25. Hydraulic conductivity field obtained in calibration of v40.

In Table 19, sensitivities and values of the HFB BC are reported, assigned as shown in Figure 26. The highest value of sensitivity is associated to hfb2 (Victoria fault), followed by hfb5 and hfb6. Hydraulic conductivity values remained low, with the exception of Maghlaq fault (hfb8) which turned to be higher than 1E-5 m/s.

Name	Group	Value (m/s)	Composite sensitivity
hfb1	hfb	1.30E-09	4.89E-04
hfb2	hfb	1.94E-08	2.07E-02
hfb3	hfb	3.18E-07	6.85E-03
hfb4	hfb	3.15E-10	2.15E-04
hfb5	hfb	8.45E-09	1.11E-02
hfb6	hfb	1.00E-10	1.10E-02
hfb7	hfb	1.75E-09	2.38E-03
hfb8	hfb	2.20E-05	8.56E-04
hfb9	hfb	1.49E-09	2.34E-04
hfb10	hfb	1.00E-10	4.01E-04

Table 19. Values and sensitivities of the faults represented in the model.

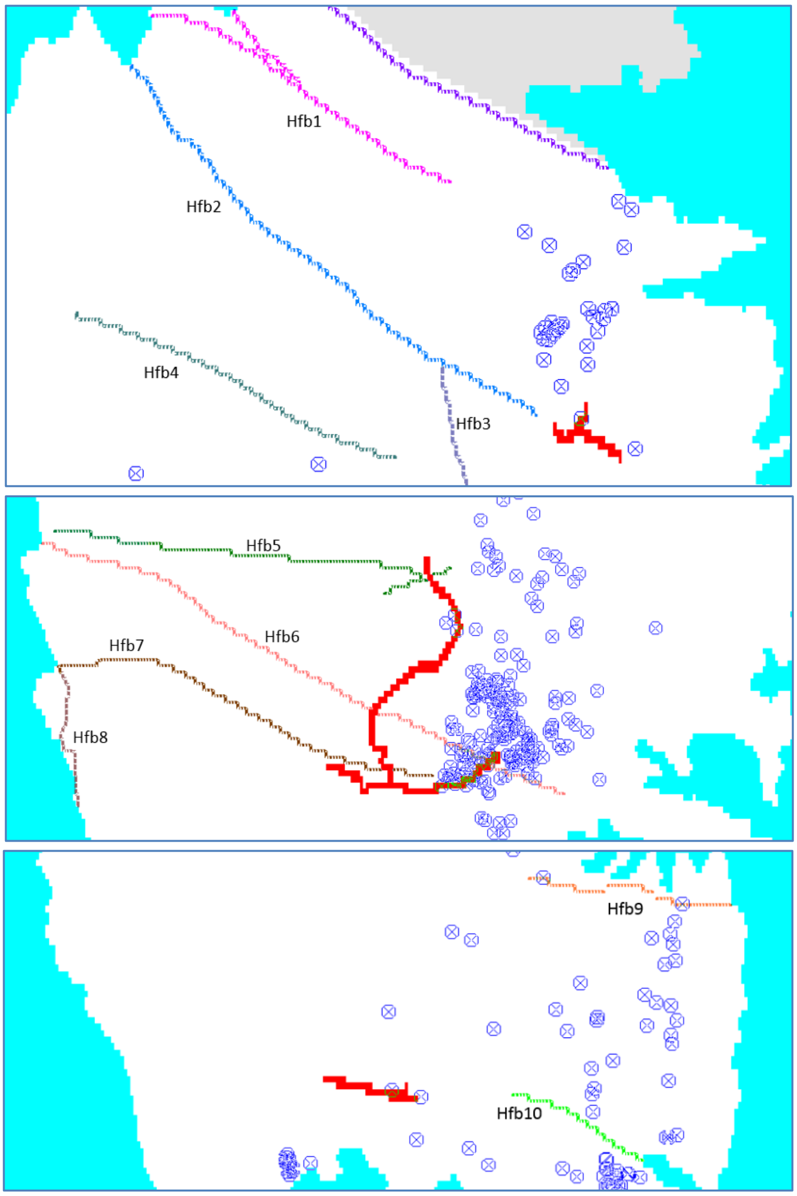

Figure 26. Positions and names of the the faults represented in the model.

Model linearity and numerical integrity was also tested plotting the observation variation *vs* parameter change. The model was run 150 times monitoring the response of observation changing 2 parameters: pilot point Kppp72 (nearby Maghlaq fault) and hfb2 (Victoria fault) (Figure 27). Results are shown in Figure 28 and Figure 29, where a nonlinear response can be noticed (the head curves are not straight lines). Nonlinearity comes with model complexity and it may also reflect contamination of finite-difference derivatives by numerical noise; this would cause a jagged plot rather than smoothly curved. In MSLA model numerical integrity does not seem to be affected by evident numerical noise.

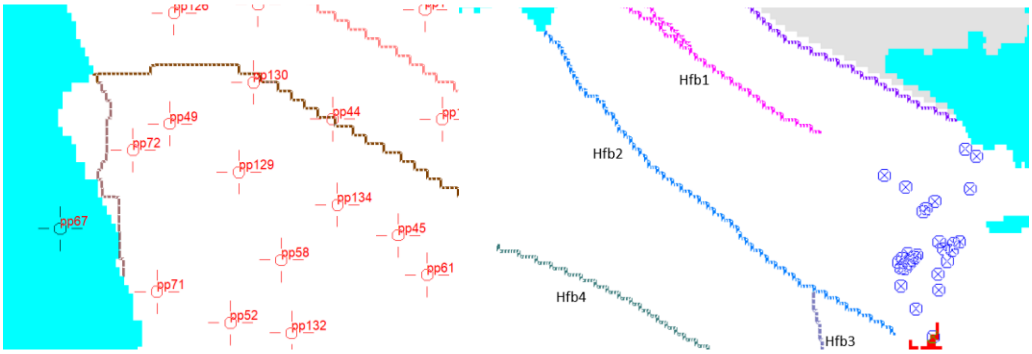

Figure 27. Position of the 2 parameters used to test model linearity and numerical noise.

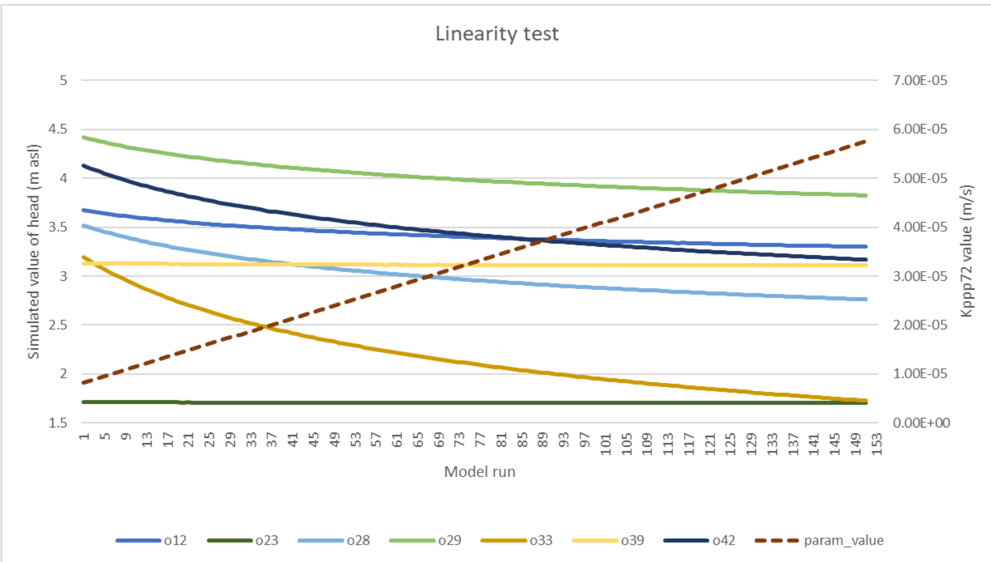

Figure 28. Linearity test for Kppp172.

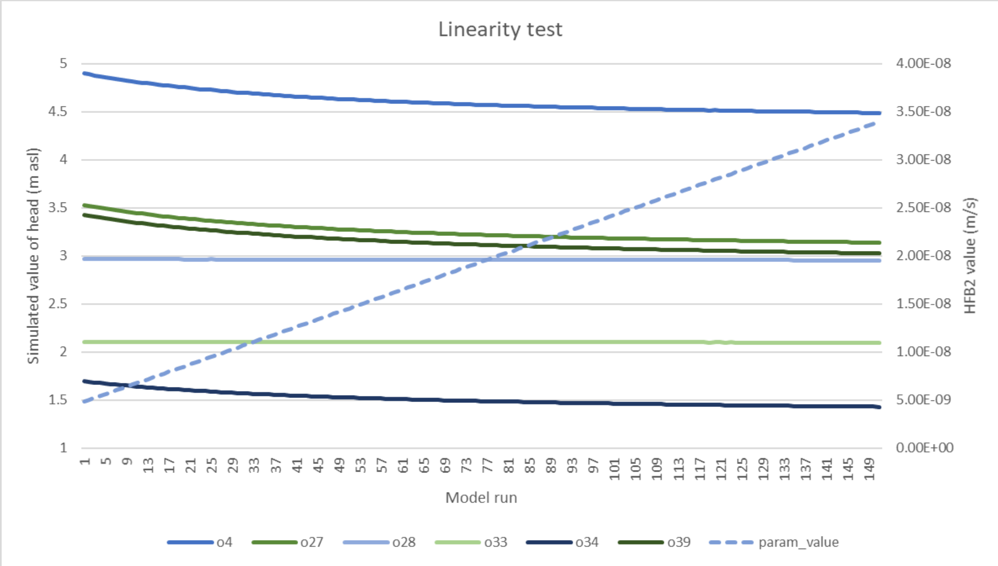

Figure 29. Linearity test for HFB2.

Water budget and head distribution

Numerical stability of the model is confirmed by the low water budget discrepancy, which is less than 0.0005%. The terms of the budget obtained in the steady state of the model are shown in m^3/s and m^3/y in Table 20. The small inflow from the sea is due to pumping nearby the coast, neglecting any effect of density-dependent flow at this stage.

	INFLOWS	OUTFLOWS		
Storage	0	0	OLF X min	0
X min	0	0	OLF X max	0
X max	0	0	OLF Y min	0
Y min	0	0	OLF Y max	0
Y max	0	0	GW to OLF	0
Top	0	0	OLF to GW	0
Bottom	0	0	OLF CH	0
Well	0	0.251668279097203	OLF Source-Sink	0
C.H.	0	0	Special Boundary	0
GHB	0.00147408500452106	0.545913066676298	OLF Recharge	0
River	0	0	OLF Evap.	0
Drain	0	0	Interception Storage	0
Stream	0	0	Precipitation	0
Recharge	0.796103400382977	0	Evp. Canopy	0
ET	0	0	Recharge to Ground	0
Lake	0	0	Total PET Possible	0
			Percent Error	
TOTAL	0.797577485387498	0.797581345773501	-0.000484012742514842	

(terms in m^3/s)

Water balance (1944)	
Inflows	
Sea (GHB) (m^3/y)	46487
Recharge (m^3/y)	25105917
Active Area (km^2)	216.6
Recharge (mm/y)	116
Outflows	
Wells (pumping station, public boreholes and private wells) (m^3/y)	7936602
Sea (GHB) (m^3/y)	17215912

Table 20. Model water balance output.

The hydraulic head resulting from the steady state model and reproducing the 1944 situation is shown in Figure 30. It is evident how the structural control over the groundwater flow is dominant.

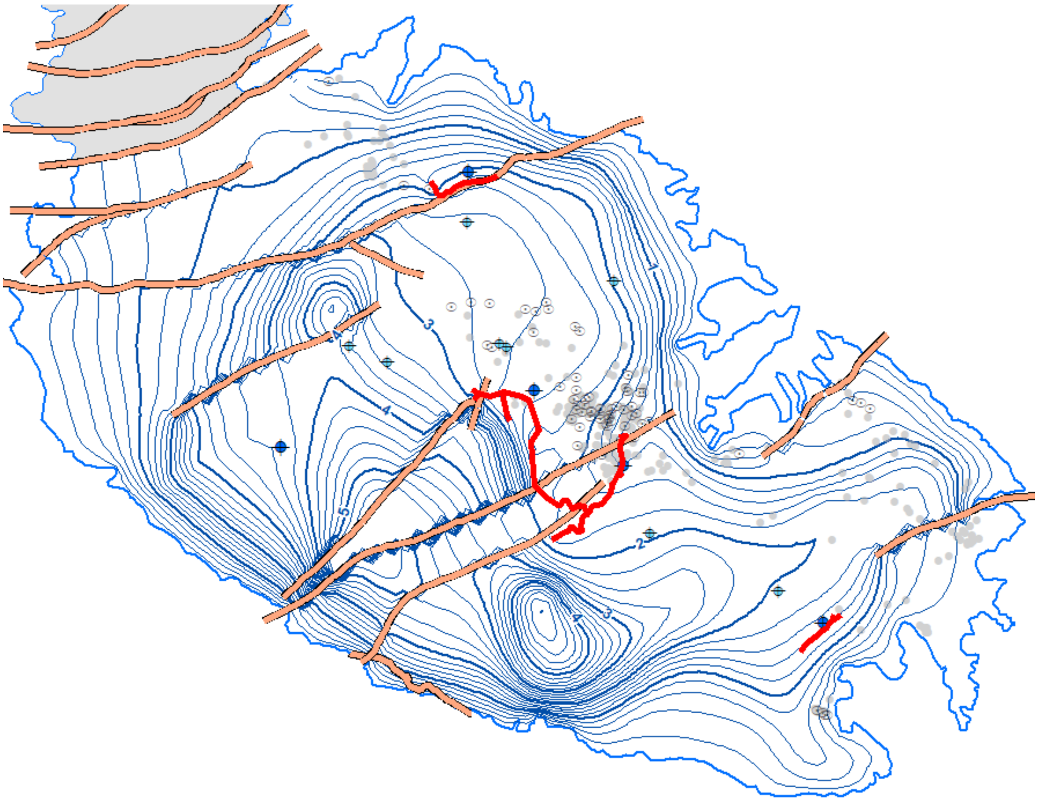

Figure 30. Model hydraulic heads output.

Residuals

Residual derived from the comparison of the calibration dataset with the simulated heads are reported in Figure 31 and Table 21. Calculated statistics of residuals and the scatter plot (Table 22) show a good agreement, even if calibration might be affected by overfitting, given the uncertainty of the original data and the RMSE of the heads interpolation: calibration RMSE is 0.2 m, while the interpolation RMSE is 0.43 m (Figure 18).

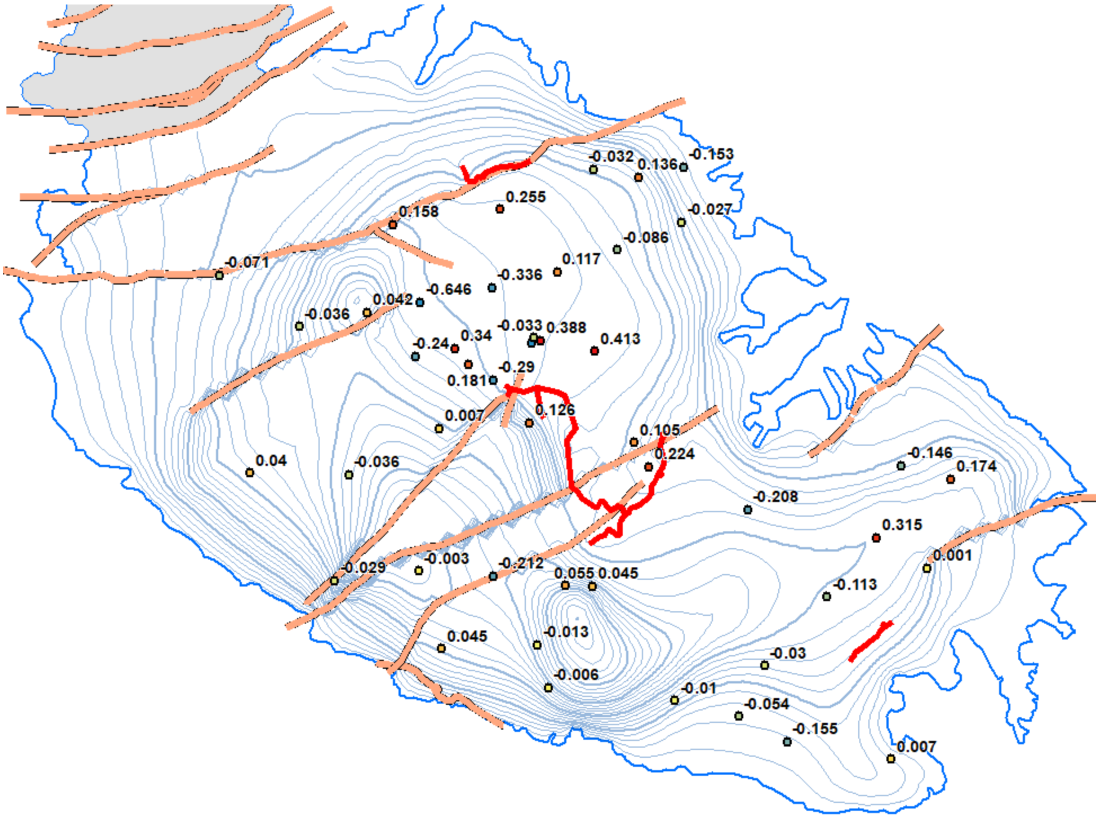

Figure 31 Map of residuals.

Name	Group	Measured	Modelled	Residual
o1	head1	1.8	1.912676	-0.11268
o2	head1	2.9	2.487464	0.412536
o3	head1	3	2.612104	0.387896
o4	head1	4.6	4.557529	4.25E-02
o5	head1	2	1.894637	0.105363
o6	head1	2.3	1.985373	0.314627
o7	head1	1.3	1.299098	9.02E-04
o8	head1	1	1.145995	-0.146
o9	head1	1.9	1.726149	0.173851
o10	head1	3.4	3.116279	0.283721
o11	head1	2.9	2.644798	0.255202
o12	head1	3.3	3.303211	-3.21E-03
o13	head1	2.2	2.286206	-8.62E-02
o14	head1	0.1	0.252953	-0.15295

Name	Group	Measured	Modelled	Residual
o15	head1	2.1	2.648309	-0.54831
o16	head1	3.2	3.159764	4.02E-02
o17	head1	3.3	3.119274	0.180726
o18	head1	0.9	0.926936	-2.69E-02
o19	head1	1.7	1.475865	0.224135
o20	head1	3.1	3.340107	-0.24011
o21	head1	2.7	2.989797	-0.2898
o22	head1	2.6	2.633333	-3.33E-02
o23	head1	1.8	1.663834	0.136166
o24	head1	2.8	2.683496	0.116504
o25	head1	2.5	2.836064	-0.33606
o26	head1	2.4	3.046237	-0.64624
o27	head1	3.2	3.235688	-3.57E-02
o28	head1	2.6	2.812039	-0.21204
o29	head1	3.9	3.844797	5.52E-02
o30	head1	4.1	4.093371	6.63E-03
o31	head1	3.6	3.628576	-2.86E-02
o32	head1	1.5	1.70781	-0.20781
o33	head1	2.1	2.055468	4.45E-02
o34	head1	1.4	1.470879	-7.09E-02
o35	head1	3.6	3.474148	0.125852
o36	head1	2.7	2.705907	-5.91E-03
o37	head1	1.9	1.931884	-3.19E-02
o38	head1	1.2	1.210336	-1.03E-02
o39	head1	3.2	3.041673	0.158327
o40	head1	1.4	1.430145	-3.01E-02
o41	head1	4.3	4.336118	-3.61E-02
o42	head1	3.3	3.312576	-1.26E-02
o43	head1	0.2	0.355475	-0.15548
o44	head1	0.4	0.393045	6.96E-03
o45	head1	3.4	3.355186	4.48E-02

Name	Group	Measured	Modelled	Residual
o46	head1	0.4	0.454346	-5.43E-02

Table 21. Residuals.

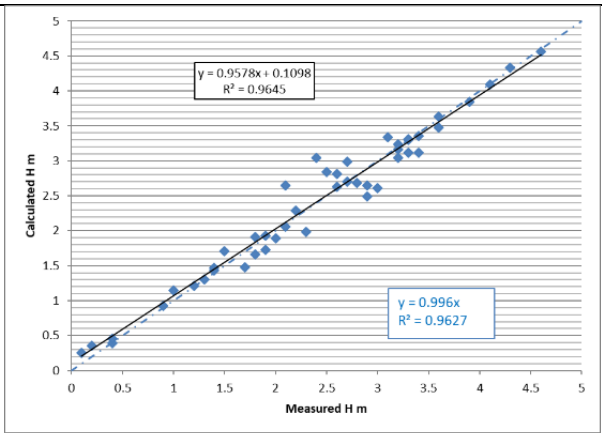

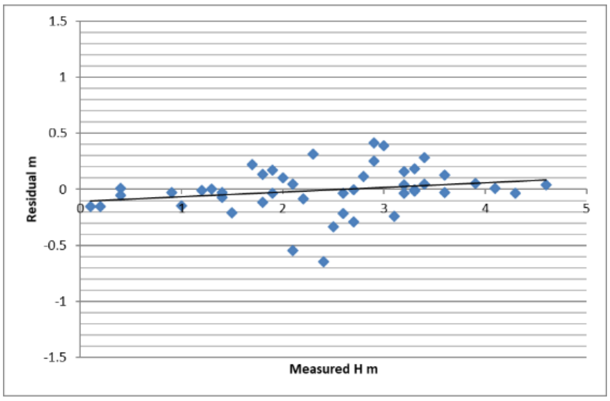

Descriptor	Unit	Value
N		46
Min	m	-0.646
Max	m	0.412
Mean	m	-0.0086
Std. error	m	0.031
Variance	m^2	0.043
Stand. dev	m	0.207
RMSE	m	0.205
Kriging RMSE	*m*	*0.46*

Table 22. Scatter plot and residuals statistics.

As previously explained, additional "parameter observations" were added to the calibration process (one for each PP) in order to make the inverse problem solvable. The weight assigned to the prior information was iteratively adjusted along the calibration process, finally obtaining a weight of 0.2 for the log-transformed hydraulic conductivities. This weight represents a compromise between respecting the head data, while trying to limit the overfitting with advantage of the parameter preferred value coherence. The full scatter plot which includes both heads observations and prior information is shown in Figure 32 and the complete table of residuals is reported in Appendix 3, resulting in a prior information RMSE equal to 2E-4 m/s if values are back-transformed.

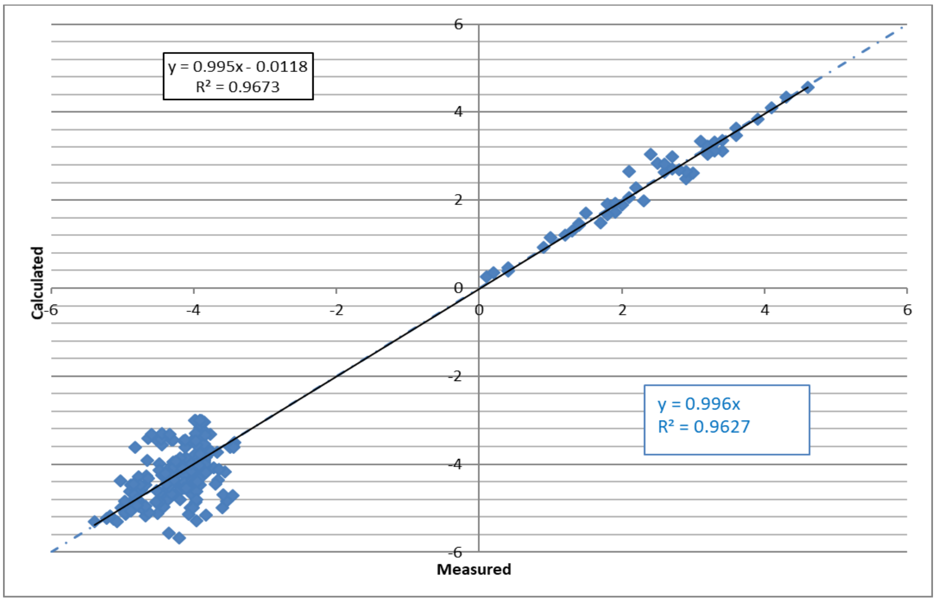

Figure 32. Scatter plot of head observations and prior information.

Mizieb and Pwales aquifers

Introduction

The conceptual models of Mizieb and Pwales aquifers are described in the Deliverable D1.3. They are separated one each other by a low conductivity fault, and are separated from the MSLA by Pwales fault, assumed to be perfectly impermeable. Elevations of top and bottom of the two aquifers allows to include them into a unique model, even if hydrogeological behavior is quite different. In both cases measured data are scarce or absent, with consequent difficulties in building a reliable conceptual model that could pass the numerical test.

The main issues approached (and not solved yet) are:

1. Mizieb: it is not clear which is the natural outflow of the aquifer; the basin seems to be close or with little exchange with the outside – but this would imply an increasing concentration in time of solutes such as nitrates, salty rainfall etc. Costain (1958) reports that there is a leakage towards the bottom through three sinkholes crossing the Blue Clay; this hypothesis has been tested. A second hypothesis of way out can be what is called the “fault breccia” in Costain, along the northern fault.
2. Mizieb: Seawater intrusion should not be an issue, but recent time series of chloride concentration show some abrupt increases. It is not clear if the supposed way out (sinkholes and breccia fault) could turn into a “way in” depending on the vertical hydraulic gradient between the aquifer and the sea level.
3. Pwales: the aquifer is affected by lateral seawater intrusion because of the low depth of the aquifer bottom (top of Blue Clay). In this specific case the bottom elevation and geometry is the dominant factor controlling seawater ingression under the pumping conditions. Information is very scarce with respect to the stratigraphy and to the water abstraction. This portion of the model has no data to be constrained by history matching; parameter adjustments have been based on supposed cautionary hydrogeological properties, but results could be totally wrong and misleading.

Domain and discretization

The Mizieb-Pwales (MP) model grid covers an area of about 15 km^2, divided into 47616 cells with dimension 12.5x25 m, rotated by 15.5 degree (Figure 33). The Mizieb aquifer surface occupies 16000 cells, Pwales 8350, the sea 3200 cells, while the southern and western portions of the domain are limited by low conductivity formations, assuming that groundwater exchanges are extremely scarce in those directions.

The model is single-layer, with a variable thickness. The bottom elevation of the model was set according to the stratigraphic interpretation of the Blue Clay top, nevertheless the bottom surface needed to be smoothed in order to control numerical instability. The original and the smoothed bottom surfaces are shown in Figure 34.

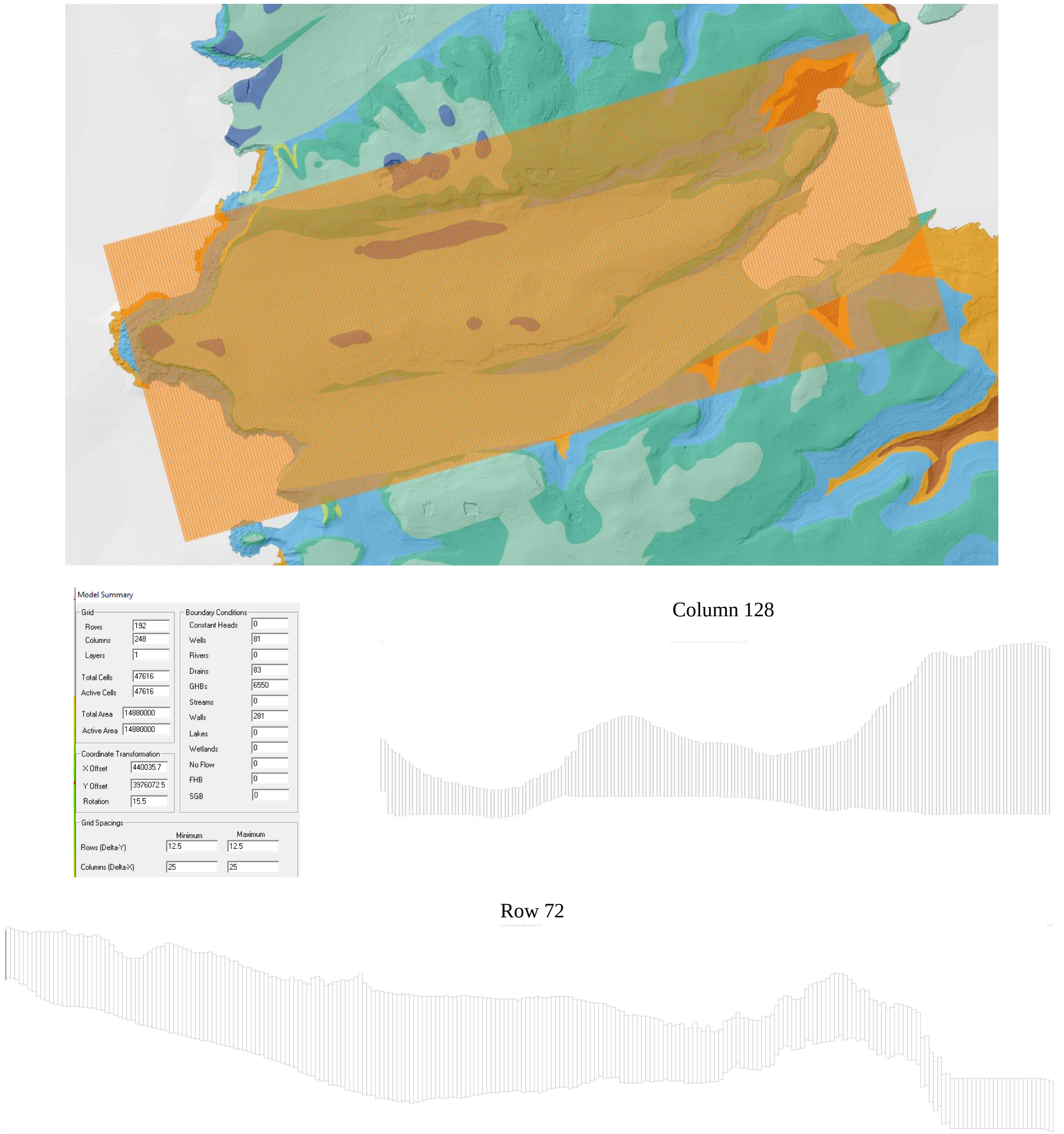

Figure 33. MP model grid.

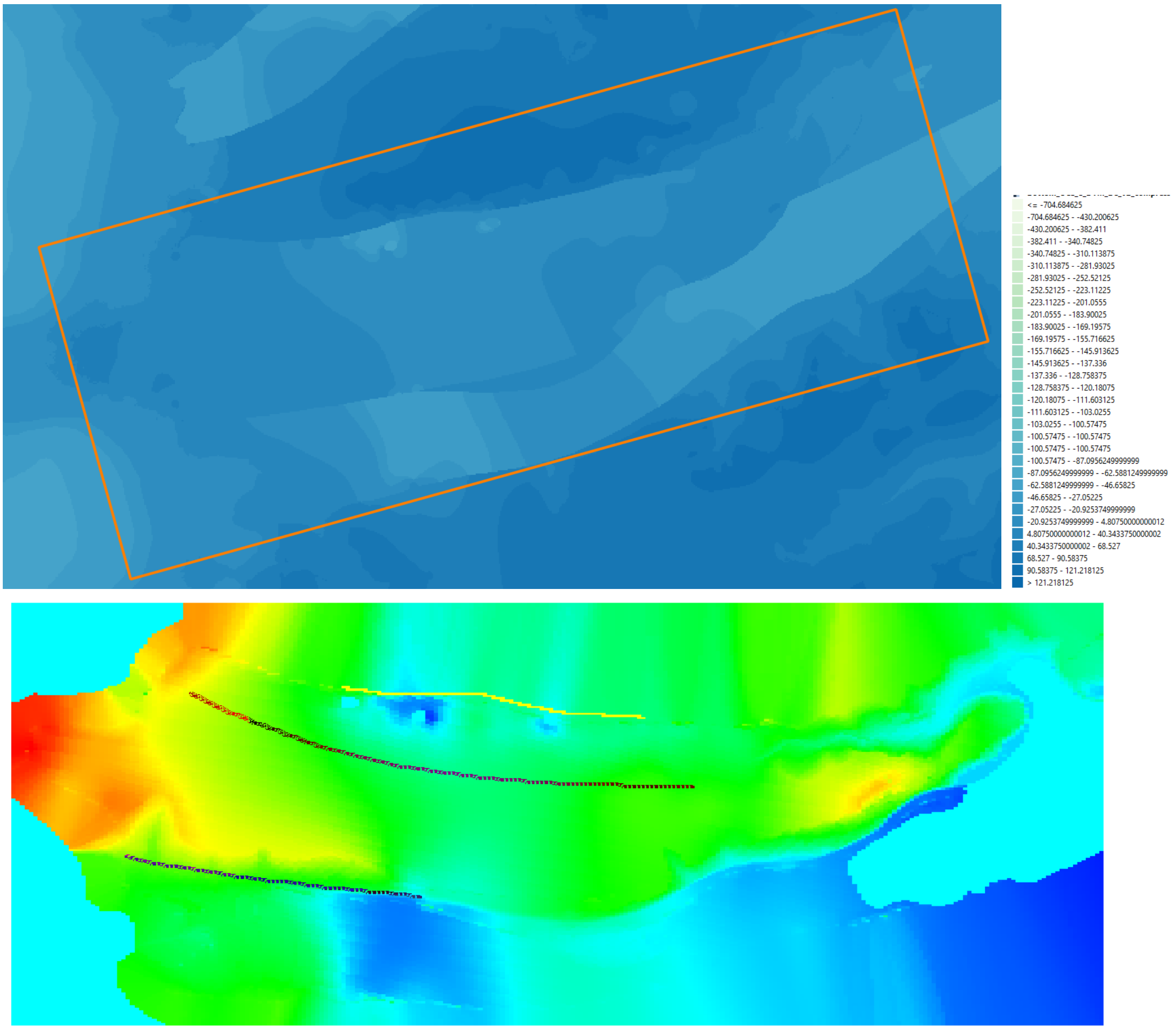

Figure 34. MP reconstructed and smoothed model bottom surface.

Boundary condition

The definition of boundary condition in the MP model was quite challenging, different settings were tried according to different conceptual models, leading to a preliminary (and probably wrong) configuration which presently includes (Figure 35):

1. General head boundary (GHB) to represent the sea, characterized by head elevation = 0 m asl;
2. General head boundary (GHB) to represent the sinkholes at the aquifer bottom in Mizieb, characterized by head elevation = 0 m asl and conductance which was varied in the preliminary adjustment process;
3. Hydraulic flow barrier (HFB) to represent the main faults discontinuities with an initial low hydraulic conductivity (1E-8 m/s);
4. Drain boundary to represent a possible outflow from the aquifer along the northern breccia fault, characterized by head elevation = 0 m asl and conductance which was varied in the preliminary adjustment process;

5. Wells (WELL) to represent the 81 private wells that were active during the period of reference (1944-45) characterized by an estimated average discharge of about 10000 m^3/y each.

The main issue encountered in boundary conditions setting was the numerical instability of the model; the peculiar geometry of Mizieb aquifer, the presence of dry areas, low permeability zones, faults and sinkholes concurred to produce a high numerical noise, as it will be discussed in later in the text. The compromises applied to the present model version (MP_3 v5) allowed to obtain numerical stability.

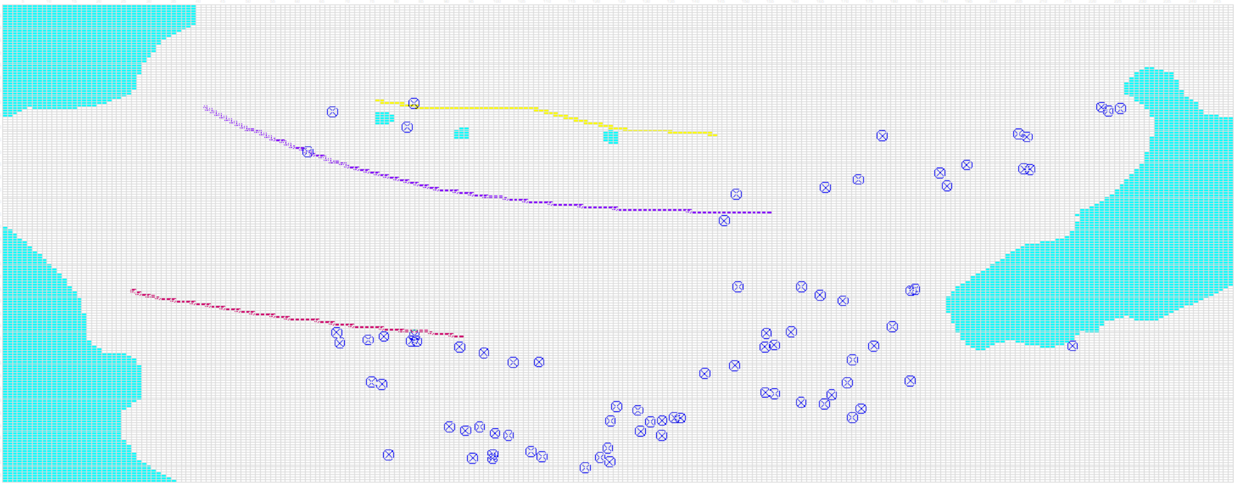

Figure 35. MP boundary conditions of MP_3 v5.

Initial properties and heads

Initial hydraulic conductivity values were assigned on the basis of results obtained in the MSLA model calibration and preliminarily adjusting the values using uniform zones (Figure 36).

The "idea" of a possible potentiometric surface (to be used as a qualitative control) was taken from the work of Constain (1958) that reports some hydraulic head elevations measured in different months between 1957 and 1958 during the Mgarr gallery works (started in 1957 and completed in 1962). Available heads and their position are shown in Table 23 and Figure 37.

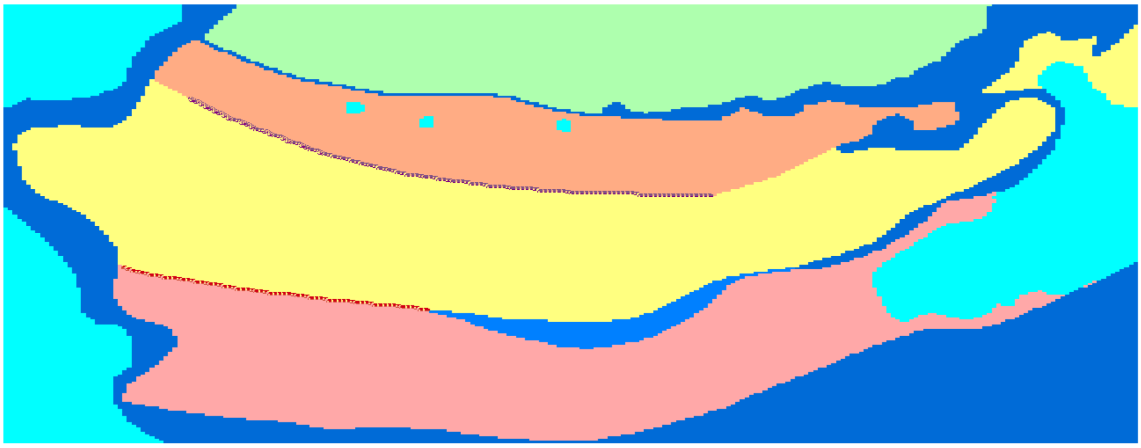

	Kx	Ky	Kz	Color
1	0.0005	0.0005	5e-005	
2	5e-006	5e-006	5e-007	
3	0.0005	0.0005	5e-005	
4	1e-006	1e-006	1e-007	
5	1e-006	1e-006	1e-007	
6	0.001	0.0001	0.0001	

Figure 36. Initial hydraulic conductivity distribution.

ID	X	Y	Ground elevation (m asl)	Borehole depth (m)	Depth to water (m)	Water head (m asl)	Date
10000	441798.8	3978405	48.768	45.72	dry	dry	Apr_1958
10001	442381	3978360	43.5864	54.864	40.8432	2.7432	Jun_1958
10002	442713.5	3978480	47.8536	62.1792	45.1104	2.7432	Jun_1958
10003	443200.9	3978559	37.4904	41.148	32.004	5.4864	Jun_1958
10004	443957.2	3978888	28.6512	30.7848	16.4592	12.192	Jun_1958
10005	442118.7	3978458	51.5112	58.5216	46.9392	4.572	Apr_1958
10006	443357.5	3978645	37.7952	42.672	dry	dry	Jun_1958
10007	443515.7	3978733	43.2816	49.3776	38.4048	4.8768	Jun_1958
10008	441799.2	3978381	46.9392	50.292	43.2816	3.6576	May_1958
10009	441800	3978368	46.6344	58.2168	43.2816	3.3528	May_1958
1074	442532.6	3978601	66.7512	78.0288	59.1312	7.62	Sept_1957
1075	442525.7	3978568	58.5216	83.82	55.4736	3.048	Sept_1957
1076	442533.1	3978537	53.6448	99.6696	49.9872	3.6576	Oct_1957
1078	442490.8	3978553	57.3024	86.5632	54.2544	3.048	Nov_1957
1079	442538.9	3978477	45.72	68.8848	42.3672	3.3528	Nov_1957
1090	441364.7	3978339	52.1208	70.104	48.1584	3.9624	Nov_1957
1096	441321.4	3978110	44.8056	44.8056	33.8328	10.9728	Jun_1958
1097	441278.2	3978273	47.8536	51.816	39.0144	8.8392	Jun_1958
1098	441629.2	3978168	44.5008	53.0352	39.3192	5.1816	Jun_1958
1099	441589.2	3978338	49.3776	63.3984	45.72	3.6576	Jun_1958

Table 23. Available data from Constain (1957).

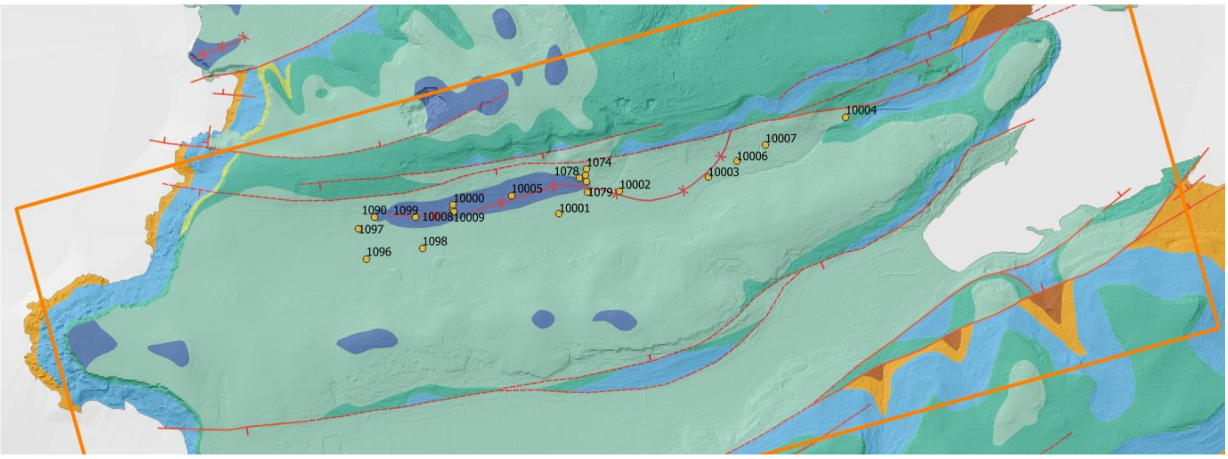

Figure 37. Available data from Constain (1957).

An attempt of interpolation of heads (points coloured differently according month) would reproduce a piezometric depression (Figure 38) clearly indicating a way out from the system. Given the little information associated to the head measurements, it is not clear if the outflow is due to the Mgarr gallery being built in that period and/or due to a natural way out. Different hypotheses have been tested during the modelling process.

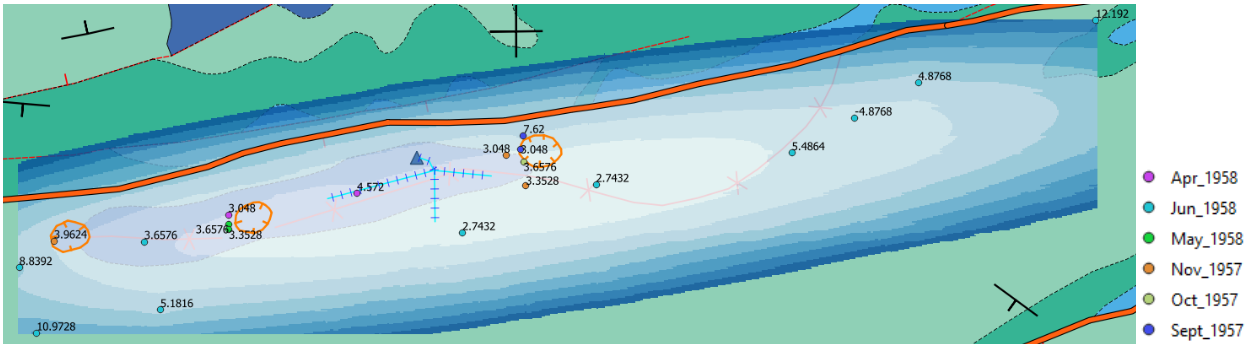

Figure 38. Heads interpolation.

Results

Sensitivities, linearity test and adjusted parameters

In order to evaluate parameter sensitivities, the heads measured in the 50s were introduced in the model, as well as 51 PP of hydraulic conductivity. Other parameters included in the analysis were the GHB conductance (sinkholes), HFB conductivity (low permeability faults) and drain conductance (breccia fault).

Sensitivities are reported in Figure 39 and Table 24. The highest values of sensitivity are associated to two PP and to the conductivity of the supposed fault (hfb100), followed by other PP. Drain conductance and one of the sinkholes (ghc3) are among the 20 highest values of sensitivity. The position of PP and of the other parameters are shown in Figure 40.

The spatial distribution of the hydraulic conductivity field obtained in the steady state preliminary parameter adjustment is shown in Figure 41.

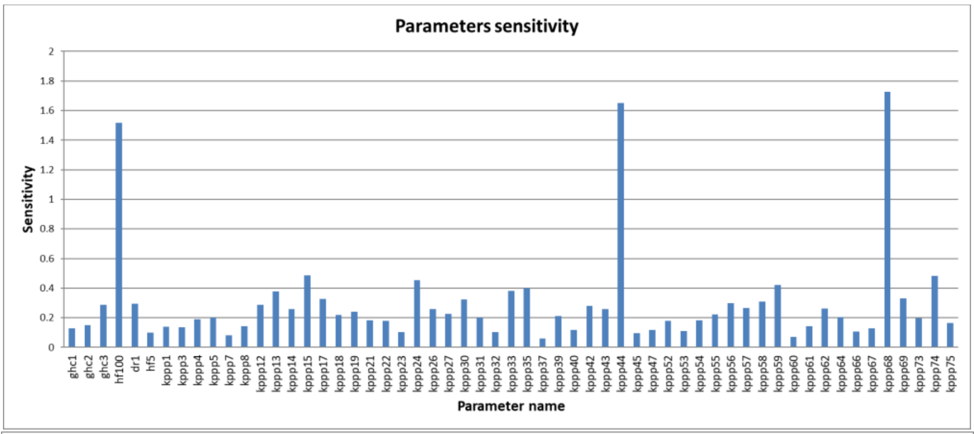

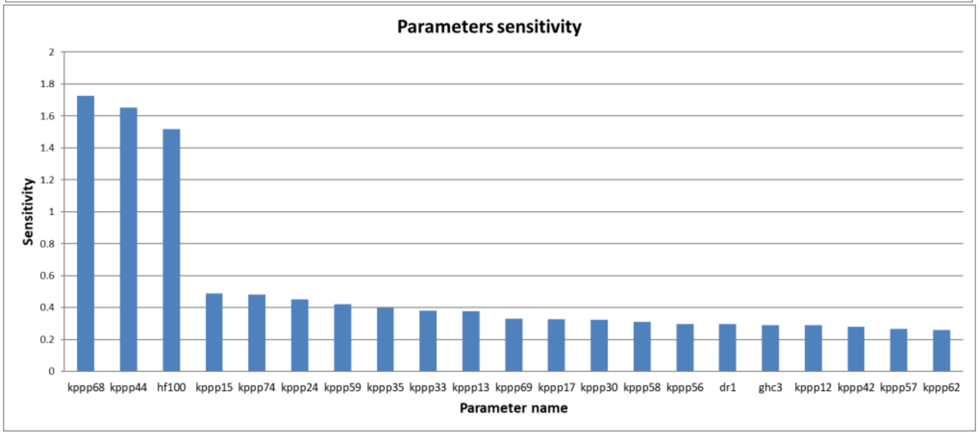

Figure 39. Parameter sensitivities.

Name	type	Value	Sens	Name	type	Value	Sens
ghc1	cond	2.46E-05	0.127	kppp35	kp	7.31E-05	0.398
ghc2	cond	6.38E-05	0.151	kppp37	kp	9.23E-05	0.060
ghc3	cond	1.06E-04	0.289	kppp39	kp	7.36E-05	0.211
hf100	hfb	2.00E-08	1.519	kppp40	kp	7.97E-08	0.116
dr1	cond	2.20E-04	0.296	kppp42	kp	5.27E-08	0.280
hf5	hfb	1.07E-09	0.099	kppp43	kp	5.22E-05	0.258
kppp1	kp	9.63E-05	0.140	kppp44	kp	9.86E-05	1.652
kppp3	kp	1.02E-04	0.137	kppp45	kp	9.31E-05	0.095
kppp4	kp	1.04E-04	0.190	kppp47	kp	9.81E-05	0.119
kppp5	kp	1.24E-04	0.200	kppp52	kp	9.30E-05	0.179
kppp7	kp	9.91E-05	0.081	kppp53	kp	7.88E-05	0.109
kppp8	kp	9.76E-05	0.144	kppp54	kp	8.74E-05	0.183
kppp12	kp	8.73E-05	0.289	kppp55	kp	9.52E-05	0.223
kppp13	kp	7.02E-05	0.377	kppp56	kp	8.64E-05	0.298
kppp14	kp	1.04E-04	0.258	kppp57	kp	6.37E-05	0.267
kppp15	kp	9.97E-05	0.488	kppp58	kp	7.80E-05	0.311

Name	type	Value	Sens	Name	type	Value	Sens
kppp17	kp	8.46E-05	0.328	kppp59	kp	7.91E-05	0.422
kppp18	kp	9.91E-05	0.219	kppp60	kp	1.02E-04	0.072
kppp19	kp	1.07E-04	0.242	kppp61	kp	8.13E-05	0.142
kppp21	kp	9.49E-05	0.183	kppp62	kp	8.98E-05	0.261
kppp22	kp	9.64E-05	0.177	kppp64	kp	9.03E-05	0.204
kppp23	kp	7.40E-05	0.103	kppp66	kp	1.00E-04	0.106
kppp24	kp	9.23E-05	0.452	kppp67	kp	1.08E-04	0.127
kppp26	kp	6.90E-05	0.258	kppp68	kp	6.49E-05	1.726
kppp27	kp	1.21E-04	0.224	kppp69	kp	9.00E-05	0.331
kppp30	kp	1.21E-04	0.323	kppp73	kp	1.13E-04	0.196
kppp31	kp	1.03E-04	0.202	kppp74	kp	9.99E-05	0.482
kppp32	kp	6.49E-05	0.103	kppp75	kp	1.15E-04	0.163
kppp33	kp	1.08E-04	0.381				

Table 24. Parameter sensitivities and preliminary values.

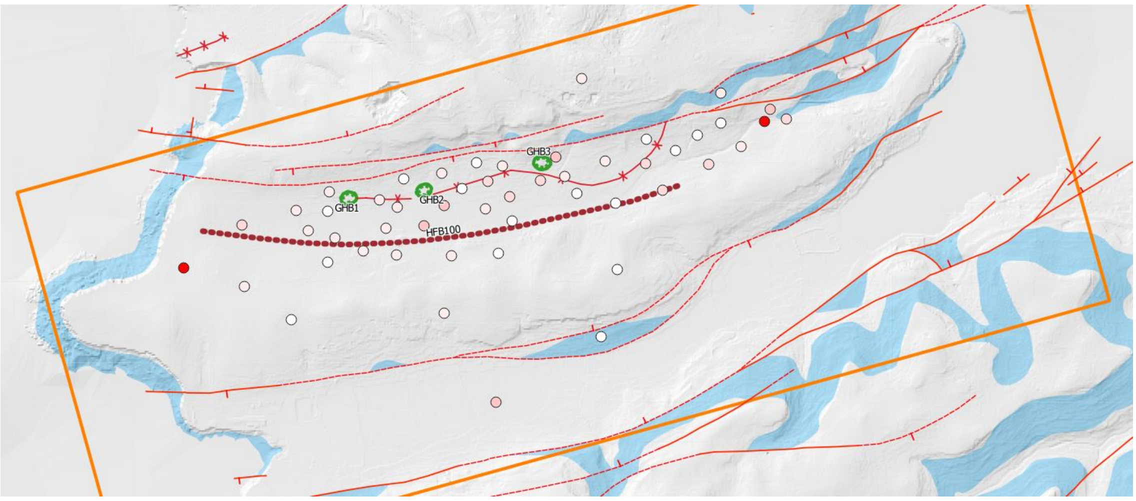

Figure 40. Parameters used in the sensitivity analysis.

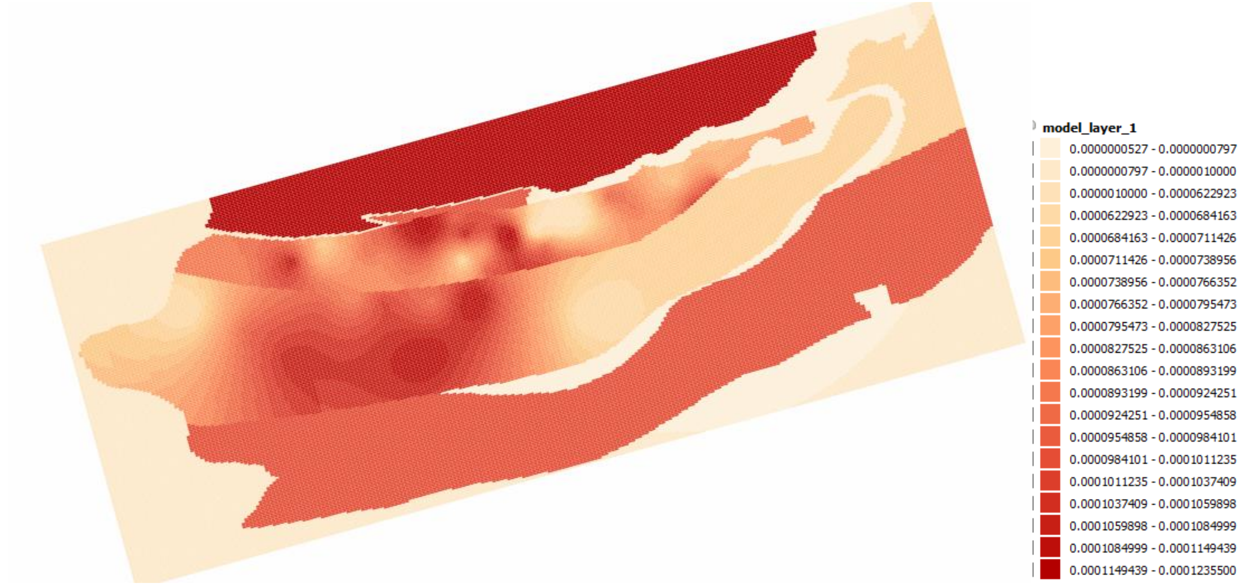

Figure 41. Hydraulic conductivity field distribution of v34.

Model linearity and numerical integrity was tested plotting the observation variation *vs* parameter change. The model was run 100 times monitoring the response of observation changing the parameter GHB3 (conductance of the sinkhole GHB3 in Figure 40). Results of one of the preliminary versions of the model is shown in Figure 28, where a high numerical noise is evident, causing random oscillation of various meters with slight parameter changes. Along the several model revisions described in Appendix 1, the model instability was made acceptable, giving the results shown in Figure 43.

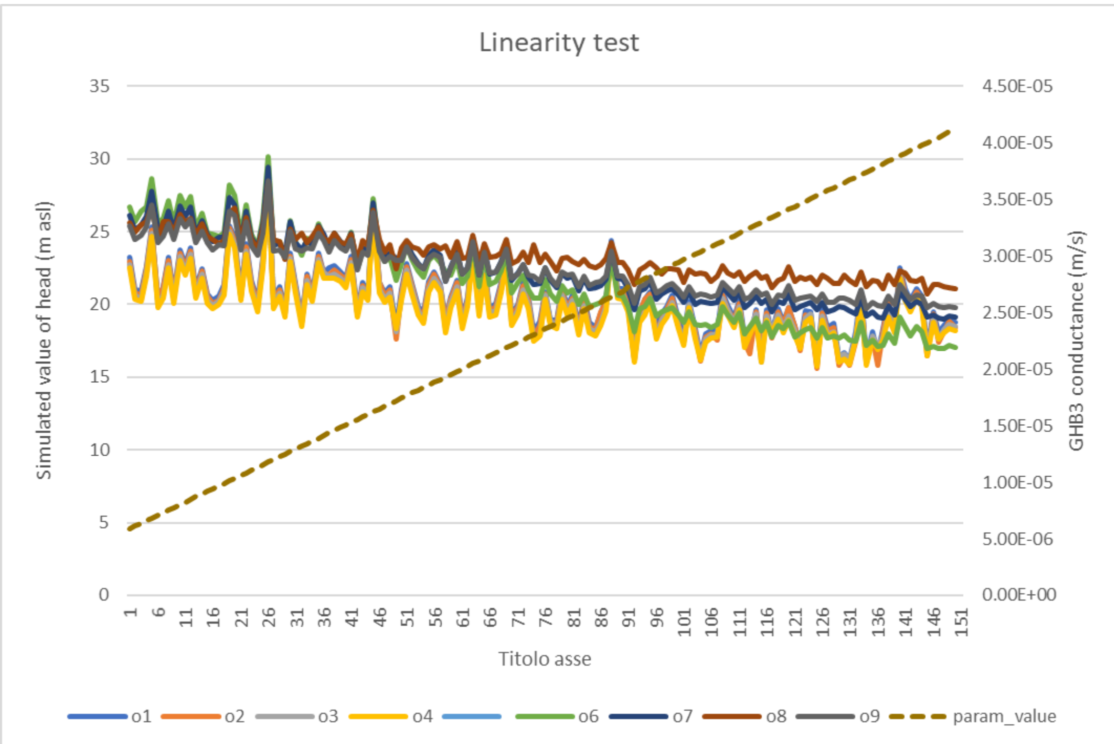

Figure 42. Linearity test (failed) of one of the early model versions.

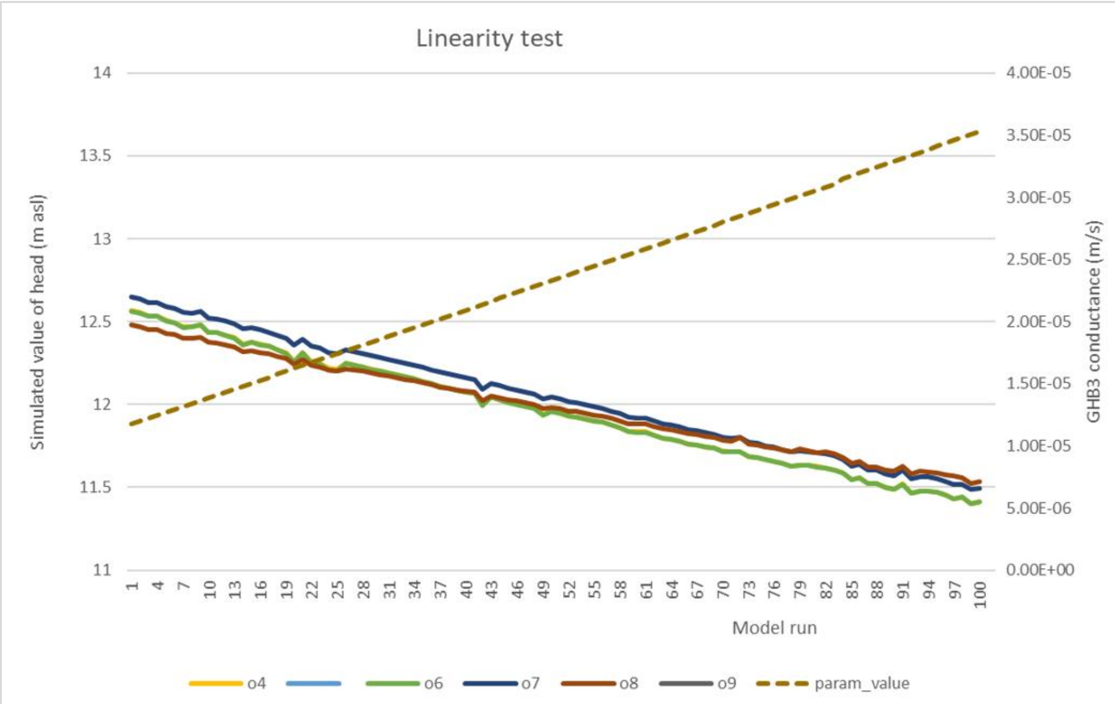

Figure 43. Linearity test of model v34.

Water budget and head distribution

Acceptable numerical stability of the model is confirmed by the water budget discrepancy, which is less than 1%. The terms of the budget obtained in the steady state of the whole domain, of Mizieb and Pwales are shown in m^3/s and m^3/y in Table 25.

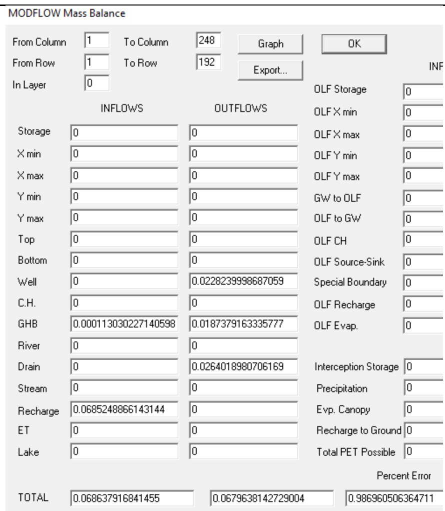

MODFLOW Mass Balance

From Column 1 To Column 248
From Row 1 To Row 192
In Layer 0

	INFLOWS	OUTFLOWS
Storage	0	0
X min	0	0
X max	0	0
Y min	0	0
Y max	0	0
Top	0	0
Bottom	0	0
Well	0	0.0228239998687059
C.H.	0	0
GHB	0.000113030227140598	0.0187379163335777
River	0	0
Drain	0	0.0264018980706169
Stream	0	0
Recharge	0.0685248866143144	0
ET	0	0
Lake	0	0
TOTAL	0.068637916841455	0.0679638142729004

OLF Storage	0
OLF X min	0
OLF X max	0
OLF Y min	0
OLF Y max	0
GW to OLF	0
OLF to GW	0
OLF CH	0
OLF Source-Sink	0
Special Boundary	0
OLF Recharge	0
OLF Evap.	0
Interception Storage	0
Precipitation	0
Evp. Canopy	0
Recharge to Ground	0
Total PET Possible	0
Percent Error	0.986960506364711

(terms in m^3/s)

Water balance (1944) Model Domain

Inflows	
Sea (GHB) (m^3/y)	3564
Recharge (m^3/y)	2161001
Outflows	
Wells (private wells) (m^3/y)	719778
Sea (GHB) (m^3/y)	418101
Sinkholes (GHB) (m^3/y)	172817
Breccia fault (DRAIN) (m^3/y)	832610

Water balance (1944) Mizieb aquifer

Inflows

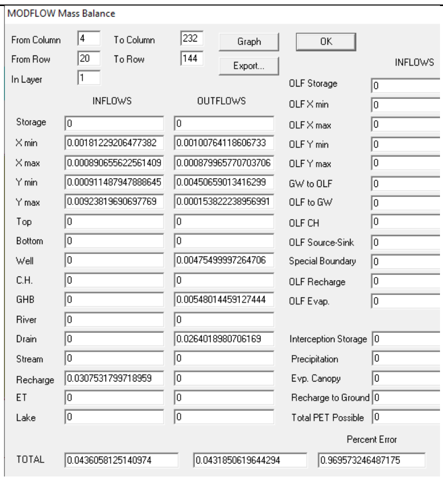

Recharge (m^3/y)	969732
Outflows	
Wells (private wells) (m^3/y)	149954
Sinkholes (GHB) (m^3/y)	172817
Breccia fault (DRAIN) (m^3/y)	832610

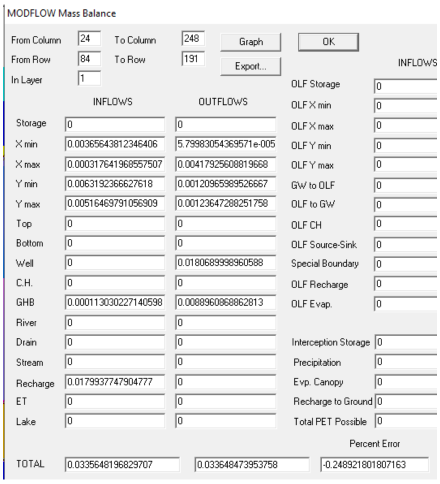

Water balance (1944) Pwales aquifer

Inflows	
Sea (GHB) (m^3/y)	3564
Recharge (m^3/y)	567332
Outflows	
Wells (private wells) (m^3/y)	569821
Sea (GHB) (m^3/y)	280544

Table 25. Model and aquifers water balances.

The hydraulic head resulting from the steady state model and presumably reproducing the 1944 situation is shown in Figure 30. It is evident how the boundary condition control over the groundwater flow is dominant.

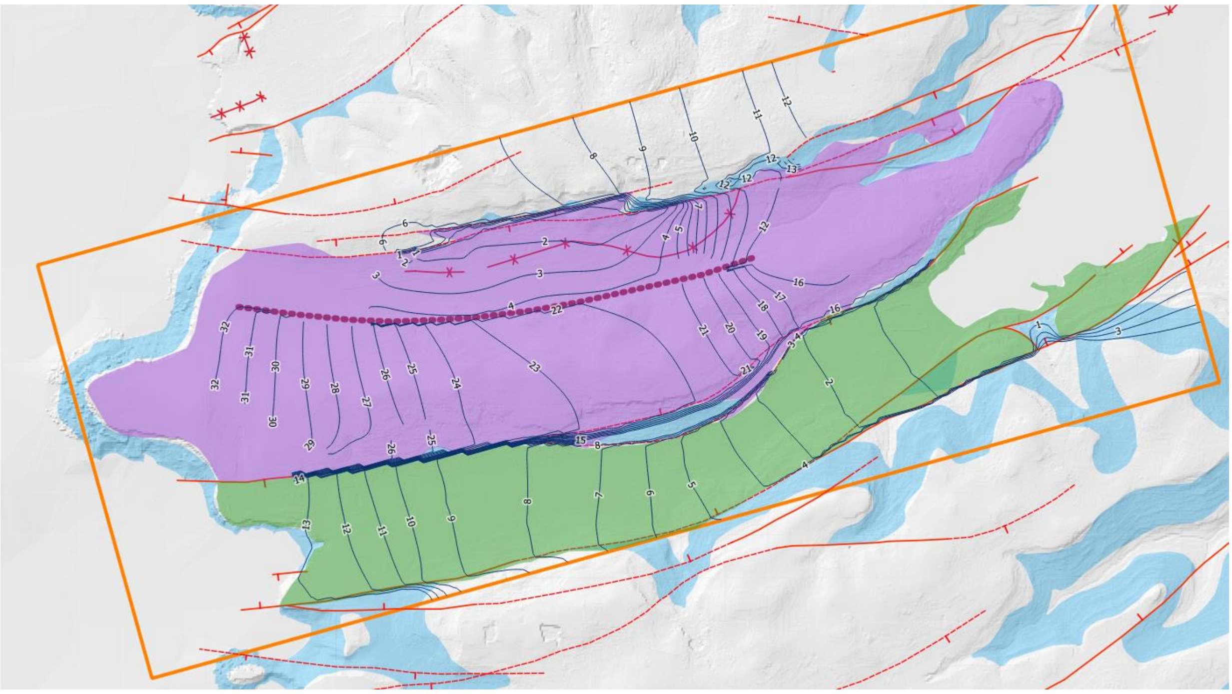

Figure 44. Hydraulic head distribution of MP_3 v5.

Seawater interface simulation

SWI2 Package

The SWI2 Package (Bakker, 2013) is the latest release of the Seawater Intrusion (SWI) Package for MODFLOW. The SWI2 Package allows three-dimensional variable-density groundwater flow and seawater intrusion in coastal systems to be simulated using MODFLOW-2005. Vertically integrated variable-density groundwater flow is based on the Dupuit approximation in which an aquifer is vertically discretized into zones of differing densities, separated from each other by defined surfaces representing interfaces or density isosurfaces. The numerical approach used in the SWI2 Package does not account for diffusion and dispersion and should not be used where these processes are important. The resulting differential equations are equivalent in form to the groundwater flow equation for uniform-density flow.

The approach implemented in the SWI2 Package allows density effects to be incorporated into MODFLOW-2005 through the addition of pseudo-source terms to the groundwater flow equation without the need to solve a separate advective-dispersive transport equation. Vertical and horizontal movement of defined density surfaces is calculated separately using a combination of fluxes calculated through solution of the groundwater flow equation and a simple tip and toe tracking algorithm. Fluid density within model layers can be represented using zones of constant density (stratified flow) or continuously varying density (piecewise linear in the vertical direction) in the SWI2 Package. The main advantage of using the SWI2 Package instead of variable-density groundwater flow and dispersive solute transport codes, such as SEAWAT and SUTRA, is that fewer model cells are required for simulations using the SWI2 Package because every aquifer can be represented by a single layer of cells. This reduction in number of required model cells and the elimination of the need to solve the advective-dispersive transport equation results in substantial model run-time savings, which can be large for regional aquifers.

Further details about the package can be found in the software documentation (Bakker, 2013), as well as examples of application. The accuracy and use of the SWI2 Package are also reported through comparison with existing exact solutions and numerical solutions with SEAWAT.

MSLA Model

General head boundary conditions were used to represent the sea boundary. The offshore bathymetry was used as top of the layer. The groundwater is divided into a freshwater zone and a seawater zone, separated by an active ZETA surface, Z, between the zones that approximates the 50-percent seawater salinity contour. Fluid density is represented using the stratified option (ISTRAT=1). The dimensionless density difference between freshwater and saltwater is 0.025. The tip and toe tracking parameters are a TOESLOPE and TIPSLOPE of 0.025, a default ALPHA of 0.1, and a default BETA of 0.1. Time of simulation includes 2 stress periods, the first representing natural conditions and lasting 250 years, and the second representing the 1944 conditions (after 20 years of development). Simulated steady-state groundwater levels for the model are shown in Figure 44. The initial freshwater-seawater interface (Figure 45) was calculated using initial heads and the Ghyben-Herzberg relation (starting Z is assumed to be smoother than head distribution to speed up convergence times). Elevations of Z which are deeper than the model bottom are set a couple of meters above the model bottom.

The SWI2 ISOURCE parameter is set to -2 in all general head boundaries representing coastal boundaries, which ensures that inflow from the coastal boundaries is saltwater and outflow is from the top zone, which can be freshwater. In all other cells, the SWI2 ISOURCE parameter was set to 1, indicating boundary conditions have water that is identical to freshwater.

The simulated saltwater surface in the 2 stress periods is shown in Figure 46. Comparison of the 2 periods are is clearer in the cross sections of the MSLA (Figure 47).

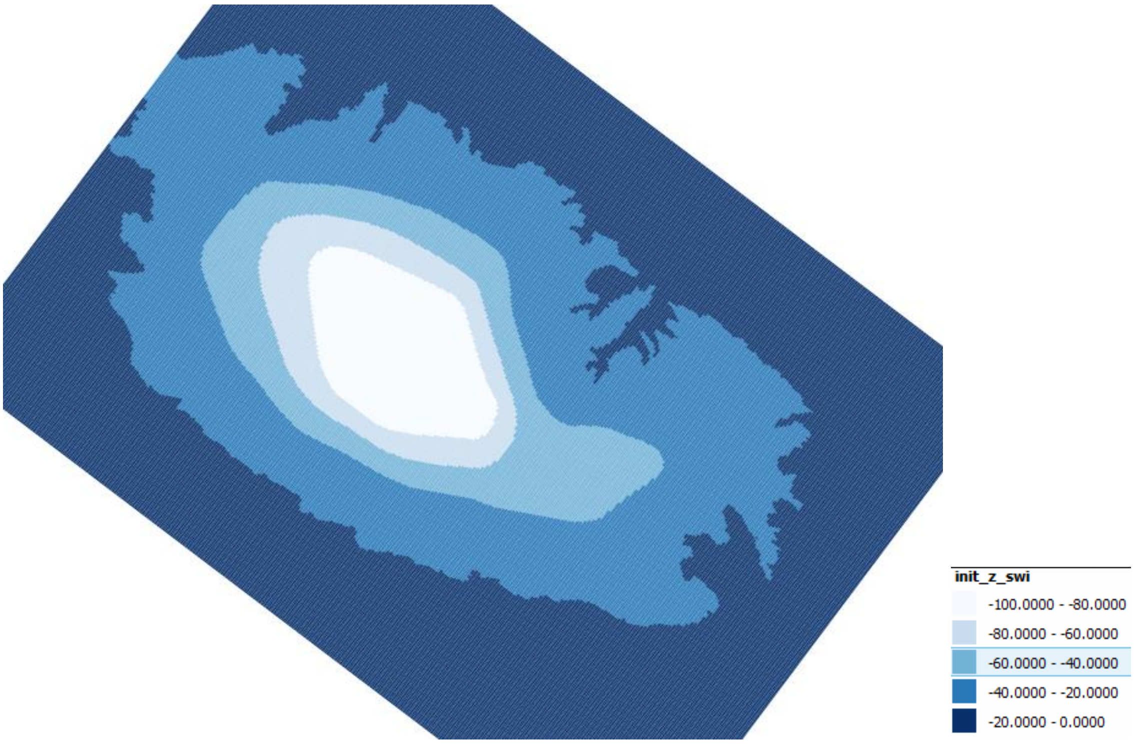

Figure 45. Initial Z surface, analytically calculated.

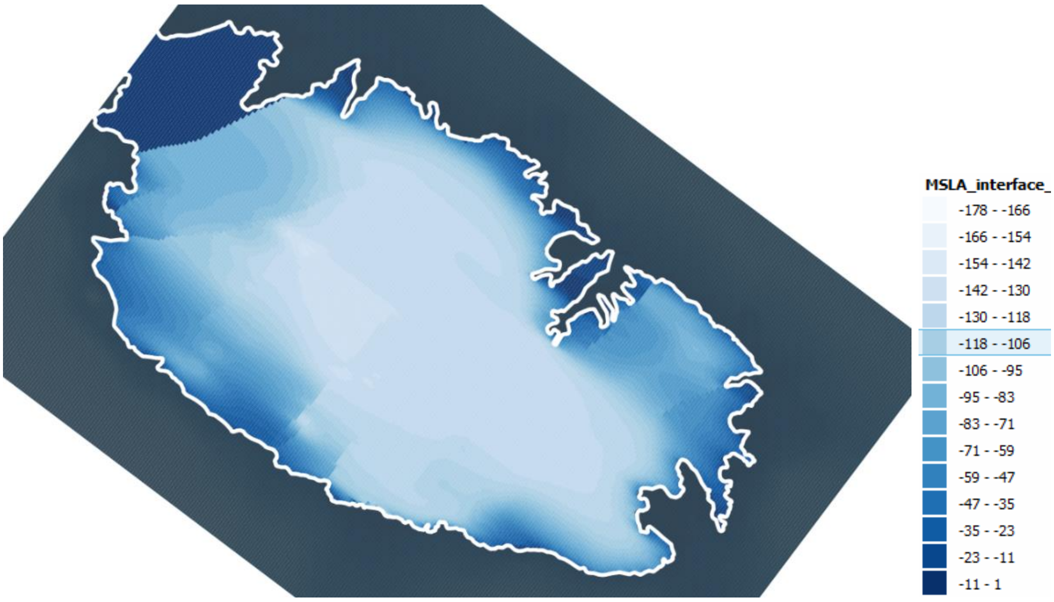

(A) Stress Period 1

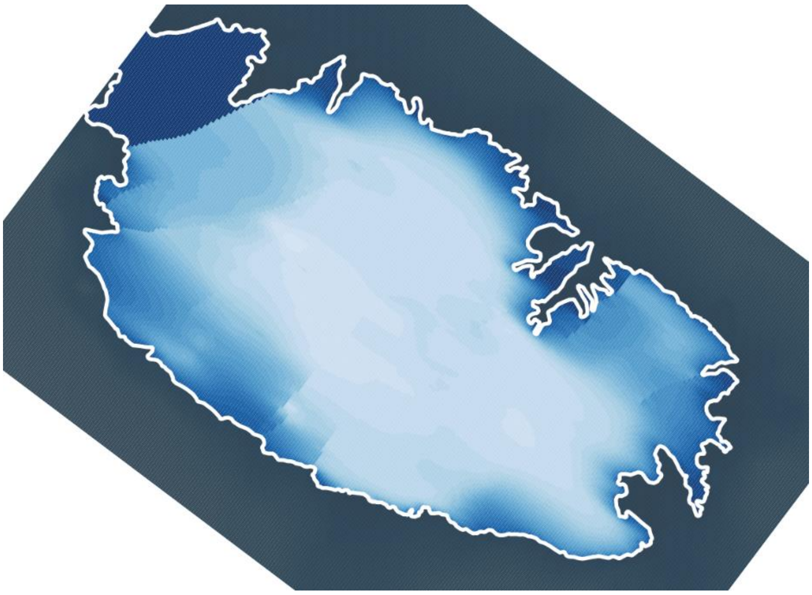

(B) Stress Period 2

Figure 46. Simulated Z surfaces at the end of Stress period 1 (A) and 2 (B).

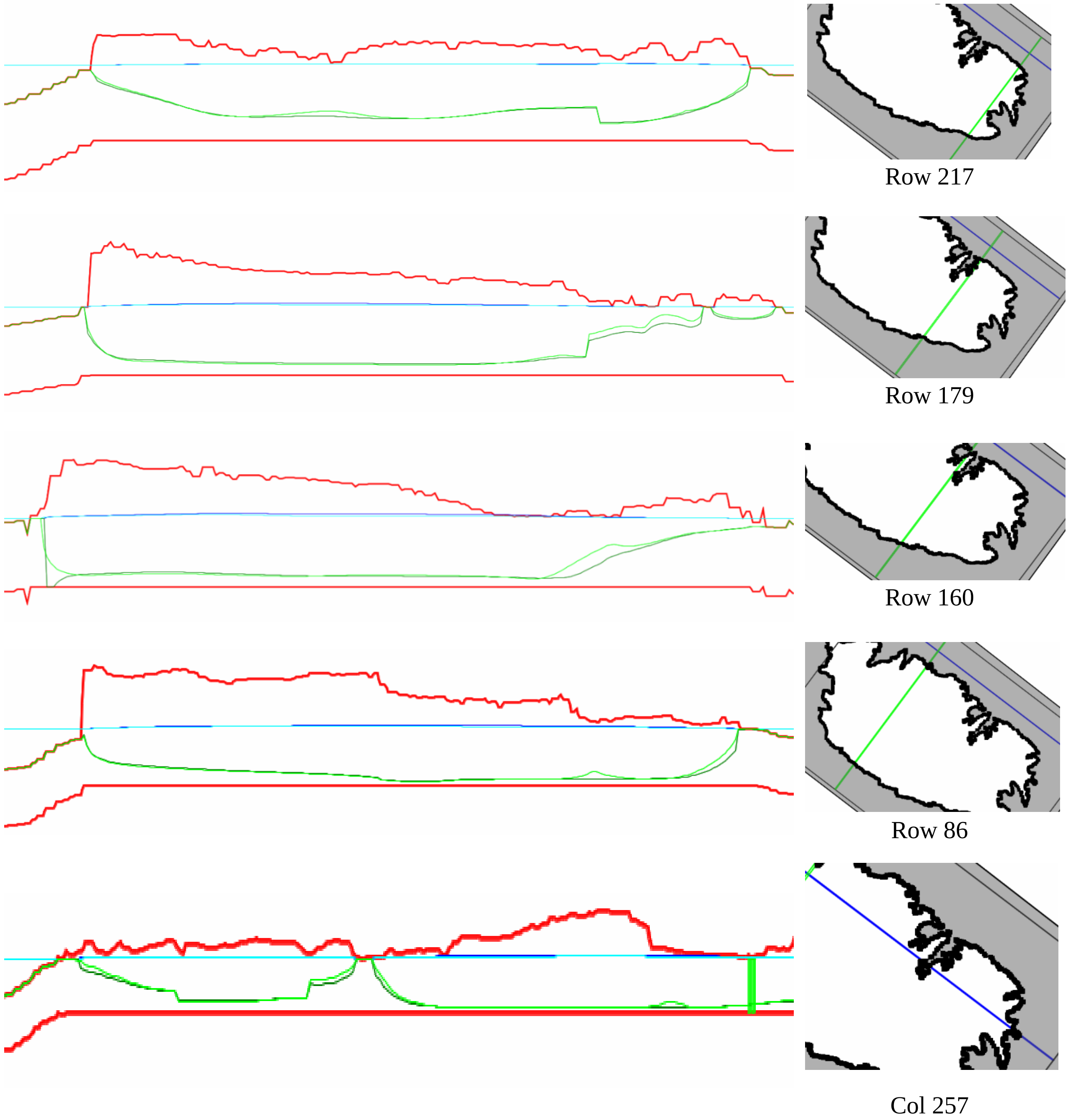

Figure 47. Cross-sections of freshwater-seawater interface; SP1 = dark green; SP2 = light green.

Mizieb-Pwales Model

The same approach was tested with the preliminary Mizieb-Pwales model. The area of the domain that can be mostly interested by seawater intrusion is the Pwales aquifer, which is in direct connection with the sea at its eastern boundary. Differently from MSLA, where the aquifer bottom is undefined, and differently from Mizieb, which is naturally protected by the Blue Clay aquifer bottom, Pwales presents a Blue Clay bottom which gradually immerses below the sea level towards the East. Risk of upconing in Mizieb is made possible through the inversion of the vertical gradient between the aquifer and the sea level in the discharge area; this is not observed in pseudo-natural conditions.

The present simulation of the seawater interface does not show effects of seawater intrusion in the two aquifers, being substantially coincident with the aquifer bottom. Given the high uncertainties and lack of important data to constraint the results of the flow model, these simulations are not considered reliable (but rather misleading) and will necessary need further checks through new datasets that should be made available.

Part 2: Models for Gozo island

Introduction

As required by EWA, the study regarding Gozo island focuses on two aquifers: the Gozo MSLA and the perched aquifer of Ghajnsielem.

The first modelling efforts were devoted to represent these two aquifers together in the same model: this approach is in general preferable not only to present the results in a way closer to the real geological settings, but also to leave the possibility to investigate potential water exchanges between the two. To this purpose the first modelling stages and sub-versions have been dedicated to have a god representation of this situation (see Appendix 1 -Modeling Journal). However, even if this approach could be promising, the main issue is the lack of information on Ghajnsielem perched aquifer, which prevents to design a model having some reference of the real-world water balance in the pre-exploitation age. Basically, the only source of information is the detailed study by Costain et al. (1958). However, this reach source of information does not give an idea on the water sinks in the aquifer (being an aquifer isolated from the sea and from MSLA). To this purpose the Ghajnsielem aquifer has been eventually taken out from the model and a specific model for the perched aquifer has been designed. This smaller model allows to define a finer grid and an easier way to activate or inactivate potential sinks, to understand their importance, having as final goal to get a support for driving additional investigation on the field.

Next sections report details for the two models developed for Gozo island.

Gozo Mean Sea Level Aquifer

Hydrogeologic characterization and conceptual model

The conceptual model has been presented in Deliverable D1.3. In Figure 48 the hydrogeological scheme is reported. The main features of the aquifer are the following.

- The Lower Coralline Limestone aquifer is present across the whole island.
- It is extensively capped by the impermeable Blue Clay and the Greensand and by less permeable strata in the Middle Globigerina Limestone.
- Its lateral boundaries are the seashore and, in the south, the Ghajnsielem-Qala fault.
- The water table is controlled by abstraction and is presently only a few meters above sea level. This abstraction also leads to extensive saline up coning and an increase in salinity.

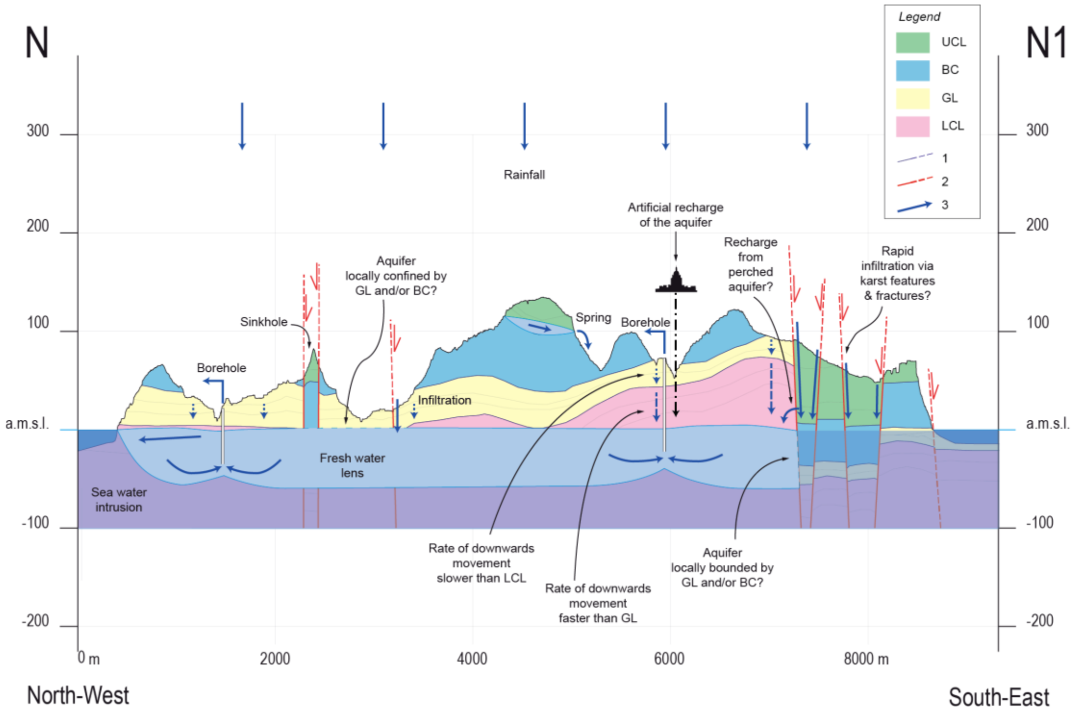

Figure 48: Hydrogeological conceptual model for Gozo MSLA.

Model design

Model domain and spatial discretization

The model domain covers all the island, having a length of around 8.6 km (along the North-South direction) and a width of around 14 km (along the West-East direction). This domain is discretized with a grid having a cell size of 50m, and resulting in 49824 cells, namely 173 rows by 288 columns (Figure 49).

The active domain counts 43208 cells (over 49824) and it represents the MSLA aquifer (Figure 50): only a portion of the aquifer (on the south east part) is neglected: here MSLA goes down the Ghajnsielem aquifer, but water storage in this zone seems negligible. Furthermore, the large buffer of active cells on the seaside is considered because of the application of SWI package (see later on).

Figure 49. Model domain and spatial discretization

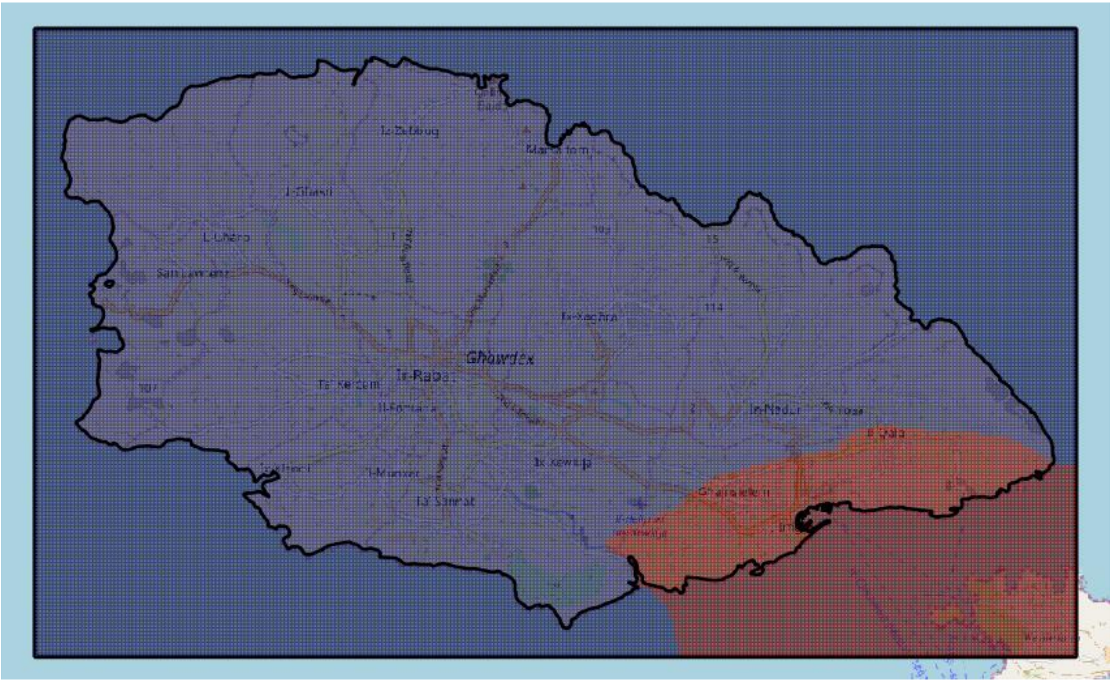

Figure 50. Active (blue) and inactive (red) cells of the model grid.

Regarding the vertical discretization, 1 model layer is considered, representing the lithology Globigerina (GL) and Lower Coralline Limestone (LCL).

The model top is taken as the top of GL (using raster layer elaborated in Activity 1), and its spatial distribution is reported in Figure 51.

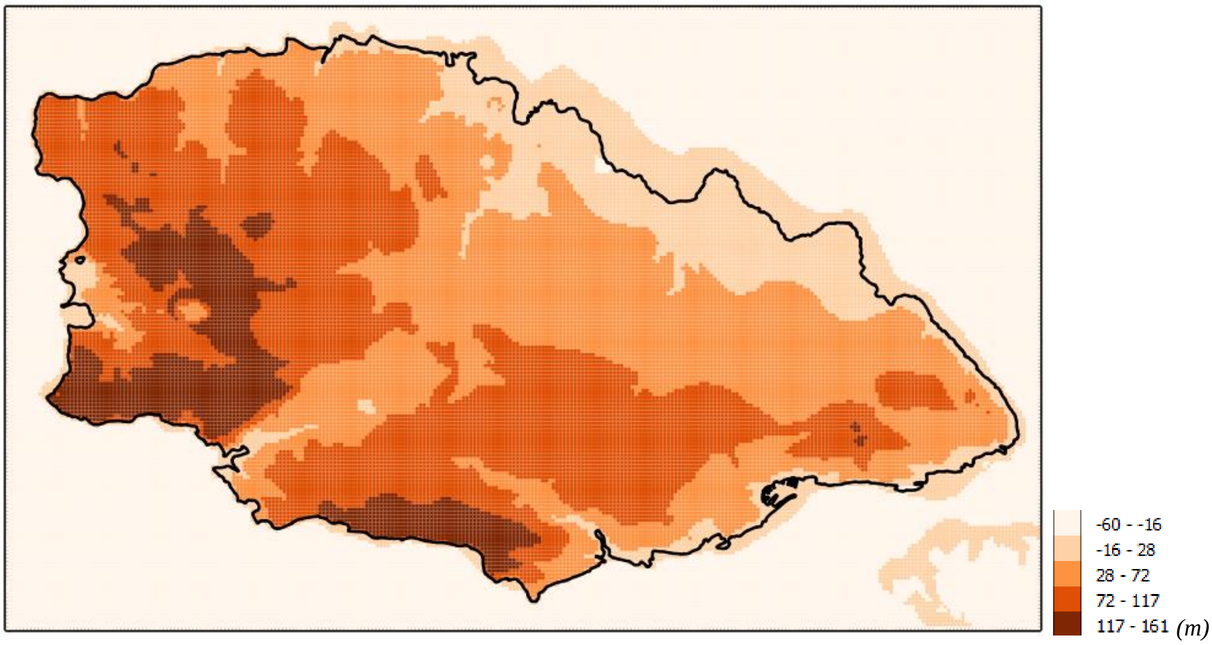

Figure 51. Model top elevation (expressed in m a.s.l.)

The elevation of model bottom is firstly calculated as (TOP-200m), to mimic a constant saturated thickness. Where this returns a bottom elevation higher than -200 m, the value is lowered to -200 m, so that eventually almost the whole aquifer has a constant bottom equals to -200 m.

Hydrodynamic parameters and faults

No estimate of transmissivity or hydraulic conductivity is available for Gozo MSLA. Therefore, the model domain has been zoned to set the hydraulic conductivity almost everywhere equal to LCL, except in zones where the bottom of GL (corresponding to the top of LCL) is under the sea level. The guess value for these parameters are the following:

- LCL (zone 1) = 13.5 m/day. This value corresponds to the geometric mean of the 8 values available for LCL in MSLA.
- GL (zone 2) = 1.35 m/day. This value is taken ten times lower than the other, as done in former modeling studies like.

However, these parameters are the object of the calibration procedure done after the first forward run of the model, as described later on.

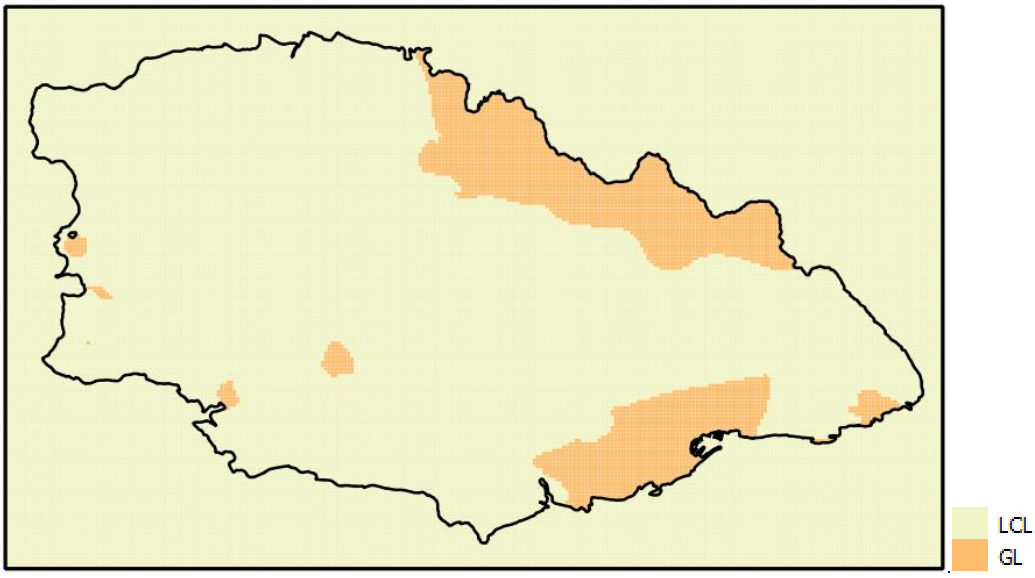

Figure 52. Zonation of hydraulic conductivity, showing the spatial distribution of LCL and GL conductivities.

The presence of several faults in the islands is accounted by applying the HFB (Horizontal Flow Barrier) package of MODFLOW code, which is activated along the fault lines, as depicted in Figure 53. For all cells the same value of HFB input parameters is used, namely K = 8.64 m/day for fault hydraulic conductivity and 1 m as fault thickness.

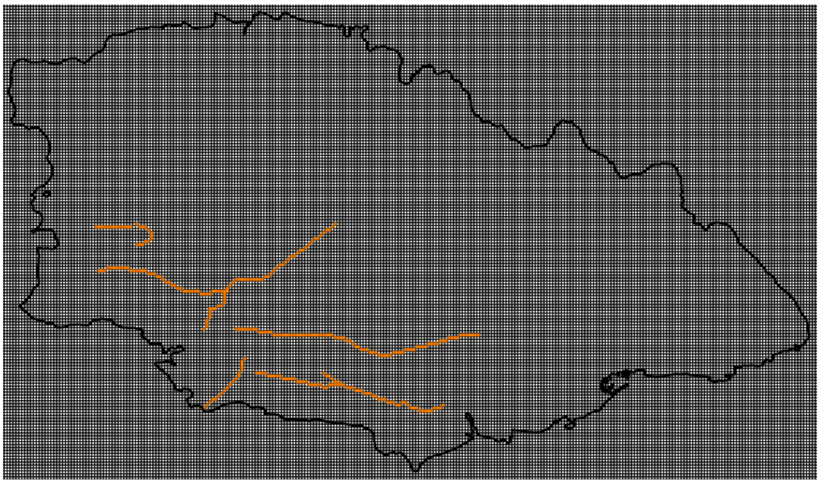

Figure 53. Cells representing the main faults within the model domain, where FHB package is applied.

Boundary condition

The model boundary condition is the potentiometric head of the sea level, namely 0 m. Although this condition could be represented by imposing a Dirichlet condition (e.g. through the Constant Head – CHD package), in this case a third type condition (GHB) is applied to represent the sea region. This artefact is due to the further application of SWI package for simulating seawater intrusion (see later on), which converges more smoothly using GHB instead. GHB is applied taking the head boundary equal to 0 m, and a conductance equal to 50 m3/day.

Aquifer recharge

The main input from which starting the recharge computation is the average annual rain recorded in Luqa weather station in the period 1941-1950, namely 550 mm/y = 1.5 mm/day. Furthermore, a uniform value for natural recharge due to infiltration (namely the difference between precipitation and evapotranspiration, accounting for 37% of the mean annual rainfall is taken as reference (BRGM, 1991). It results in a reference recharge of 5.57E-4 m/day.

To obtain a more detailed spatial distribution of recharge, the same procedure applied for Malta MSLA is used. However, it is worth mentioning that no similar data are available for Gozo island. Therefore, the same values used in Malta are applied for Gozo and we do not report here the procedure for obtaining this result through the application of Thornthwaite method. In particular, the same approach is used to obtain the spatial value of Thornthwaite term *Surplus*. The calculation of this term based on Malta island data is a feasible assumption in case of lack of data, but of course this clearly affects the computation results.

As for Malta models, the *surplus* is used in a weighted sum taking into accounts the following features: urbanized area, geology (type of formation characterizing the model layer), morphology (terrain slope). Therefore, the weighted natural recharge value is computed according to the following formula:

$$NatRCH = Surplus*CIPS*U$$

where:

- *NatRCH* is the computed value of natural recharge (m/day).
- *Surplus* is the surplus computed using Thornthwaite method and the soil classification obtained from Lang (1960).
- *CIPS* coefficient (Viaroli et al. 2018), calultated as *CIPS* = *G*SL*, where:
    - *G* is the dimensionless coefficient accounting for the geology types distribution (see map and details below).
    - *SL* is the dimensionless coefficient obtained as the complement to 1 of the terrain slope, namely (1-slope*0.1), and so ranging from 0.0 (100% of slope) and 1.0 (flat surface, 0% of slope). Map of the slope value is reported below.
- *U* is a dimensionless coefficient, which is equal to 0.1 in urbanized areas and 1.0 in non-urbanized areas (Figure 54). The coefficient for urbanized zones is taken as 0.1 instead of the theoretical null value because of the potential infiltration due to anthropic activities, mainly the infiltration from water supply network. Such a contribution could be better assessed (both quantitatively and spatially) by using specific data on this topic.

In the following paragraphs we report, for each coefficient, the spatial distribution and details on its derivation, as well as the derivation of the additional terms due to leakage from perched aquifers and dams.

Urbanized areas (U)

Urbanized areas are derived from the land use map dated 1957, provided by EWA in May 2019.

Figure 54. Map of urbanized areas on Gozo island.

Soil type

Regarding the soil influence, the surplus is spatially modulated according several factors, as explained below.

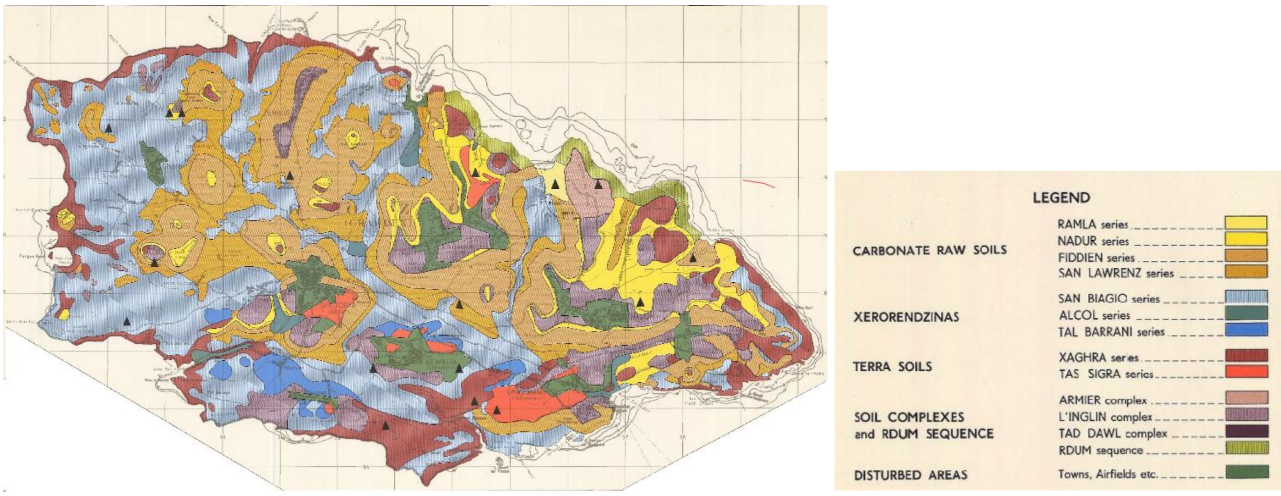

Figure 55. Soil map derived by Lang (1960).

Focusing on Gozo island, the following types of soil have been considered to get a digitized version of the spatial classification:

Class	Rank	Weight (S)
San Lawrenz/Fidden	1	0.3
Tal Barrani	2	0.5
L'Inglin	3	0.7
San Biagio	3	0.7
Nadur	4	0.7

Table 26. Weights assigned to each soil type and used in the formula to get the spatial distributed recharge.

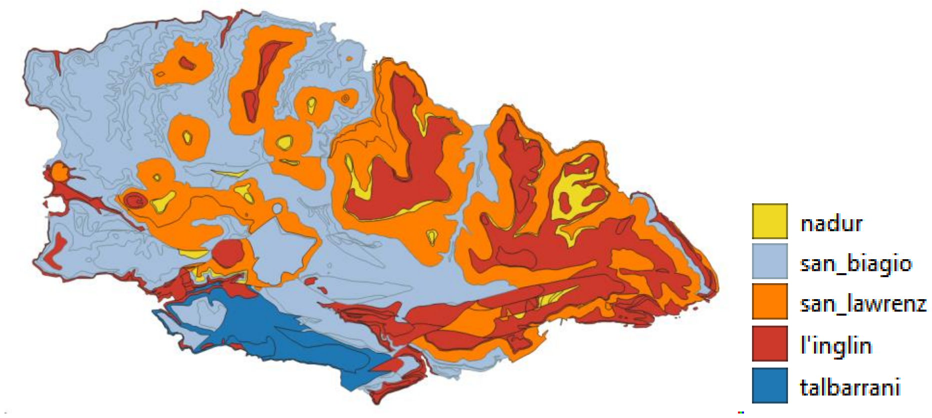

Figure 56. Digitized version of soil map derived from the original one (Figure 55).

Geology type (G)

Recharge is also influenced by the lithology: to take into account this effect, a weight to each geology type has been assigned (Table 27):

Geology type	Weight (G)
Blue Clay	0.1
Globigerina	0.6
Lower Coralline Limestone	0.9
Upper Coralline Limestone	1.0
Greensand	1.0

Table 27. Weights assigned to different geological types.

The map of the spatial distribution of such coefficients is reported in Figure 57.

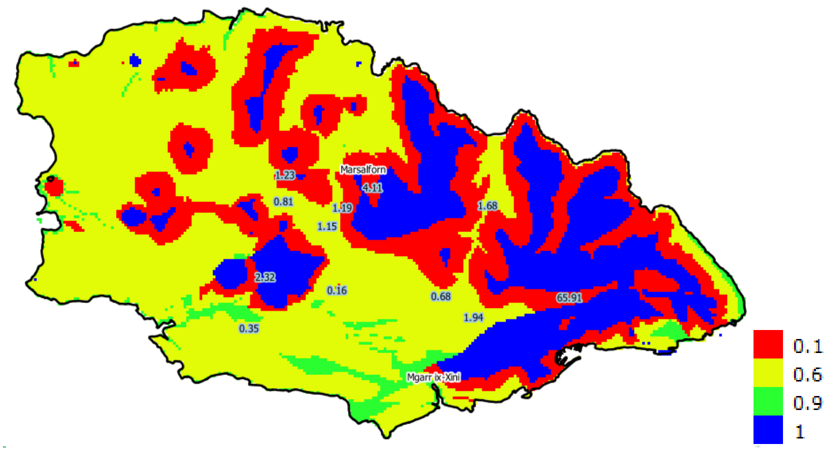

Figure 57. Map of the weights assigned to geology types.

Terrain slope (SL)

The terrain slope in Gozo has been computed using GIS tools (through QGIS software), taking as reference a DEM of 1m in resolution. The corresponding map is reported in Figure 58.

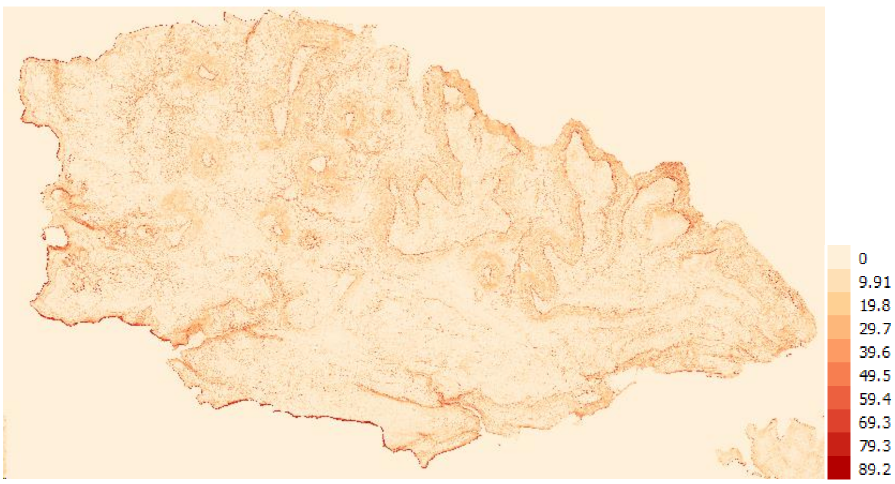

Figure 58. Map of the slope coefficient (SL, dimensionless) calculated for Gozo island.

The distribution map of spatially weighted natural recharge resulting from this calculation is reported in Figure 59.

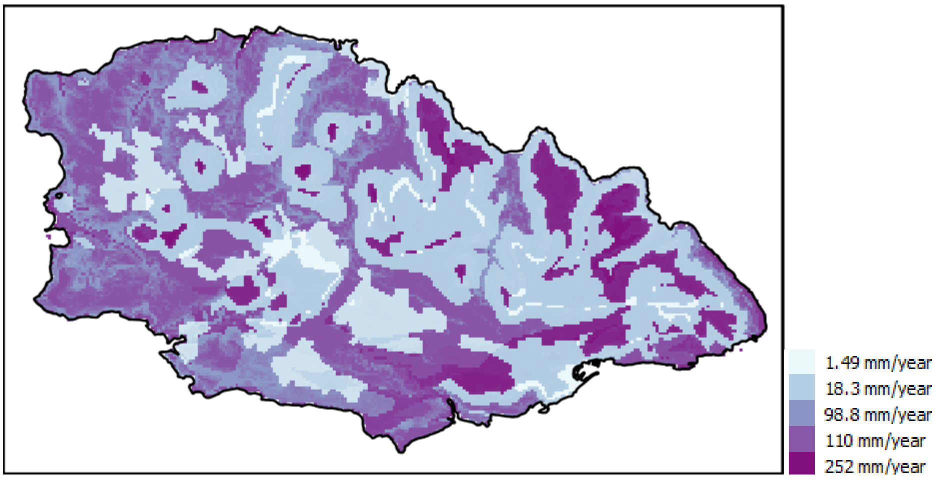

Figure 59. Map of the spatially distributed and weighted natural recharge.

The value of natural recharge is then summed up with two additional terms:

- Leakage from perched aquifers,
- Contribution of dams,

as described hereafter.

A recharge rate due to leakage from perched aquifer, through Blue Clay formation, has been estimated in 63 mm/year (1.7E-4 m/day), based on BRGM models (BRGM, 1991). This additional recharge term is applied on the top layer in regions corresponding to perched aquifers limits, as represented in the Figure 60.

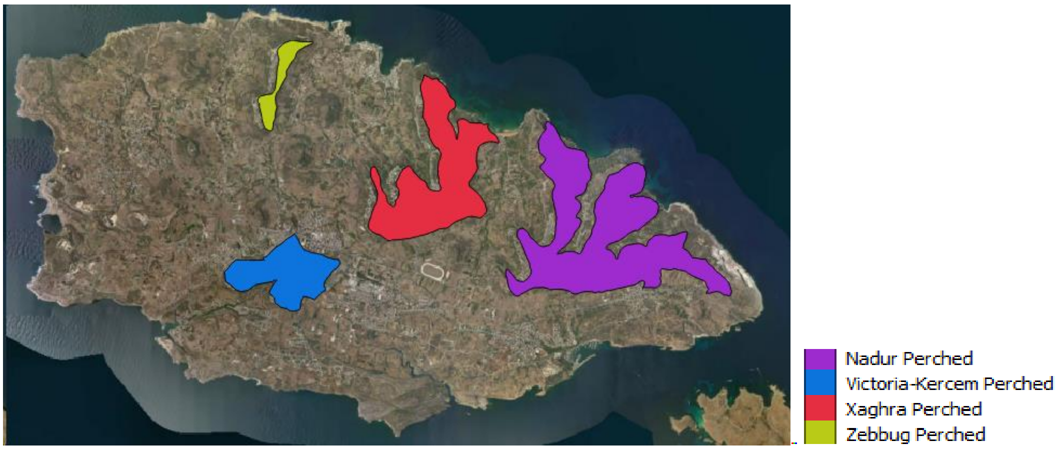

Figure 60. Limits of perched aquifers in Gozo island (with the exception of Ghajnsielem aquifer, not belonging to the model active domain).

Furthermore, according to the dataset provided by EWA, 32 dams have been recognized in Gozo island.

However, no information on the storage volume is available. For this reason, the averaged value of volumetric flow rate computed for dams in Malta island is taken as reference, namely 38.5 m3/day. The latter is obtained taking the average value of 2800 m3 of storage volume (referred to Malta island), and multiplying it by the estimated times per year when a complete filling of the dam is observed, namely 5 (according to information available by EWA's Officers).

To redistribute this recharge volume rate not only on the local point, a buffer of 100m has been applied to each dam-point. Therefore, the specific volume rate (namely the volume rate divided by area) is obtained in each buffer by dividing the volume rate per the total area of cells intersected by each buffer (Figure 61).

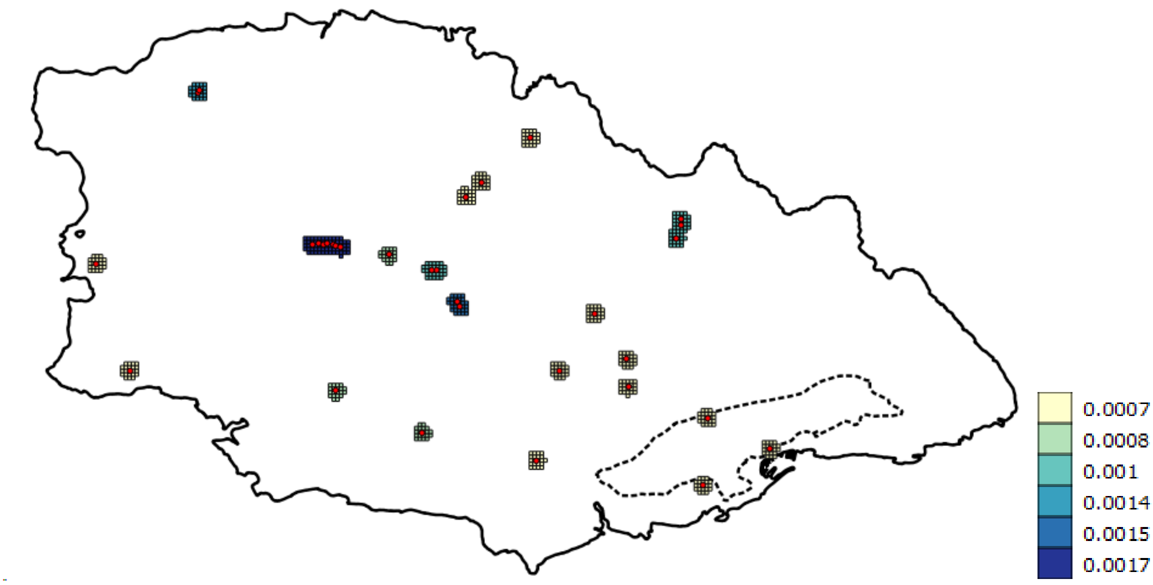

Figure 61. Map of Dams points (in red) and the cells to which the additional recharge (m/day) is applied, as reported in the legend. Notice that three dams belongs to the no-flow area in the south-east part, and therefore they have not been considered in the model run.

The final value of spatially distributed recharge is shown in the map reported in Figure 62.

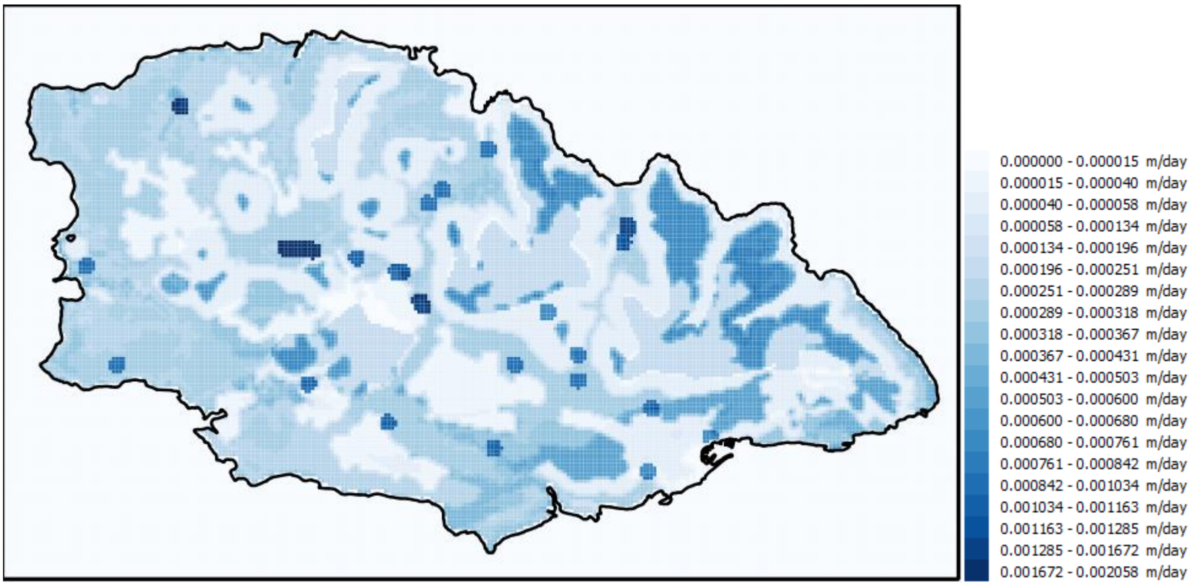

Figure 62. Map of the spatially distributed recharge (in m/day) assigned as input to package RCH.

Abstraction rate

According to EWA dataset, in 1940's, only two pumping stations were active in Gozo, while no borehole was active at that time (neither public nor private).

Pumping stations active since 1941 are:

- Marsalfolrm, with an average abstraction rate of 230 m3/day;
- Mgarr ix-Xini, with an average abstraction rate of 400 m3/day.

These pumping rates have been distributed along the water galleries corresponding to the related pumping stations, as shown in Figure 63.

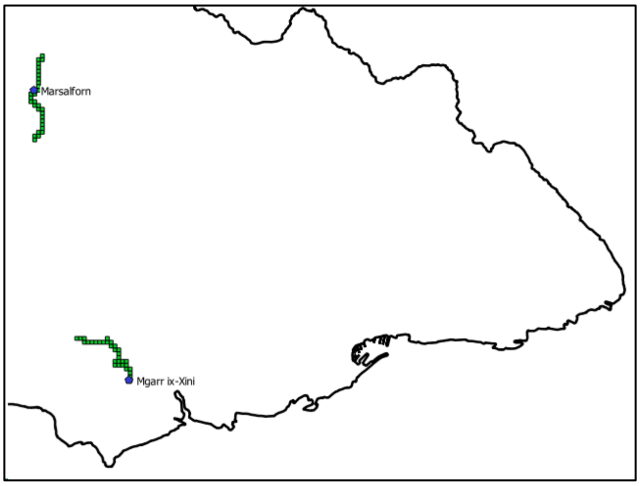

Figure 63. Localization of the two water galleries and pumping stations active in the time frame considering by the model.

Model run (not calibrated)

The model with not calibrated values of hydraulic conductivity is run using the PCG (Pre-Conjugate Gradient) solver, available in MODFLOW, with the following settings.

Outer iterations: 500; Inner iterations: 50; HClose (first tolerance convergence criterium) = 0.001; RClose (second tolerance convergence criterium) = 0.001.

The convergence is reached in few seconds (2.2 s.). The map of spatial distribution of potentiometric head computed by the model is reported in Figure 64, along with its contour lines.

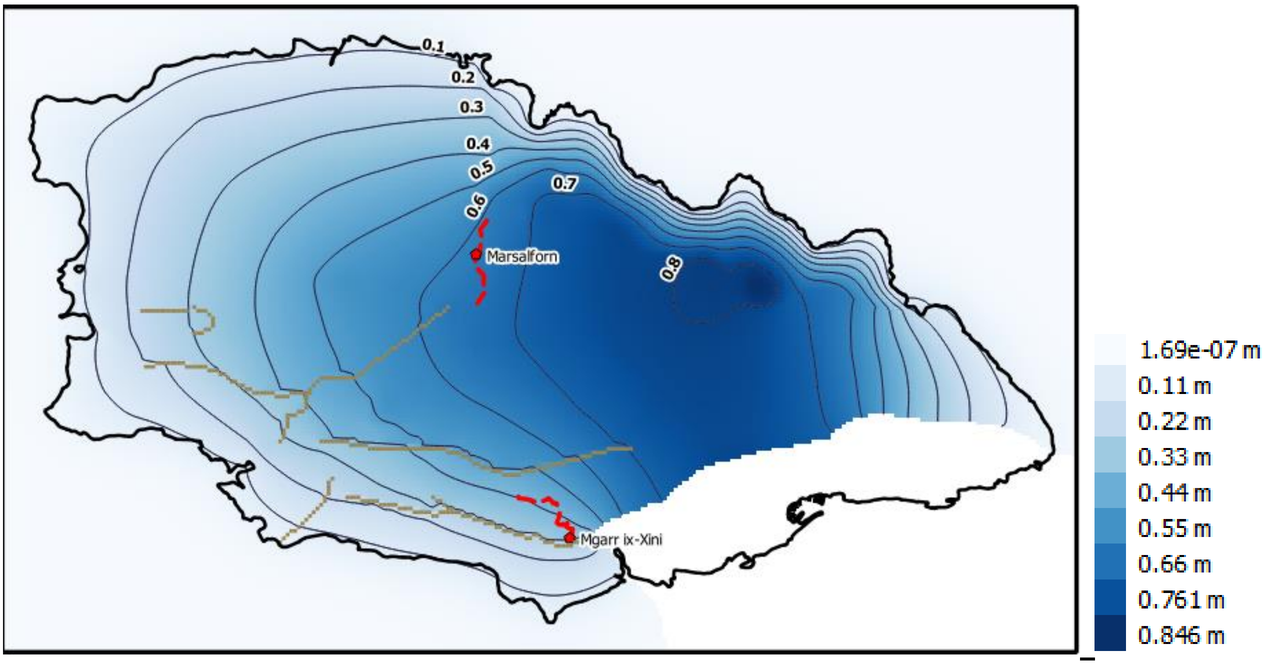

Figure 64. Map of the head distribution 8and its contour lines). Values expressed in m.

Sensitivity and calibration

The calibration study focuses on getting the best value for the two conductivity parameters, KLC and KGL. Firstly, a sensitivity analysis has been run before starting the calibration, to investigate the effect of these parameters on model results, and to understand the importance of the observations on estimating such parameters.

Observations (calibration targets)

The available data set includes only 12 observations of the observed piezometric level in Gozo MSLA (Figure 65), each one reporting only one reading, as shown in Table 28. Piezometric readings available for Gozo MSLA. No information is available on the exact timeframe which these measurements refer to. Therefore, even these observations are used in the calibration as targets, the final aim is to obtain a piezometric level with a good agreement of the measured values, without asking for any specific performance of the calibration statistics. For instance, it is likelihood that these observations refer to a time frame corresponding to a more intensive exploitation of groundwaters (namely after 1940's).

Furthermore, there are two observations having measurements and eventually taken out from the target list: the first one (boreholes ID 10802) belongs to the perched aquifer (not to MSLA). The other one (boreholes ID 10843) reports a measured value that could be an outlier.

ID	Borehole Name	Locality	Benchmark (m)	B.H.Depth (m)	Water Level (m)	Piezometric Level (m)
W10834	Taflija (foreman str)	Rabat	71.46	77.7	70.65	0.81
W10821	Wied Sara	Rabat	56.27	68.46	55.04	1.23
W10843	Gharb road (Tat-Torri)	Rabat	114.96	134.11	110.85	4.11
W10823	Xlendi	Xlendi	41.5	56.39	39.18	2.32
W10872	Ghalaq	Munxar	108.47	126	108.12	0.35
W10870	Garzelli	Sannat	87.25	103.94	87.09	0.16
W10816	St. Cecilja	Ghajnsielem	100.86	111.56	98.92	1.94
W10802	Mgarr Road	Nadur	93.3		27.39	65.91
W10860	Hniena	Xewkija	104.33	123.44	103.65	0.68
W10868	Wied l-Ghejjun	Xaghra	60.7	81	59.02	1.68
W10866	*Republic Street	Rabat	71.02	91.4	69.87	1.15
W10836	*Ta' l-Ghattuq	Rabat	49.26	62.18	48.07	1.19

Table 28. Piezometric readings available for Gozo MSLA.

Figure 65. Map of the observation points available for Gozo MSLA.

Parametrization and Sensitivity

The two values of hydraulic conductivity have been parameterized: KLC refers to LCL conductivity, while KGL to GL conductivity. The sensitivity analysis has been implemented by using the UCODE automatic-calibration software (Poeter et al., 2014), through the FREEWAT interface. Results show that KCL and KGL are highly correlated (correlation coefficient = -0.913), however the coefficient is not greater than the critical value (0.95) indicating that there may not be enough information in the observations used in the regression to estimate parameter values individually. Therefore, both parameters will be considered for calibration.

Other statistics (fit-independent) are useful to understand the importance of parameters and observations are reported as plots below. In particular:

- The Composite Scaled Sensitivity (CSS), a statistic indicating the overall importance of each parameter on the simulate values evaluated at all targets. Results show that great importance of KLC compared to KGL, as expected (Figure 66).
- The Dimensionless Scaled Sensitivity (DSS), which shows the importance of each observation to estimate the single parameters (). The DSS is useful to rank the observations in terms of their importance to estimate the conductivity (for instance KLC), as shown in Table 29. This information can help to guide future field investigations for getting more information in region of the aquifer where conductivity value has a more effect on the hydrodynamics of the groundwater.

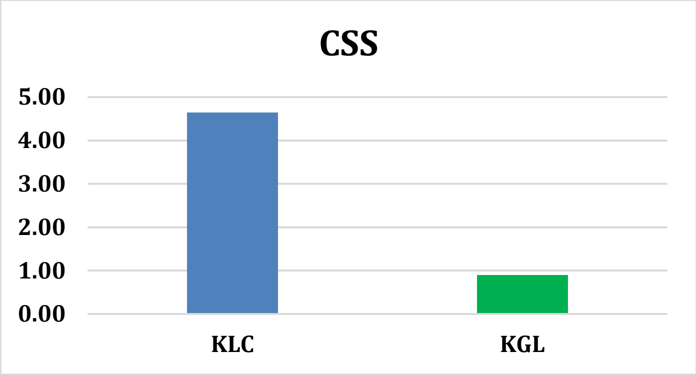

Figure 66. CSS (Composite Scaled Sensitivity) computed for KLC and KGL, before calibration.

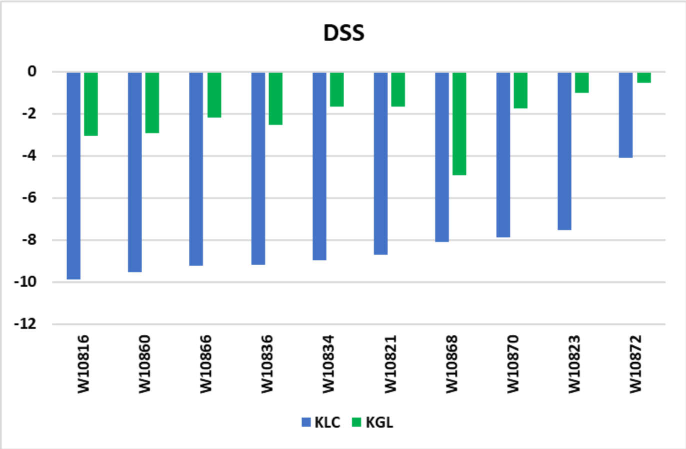

Figure 67. DSS (Dimensionless Scaled Sensitivity), which shows the importance of each observation to estimate the single parameters.

Rank	ID	Name
1	W10816	St. Cecilja
2	W10860	Hniena
3	W10866	Republic Street
4	W10836	Ta' l-Ghattuq
5	W10834	Taflija (Foreman str)
6	W10821	Wied Sara
7	W10868	Wied l-Ghejjun
8	W10870	Garzelli
9	W10823	Xlendi
10	W10872	Ghalaq

Table 29. Ranking of observations according to DSS calculated for KCL.

Calibration and residual analysis

Model optimization algorithm converged smoothly, and it gets the following optimal values for the hydrodynamic parameters:

KLC = 5.528 m/day

KGL = 1.446 m/day

However, from an analytical point of view, the quality of the model fit is poor, as evident by the correlation plot (Figure 68) and residuals (

Figure *69*), and model fit statistics (Table 30). The convergence is reached by imposing a strong tolerance value (coefficient TolPar in UCODE equal to 1E-03, expressing the tolerance of maximum fractional change in parameter values between two consecutive iterations), and it is achieved in only 4 iterations (out of 20 imposed as maximum number of iteration). It means that there is no potentiality of getting a best model fit, considering the current observations available and model settings. Therefore, the calibration results should be considered rather in a qualitative way. For instance, looking at the spatial distribution of residuals on the model domain (Figure 70), it is evident that there are specific zones of the model domain where the model misfit is larger. From this information we could figure out that a more precise zonation of the hydraulic conductivity could help to get a better representation of the real system. This conclusion is supported also by the bad results got for some specific observation, where the residual of calibrated model is greater than the not-calibrated one. It means that a unique parameter for hydraulic conductivity could not be feasible.

Further comments and a summary of these conclusions are also given in next section.

Finally, a model linearity test has been performed by means of the subroutine MODEL_LINEARITY distributed within UCODE-suite (Poeter et al., 2014). In particular, model linearity is evaluated using the *modified Beale's measure*, documented in Hill and Tiedman (2007). The measure for the present model is 0.48210: for values greater than 0.22, as it is in this case, the model is surely nonlinear.

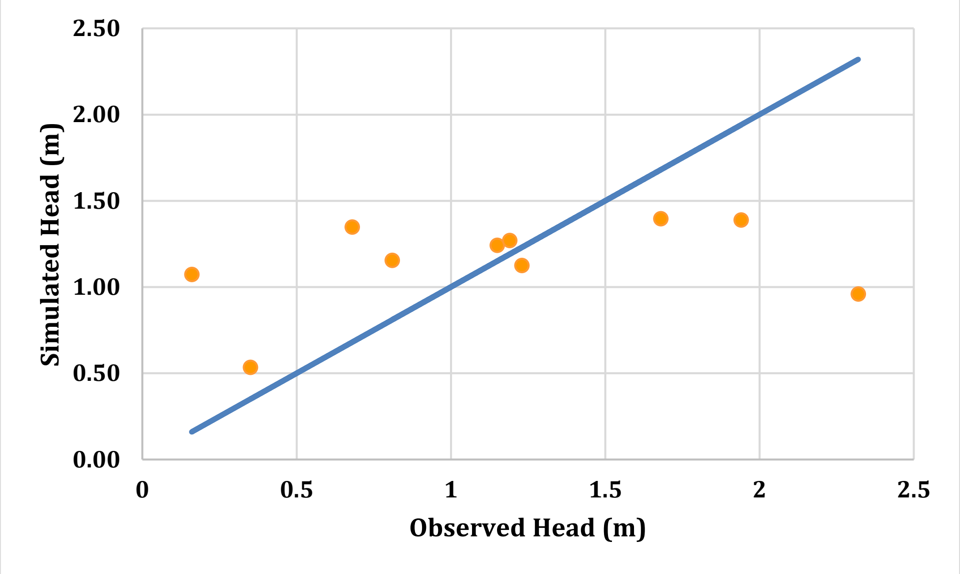

Figure 68. Plot of observed vs simulated values, after automatic calibration

	NotCalibrated	Calibrated
ME	-1.91	-0.14
MAE	3.74	3.35
RMSE	18.00	3.65
NRMSE		32%
Pearson Correlation Coefficient	0.66	0.65

Table 30. Statistics for evaluating the model fit. ME = Mean Error; MAE = Mean Absolute Error; RMSE = Root of Mean Squared Error; NRMSE = Normalized RMSE (with respect to the range of variation of observations).

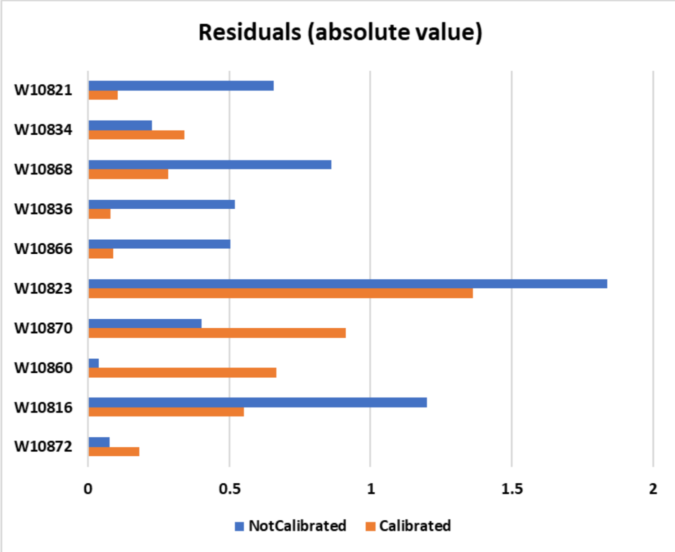

Figure 69. Comparison between calibrated and not calibrated model, according to the absolute value of error (residuals) for each observation included as targets (boreholes names are reported in Table above).

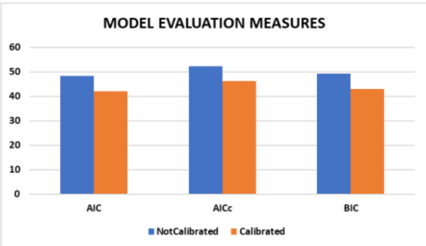

	NotCalibrated	Calibrated
AIC	48.289	42.091
AICc	52.289	46.091
BIC	49.197	42.999

Table 31. Values of model evaluation measures (Anderson et al. 2015; Hill and Tiedmann, 2007).

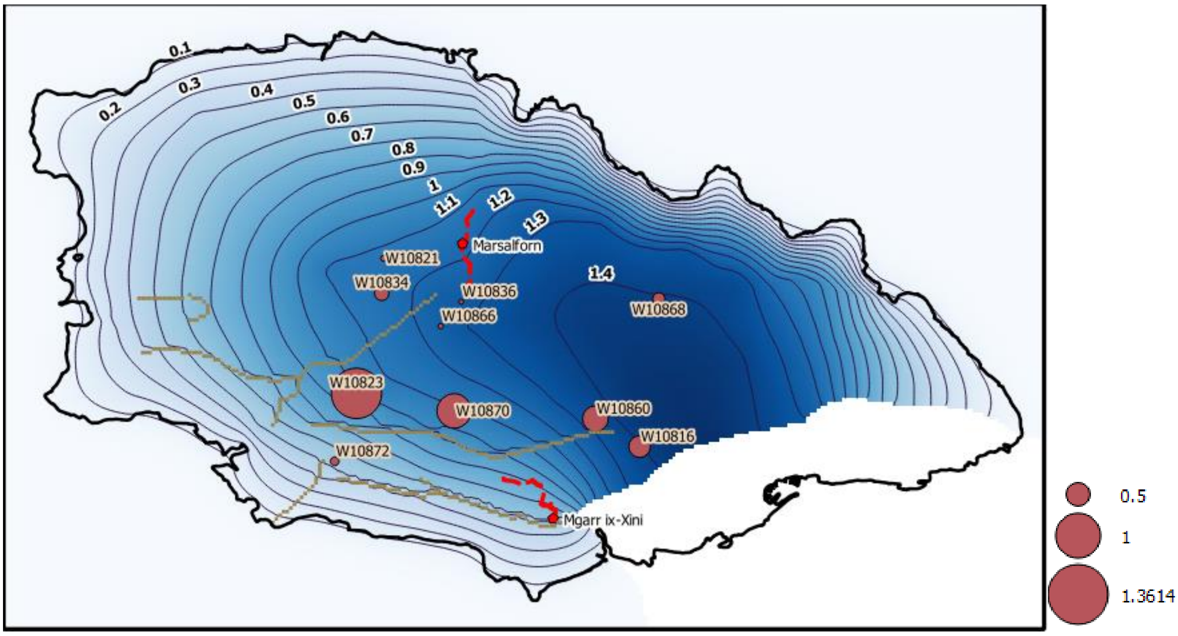

Figure 70. Bubble plots of absolute residuals (in m).

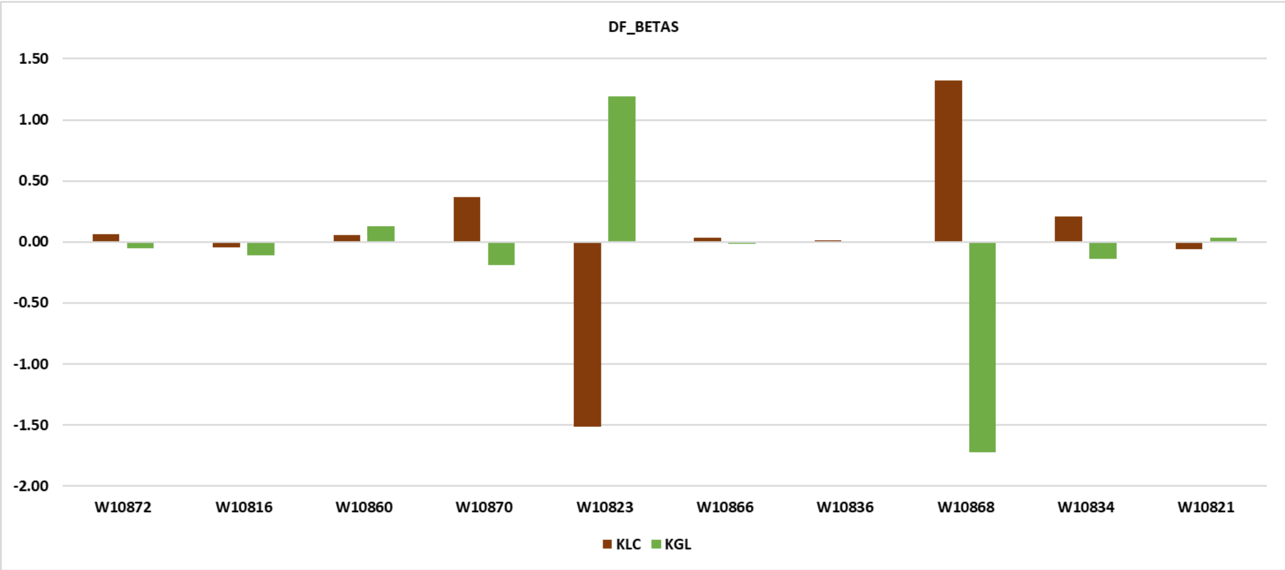

Figure 71. DFBetas Statics for each parameter, showing the influence of each observation on optimizing the single parameter (Hill and Tiedeman, 2007). Computed critical value for this statistics is 0.632: observation having an absolute value greaten than this can be considered "influential". In this case, for both parameters, they are W10823 and W10868.

Water balance and head distribution

The water budget obtained by the calibrate model is reported below.

Inflow	**m3/day**
RECHARGE	14963.2373
Total In	14963.2373

Outflow	**m3/day**
WELLS	-630.000
FLOW TO THE SEA (GHB)	-14333.2451
Total Out	-14963.2451

IN-OUT	-7.80E-03

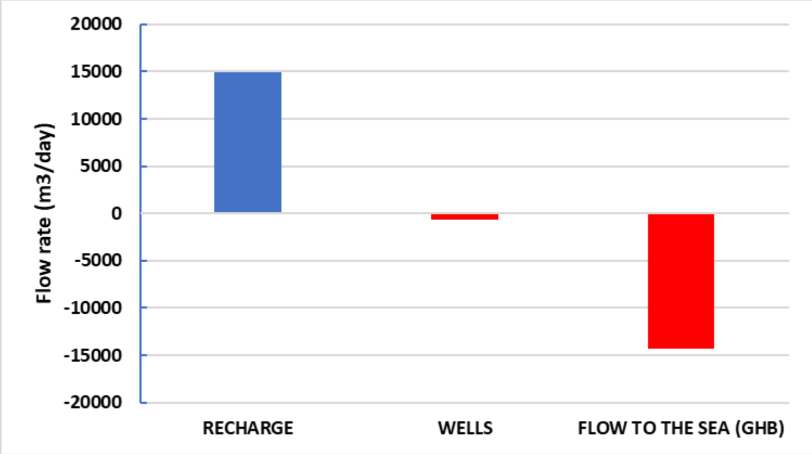

The water budget confirms that the time frame considered can be taken as a pre-exploitation period, since the influence of pumping stations is very low (around 4% of the total outflow). This result is well explained also by the map of spatial distribution of potentiometric head computed by the model (Figure 72) and its contour lines, which prove that the model solution is driven by the boundary condition at the cost line.

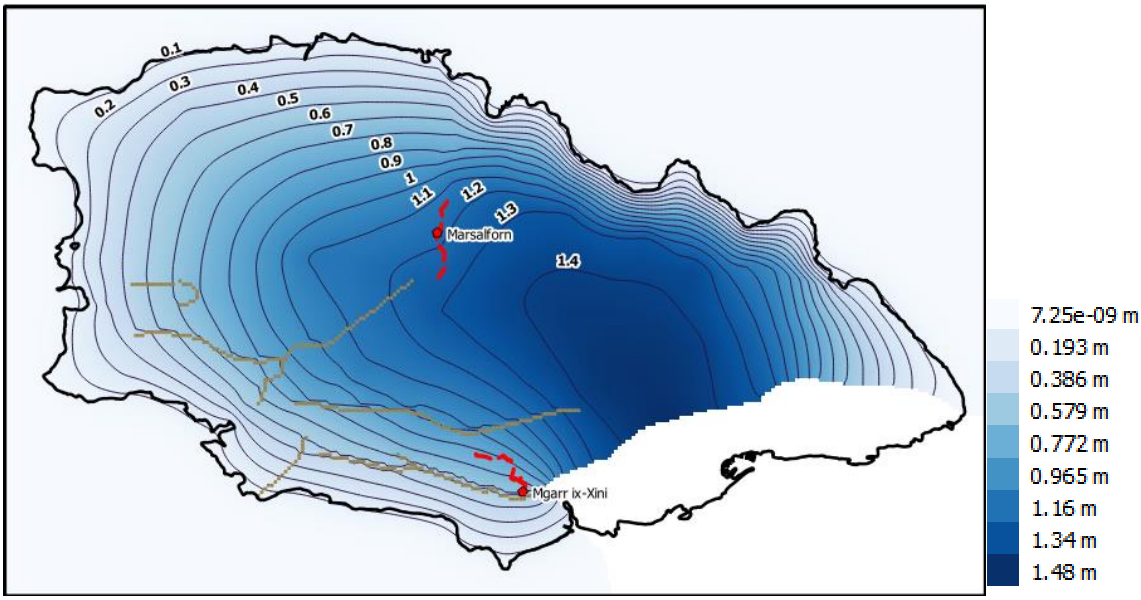

Figure 72. Map of the head (expressed in m) provided by the calibrated model, along with related contour lines.

Insights derived from the calibration process

Results of calibration process should be taken in a qualitative way, due to the following limitation of the data set available:

- The number of observations is very low (only 10 points) on a domain of around 66 km^2 of spatial extension, not uniformly distributed on the domain.
- There is not precise indication on the date of recording, neither on the real stresses present at time of recording (e.g. additional wells). Furthermore, there is only one 1 value for each point, while the model considers an annual average of all the other stresses (e.g. rainfall rate and pumping rate).
- There is no estimate for recording error, so that all readings are taken as "precise" measurement, without the possibility to weight their importance.

Even if the calibration produces a slight increase of the model performance, the model fit is not satisfactory. However, the statistics computed through the calibration give interesting suggestions:

- Measurements campaigns to get estimate of transmissivity can be done in the zone showed as more influencing in terms of KLC (Figure 67 and Table 29).
- The comparison between DSS and DFBetas results (Figure 67 and Figure 71) shows that most sensitive observations are not the ones influencing more the calibration performance.
- Results suggested that a better model fit can be achieved only by setting a more distributed value of conductivity, since the selection of only two zones seems not promising. However, it is clear that not having (currently) any estimate of transmissivity, it makes no sense to define a finer zonation for conductivity.
- A part the estimate of parameters, the water budget the head distribution shows that the model solution is dominated by the sea-side boundary condition. Therefore, it could represent a good initial condition for next transient simulations, since it is a feasible representation of the pre-exploitation age.

Seawater Intrusion

The calibrated version is used to calculate the interface freshwater/saltwater by means of the package SWI - Sea Water Intrusion (Bakker, 2013). The latter is applied with the following settings:

- Initial guess of the interface set according to the Ghyben-Herzberg formula (z = -40*h) using as potentiometric head (h) the solution of the calibrated flow model.
- TIP and TOE Slope parameters (dimensionless values) are taken as the default values (namely both equal to 0.05).
- Effective porosity is taken equal to 0.2.

Application of SWI gives the spatial distribution of the interface showed in Figure 74. A 3D representation of the interface is reported in Figure 75.

The minimum of the interface is achieved almost in the east part of the aquifer. The most influent pumping gallery generates a slight and local up-coning of the interface, even if not so relevant, since the peak of the interface is not achieved near the pumping gallery localization.

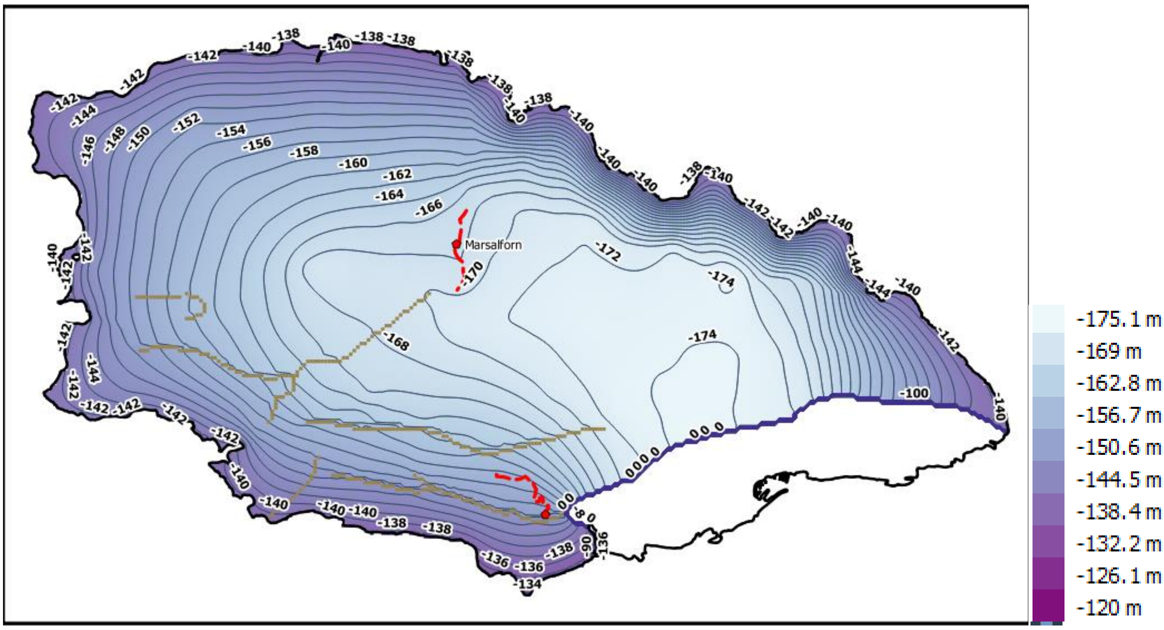

Figure 73. Map of the computed elevation of saltwater interface.

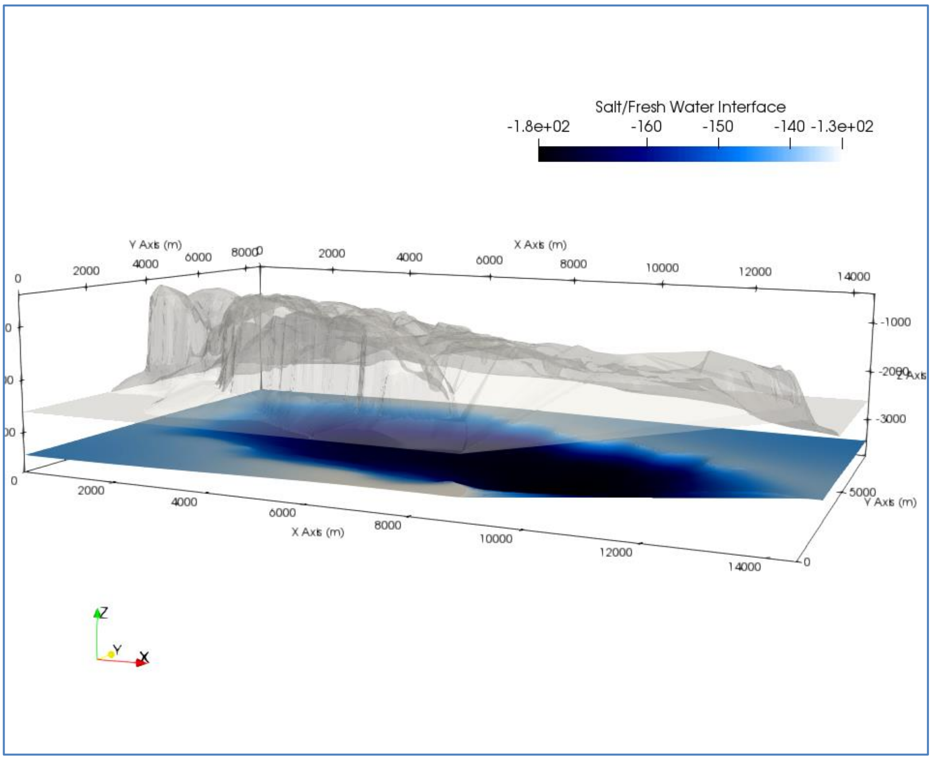

Figure 74. 3D representation of the interface (showed with a vertical exaggeration of 10 times along z-axis)

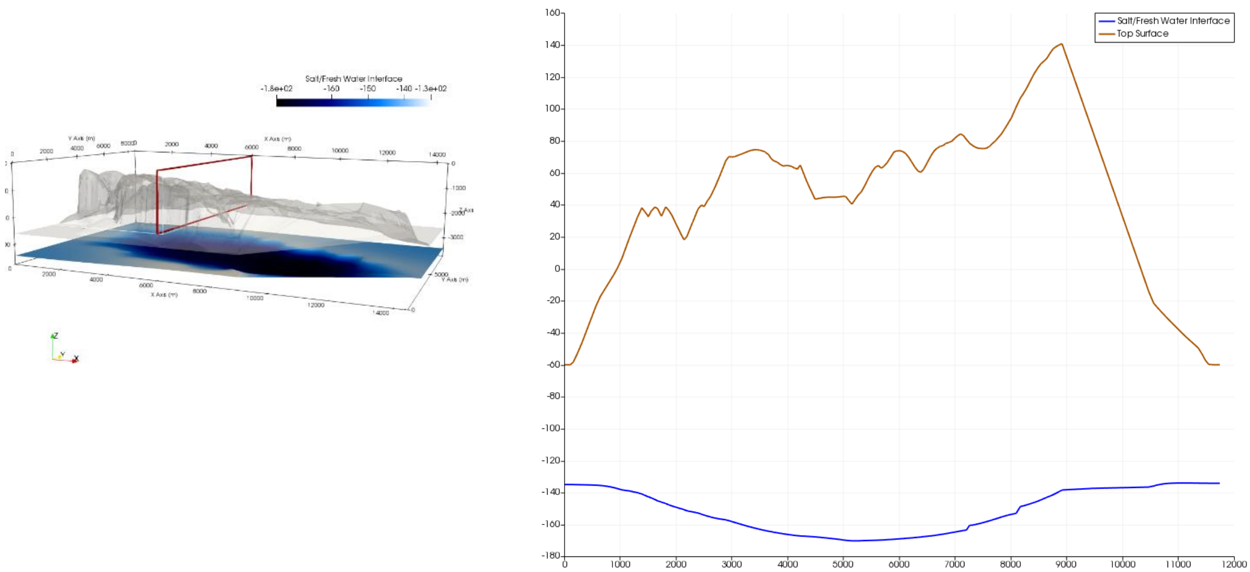

Figure 75. Cross section of the 3D image (along South-North direction), showing the interface elevation vs the top surface elevation.

Ghajnsielem Perched Aquifer

Hydrogeologic characterization and conceptual model

The Ghajnsielem perched aquifer lies within the UCL which reaches a maximum thickness of 87 m and shows considerable variations in permeability and porosity. In general, the formation is highly fractured and cavernous whilst the piezometric height varies from west to east. Within this groundwater body two synclinal structures occur. The main one is a downthrown trough or graben produced by subsidence between two normal faults; the Ghajnsielem-Qala fault to the north and to the south by a subsidiary fault down throwing to the north. The trough lies north of Ghajnsielem village and is crossed by the Victoria – Qala road.

The floor of the graben is synclinal and corresponds with the top of the BC placed at sea level. At the western flank of the graben, the BC rises to around 60 m a.m.s.l. whereas to the east the clay reaches around 40 m a.m.s.l.

Further details about the conceptual model have been presented in Deliverable D1.3. The hydrogeological scheme there depicted is reported in Figure 76

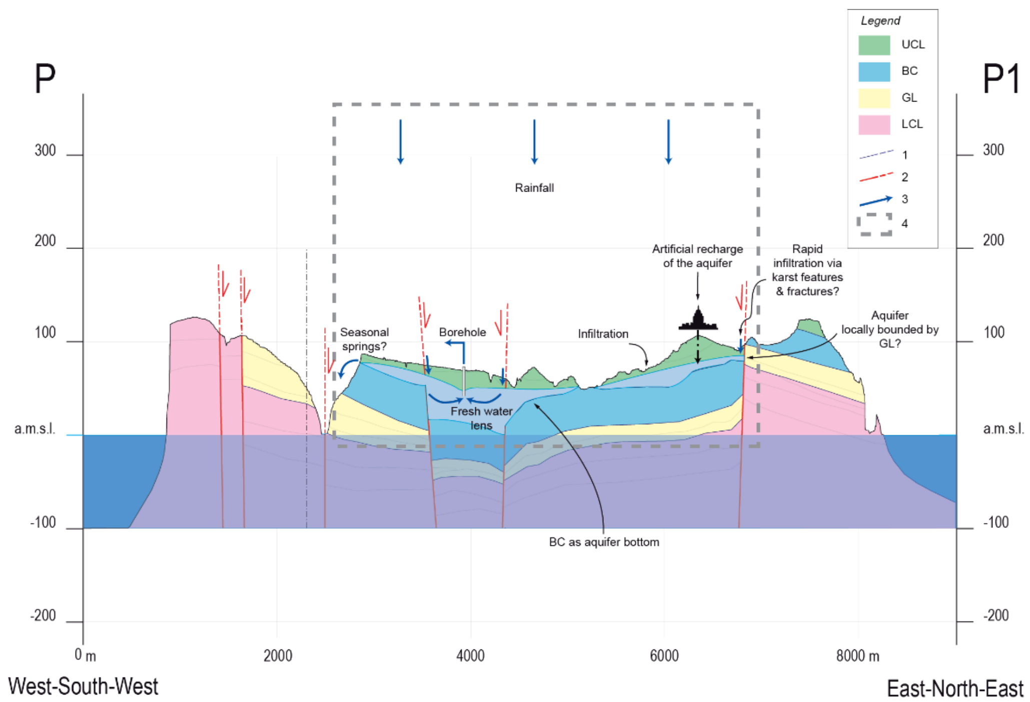

Figure 76. Ghajnsielem perched aquifer hydrogeological conceptual scheme: filled polygons – hydrogeological units; 1 – hydrogeological units contacts; 2 – faults (observed or inferred); 3 – flow directions; 4 – Area of Interest of Ghajnsielem perched aquifer.

The approach of treating the perched aquifer as a separate model (see the Introduction) allows to isolate the aquifer from the sea and from the underlying formations. However, it implies that outflow in the aquifer have to be assumed, since the simulated age (1941 – 1944) did not present any abstraction. To this purpose, two different type of (potential) water outflows are set up, as described in the Boundary Conditions section later on.

Model design

Model domain and spatial discretization

The model domain covers all the aquifer, having a length of around 2 km (along the North-South direction) and a width of around 4.5 km (along the West-East direction). This domain is discretized with a grid having a cell size of 20m, and resulting in 23175 cells, namely 103 rows by 225 columns. In the vertical direction the aquifer is represented by only one layer. Top of the layer corresponds to the top surface (passed to the model through the DEM available in the data set), while the bottom is represented as the physical limit of the UCL formation, derived by the new stratigraphy and geological surfaces obtained in Activity 1. The bottom elevation is reduced to (top-15m) wherever this quota exceeds the top surface. The active domain consists of 6776 cells (Figure 77).

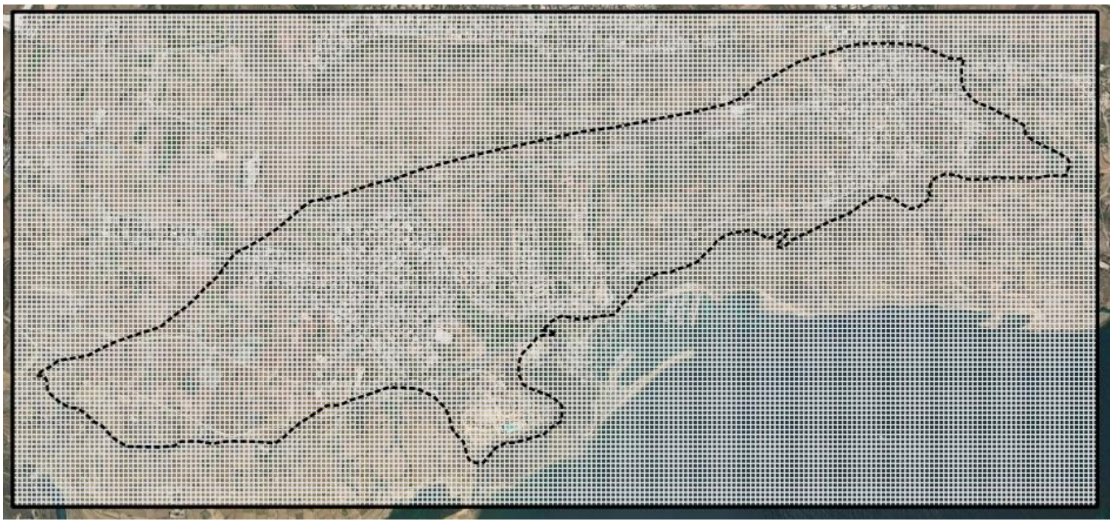

Figure 77. Model domain and model grid.

Hydrodynamic parameters and faults

No estimate of transmissivity or conductivity is available for this aquifer. Information about the permeability of UCL in this region is available in Bakalowicz and Mangion (2003) the primary matrix permeability is estimated to be around 8.64E-04 m/day. However, the formation has a high variable composition, even with presence of karst phenomena. This suggests that the effective hydraulic conductivity is comparable with the LCL, and thus in this model it has been set as almost everywhere equal to 13.5 m/day (the LCL-geometric mean used also in Gozo MSLA model), except where faults are present. The latter are represented with a value of K = 8.64E-3 m/day. The value of the main conductivity has been furtherly investigated during the calibration process.

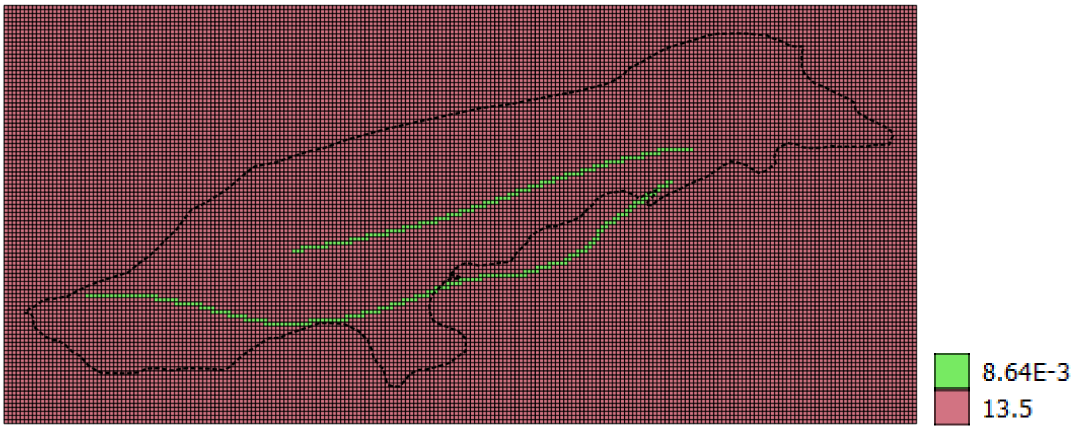

Figure 78. Value of the hydraulic conductivity and its distribution expressed in m/day.

Boundary condition

The model boundary is everywhere a no flow boundary. Since it is needed to define outflows boundaries (to close the water budget), the bottom of the aquifer is assumed to produce a slight leakage towards the underlying formation. This setting serves to include in the model as a hydrogeological assumption, to be evaluated and potentially assessed/confirmed by on field investigations.

To set the conductance as leading parameter, the head boundary in GHB is set to 0 m. a.s.l. This assures that this condition is always a sink term (i.e. the imposed boundary head is always below the simulated one).

A constant conductance is then applied. Since in (BRGM, 1991) an estimate of 1.7E-4 m/day is given as leakage from perched aquifers, this value is taken as reference: from this information, a first guess value for the conductance is derived equal to 1E-3 m^2/day. This value is assessed later on in the calibration phase.

The other potential water sinks are drains (springs) assumed to existing on two regions:

- The west side of the aquifer, where the boundary is represented by a fault (see the geological section above).
- A region almost on the center of the aquifer, where the bottom of UCL outcrops the ground surface.

These assumed sink zones are represented as drain cells as depicted in Cells where the Drain package (DRN) is applied to mimic potential springs. (Figure 79). The guess value for drain conductance is taken as follows:

- C = 8 m^2/day for the west-side drain.
- C = 10 m^2/day for the central-east drain.

Figure 79. Cells where the Drain package (DRN) is applied to mimic potential springs.

Aquifer recharge

The computation of spatially distributed recharge rate done for Gozo MSLA model has the whole island as domain. Therefore, this result is used in this model as well, once clipped on the model domain (Figure 80).

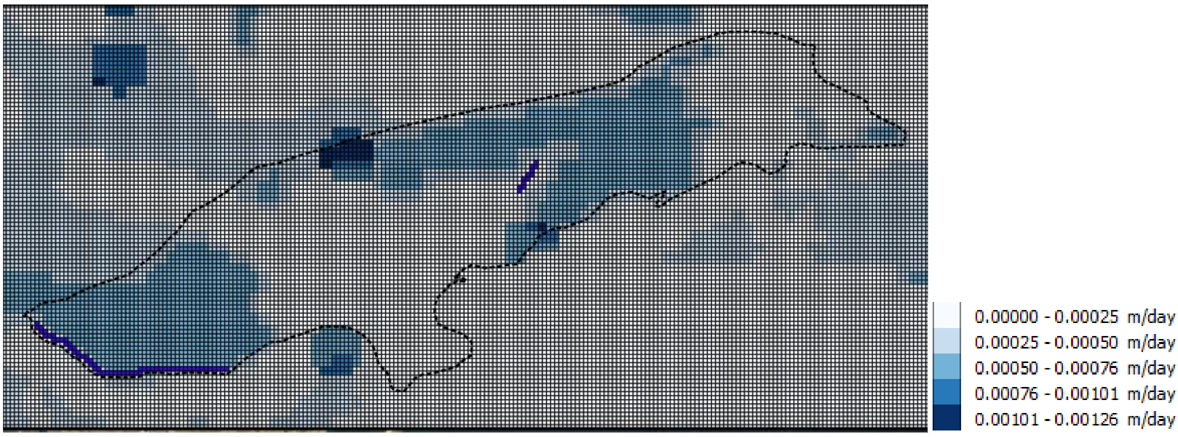

Figure 80. Spatially distributed recharge applied by means of the RCH package.

Model Run (not calibrated)

The head resulting from the not calibrated model are higher than expected. The calibration process (see later on) will make use the measurements done in Costain (1968) to assess the value of leakage conductance and drains conductance. However, the not calibrated model is already compliant with the following expectations:

1. The contribute of the drains to outflow terms in the water budget is larger than the one of leakage. It means that conductance values (even if to be calibrated) are in a reliable range.
2. The dry cells obtained on the east-north and south-west parts of the model reflects the real presence of a very low saturated thickness: it means that model reproduces correctly the morphology of the aquifer. To show evidence of this, in Figure 78 a detail of the aquifer thickness and head elevation is reported.

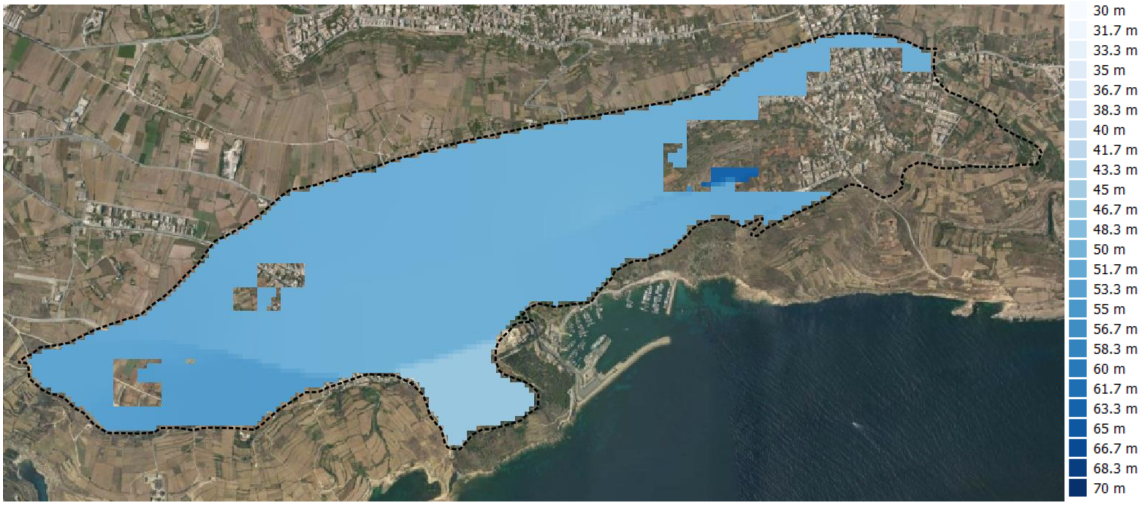

Figure 81. Distribution of head on the model grid (active cells). Dry cells are not represented

Sensitivity and calibration

Observations (calibration targets)

A set of 25 observation points are available from the study documented in (Costain, 1958). Among these, only 18 have been selected (Table 32). Some target was excluded because not belonging to the model domain (corresponding to the 5 points reported with a light red background color in the table). Some 2 other measurements have been excluded because presenting a negative value of depth to water table (light blue background color in the table). A map of these targets is shown in Figure 82where the points are classified according to the regions identified in (Costain, 1958), namely:

- Trough,
- Basin,
- Wied Biljun,
- West Ghajnsielem,
- Qala West,
- Chambray.

As stated in (Costain, 1958), the most relevant regions from a groundwater storage point of view are the Trough and the Basin. Measurements were made in July 1957, which was documented as the middle of dry season in that year.

ID	Point Name	Region	Height	Tot Depth	Depth to Top BC	Depth to Water Table	Height of BC	Height of Water	Saturated Thikness
1412	bh1412	Chambray	69.1896	14.0208	13.1064	11.5824	56.0832	57.6072	1.524
1416	bh1416	Qala_west	78.0288	30.7848	28.956	23.4696	49.0728	54.5592	5.4864
1418	bh1418	Qala_west	68.58	14.6304	14.0208	11.2776	54.5592	57.3024	2.7432
1429	bh1429	Qala_east	87.4776	8.2296	7.62	7.3152	79.8576	80.1624	0.3048
1435	bh1435	Qala_east	109.728	15.5448	14.9352	-304.495	94.7928	-304.495	-399.288
1436	bh1436	Qala_east	78.0288	28.956	28.956	24.9936	49.0728	53.0352	3.9624
1443	bh1443	Basin	91.1352	44.5008	43.8912	32.004	47.244	59.1312	11.8872
1449	bh1449	Trough	89.6112	63.3984	58.8264	40.8432	30.7848	48.768	17.9832
1458	bh1458	West Ghaj	64.008	20.1168	19.812	10.9728	44.196	53.0352	8.8392
1461	bh1461	Trough	75.8952	56.0832	53.9496	27.1272	21.9456	48.768	26.8224
1464	bh1464	Trough	88.0872	81.3816	79.5528	39.9288	8.5344	48.1584	39.624
1466	bh1466	Trough	66.1416	39.624	38.7096	17.3736	27.432	48.768	21.336
1469	bh1469	North Ghaj	59.7408	13.4112	11.2776	9.144	48.4632	50.5968	2.1336
1471	bh1471	West Ghaj	67.056	11.2776	9.7536	9.7536	57.3024	57.3024	0
1473	bh1473	Wied Biljun	79.248	15.8496	14.3256	-304.495	64.9224	-304.495	-369.417
1475	bh1475	Trough	70.7136	42.9768	42.3672	21.9456	28.3464	48.768	20.4216
1476	bh1476	West Ghaj	81.6864	37.7952	37.7952	28.956	43.8912	52.7304	8.8392
1478	bh1478	Trough	80.772	60.3504	60.0456	31.3944	20.7264	49.3776	28.6512
1479	bh1479	Trough	79.5528	64.9224	64.3128	30.7848	15.24	48.768	33.528
1480	bh1480	Trough	81.3816	62.7888	60.6552	30.7848	20.7264	50.5968	29.8704
1481	bh1481	Basin	85.344	50.292	48.768	25.6032	36.576	59.7408	23.1648
1485	bh1485	Basin	75.5904	32.9184	31.3944	15.5448	44.196	60.0456	15.8496
1497	bh1497	Wied Biljun	52.1208	4.8768	3.6576	2.7432	48.4632	49.3776	0.9144
1499	bh1499	Wied Biljun	53.9496	7.62	--	6.4008	--	47.5488	--
14006	bh14006	Trough	84.4296	40.2336	--	29.8704	--	54.5592	--

Table 32. Observations point for piezometric level. Values expressed in m.

Figure 82. Position of the 18 target points used for sensitivity and calibration, colored according to the region classification identified in (Costain, 1958).

Parametrization and Sensitivity

A first sensitivity procedure has been applied to study the model dependence upon the different stresses imposed. The model has been parametrized using the 5 parameters reported in Table 33.

Parameter	Description	Starting value
KA	Aquifer hydraulic conductivity (horizontal component)	13.50 m/day
KF	Hydraulic conductivity assigned to faults (horizontal component)	8.64E-3 m/day
GHC	Conductance of GHB condition on bottom	1.00E-3 m^2/day
DRWC	Conductance of west-side drain	8.0 m^2/day
DREC	Conductance of east-side drain	10.0 m^2/day

Table 33. Parameters defined for studying the sensitivity of the model

The sensitivity analysis was run by applying UCODE automatic calibration program (Poeter et al., 2014). Results summarize in the following findings:

- There is a high correlation between KF and DREC (0.98), which could indicate that there may not be enough information in the observations used in the regression to estimate these parameter values individually (Table 34). Other important correlations (namely larger than 0.90) are between KF and DRWC (0.94) and DRWC and DREC (0.91).
- Composite Scaled Sensitivity (CSS) shows that DREC is the most important parameter, followed by KF and KA. A negligible importance, conversely, is showed by DREWC.

These results suggest the following settings for the calibration process:

(i) Excluding KF from the calibration, since it is highly correlated with DREC and not much more influent than KA; furthermore, it is a value to simulate a quasi-no flow condition, and therefore it can be justified as a modeling approach than an hydrogeological parameter.
(ii) Excluding also DRWC, having a low importance, and being correlated to DREC.

Finally, the calibration involved firstly only KA, GHC and DREC parameters (see next section).

	KA	KF	GHC	DRWC	DREC
KA	1	0.20	-0.81	0.12	0.17
KF		1	-0.65	0.94	0.98
GHC			1	-0.54	-0.67
DRWC				1	0.91
DREC					1.0

Table 34. Parameters correlation matrix.

PARAMETER	CSS	RATIO to Maximum
DREC	77.67	1.00E+00
KF	33.15	4.27E-01
KA	32.67	4.21E-01
GHC	26.19	3.37E-01
DRWC	3.08	3.96E-02

Table 35. Composite Scaled Sensitivities (CSS), to show the overall importance of each parameter on the simulate values evaluated at all targets (Hill and Tiedeman, 2007).

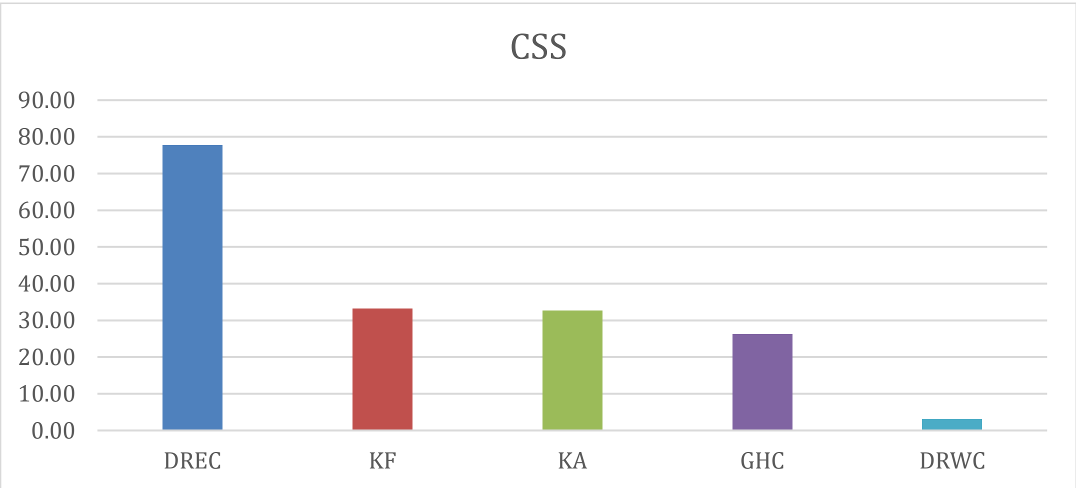

Figure 83. Plot of CSS values (see Table 35).

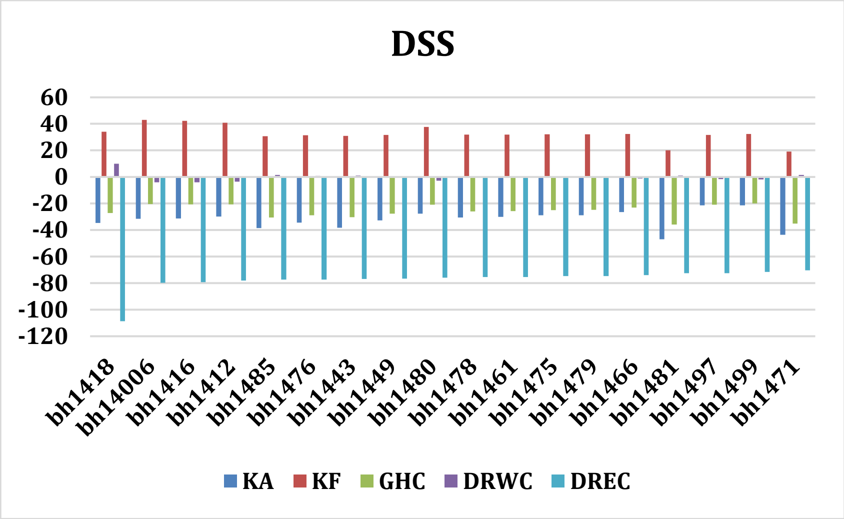

Figure 84. DSS – Dimensionless Scaled Sensitivity, which shows the importance of each observation to estimate the single parameters. Notice that this statistics is fit-independent (Hill and Tiedeman, 2007).

Calibration and residuals analysis

Using the 3 selected parameters (KA, GHC and DREC) for calibration, the following results are obtained:

- KA = 1.0 m/day (equal to the lower constraint set up for KA)
- GHC = 2.352E-03 m^2/day
- DREC = 392.8 m^2/day

Convergence of the optimization algorithm is achieved smoothly (even imposing a stringent convergence criterium), however it is evident that the calibrated value for KA is not realistic, being a value for UCL which is even lower than what measured for LCL in Malta MSLA. Therefore, the result is annalistically correct but far away from the hydrological meaning of this parameter. Furthermore, this result is the lower bound imposed by the modeler: it means that optimization would suggest (in this setting) a value potentially even lower than what obtained, and so even more far away from reality.

To cope with this issue, KA is taken out from calibration process. This choice is also supported by the value of CSS for KA (Table 35), which is not the most important.

Finally, the automatic optimization procedure to calibrate GHC and DREC, led to the following values

- GHC = 1.00E-03 m^2/day.
- DREC = 22.37 m^2/day.

However, as for Gozo MSLA, from an analytical point of view, the quality of the model fit is poor, as evident by the correlation plot (Figure 85), (Figure 86) and model fit statistics (Table 36). The convergence is reached by imposing a strong tolerance value (coefficient TolPar in UCODE equal to 1E-03, expressing the tolerance of maximum fractional change in parameter values between two consecutive iterations), and it is achieved in only 4 iterations (out of 20 imposed as maximum number of iteration).

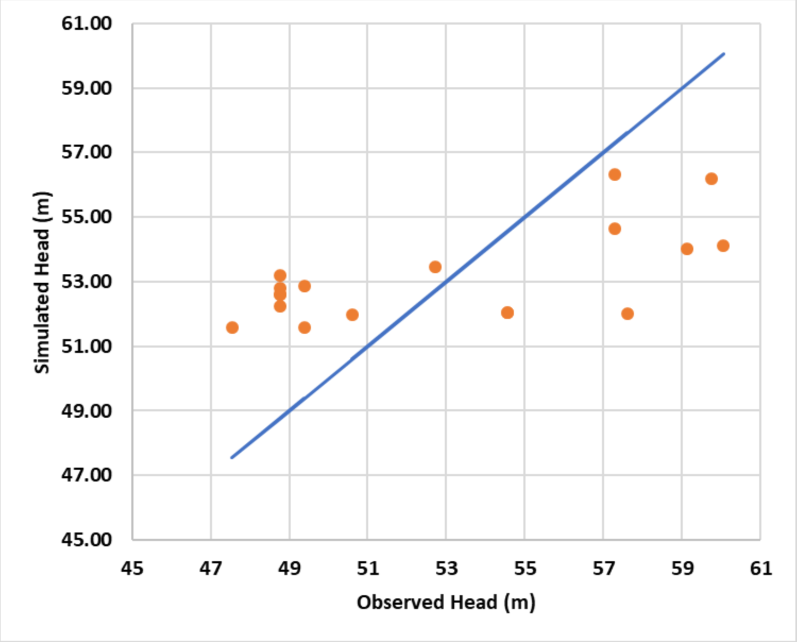

Figure 85: Simulated vs Observed values of head (expressed in m.).

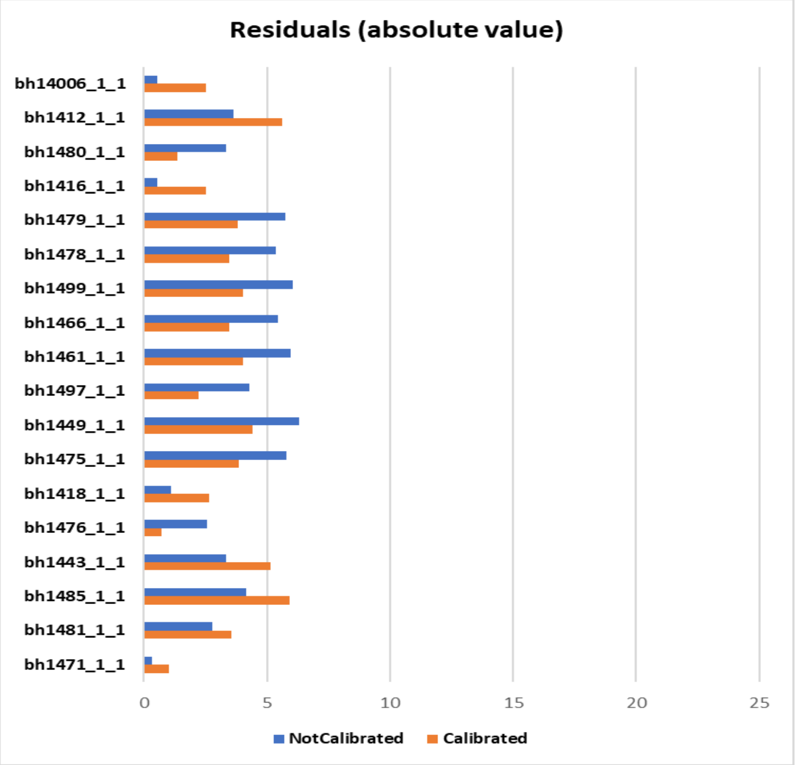

Figure 86. Comparison between calibrated and not calibrated model, according to the absolute value of error (residuals) for each observation included as targets (boreholes names are reported in Table above).

	NotCalibrated	Calibrated
ME	-1.91	-0.14
MAE	3.74	3.35
RMSE	18.00	3.65
NRMSE		32%
Pearson Correlation Coefficient	0.66	0.65

Table 36. Statistics for evaluating the model fit. ME = Mean Error; MAE = Mean Absolute Error; RMSE = Root of Mean Squared Error; NRMSE = Normalized RMSE (with respect to the range of variation of observations).

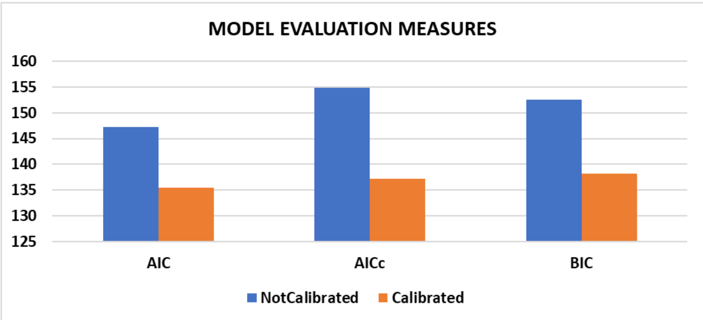

	NotCalibrated	Calibrated
AIC	147.25	135.45
AICc	154.88	137.17
BIC	152.59	138.12

Table 37. Values of model evaluation measures (Anderson et al. 2015; Hill and Tiedman, 2007).

Figure 87. Bubble plots of absolute residuals (in m). Points are colored according to the different region classification, according to Costain (1958).

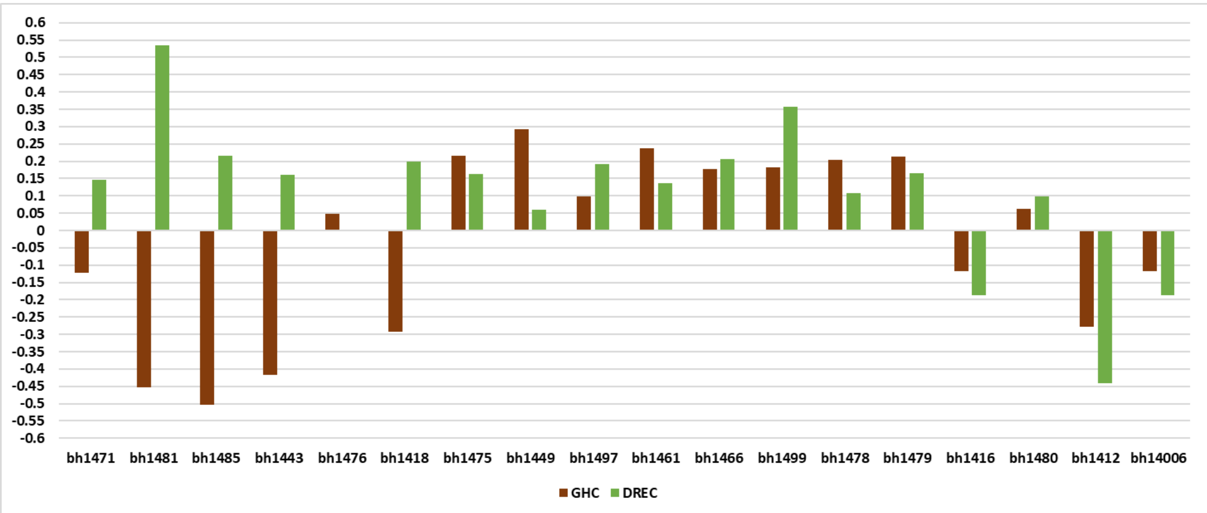

Figure 88. DFBetas Statics for each parameter, showing the influence of each observation on optimizing the single parameter (Hill and Tiedeman, 2007). Computed critical value for this statistics is 0.471: observation having an absolute value greaten than this can be considered "influential". In this case, for DREC parameters it is observation bh1481; for GHC parameter it is observation bh1485.

Water Balance and head distribution

The water budget obtained by the calibrate model is reported below. The numerical accuracy of the model is confirmed by the water budget discrepancy, which is basically 0% (at the third decimal figure).

Inflow	
RECHARGE	715.3686
Total In	715.3686

Outflow	
DRAIN WEST	0.00
DRAIN EAST	-421.96
LEAKAGE	-293.4065
Total Out	700.667

IN-OUT	-0.00153

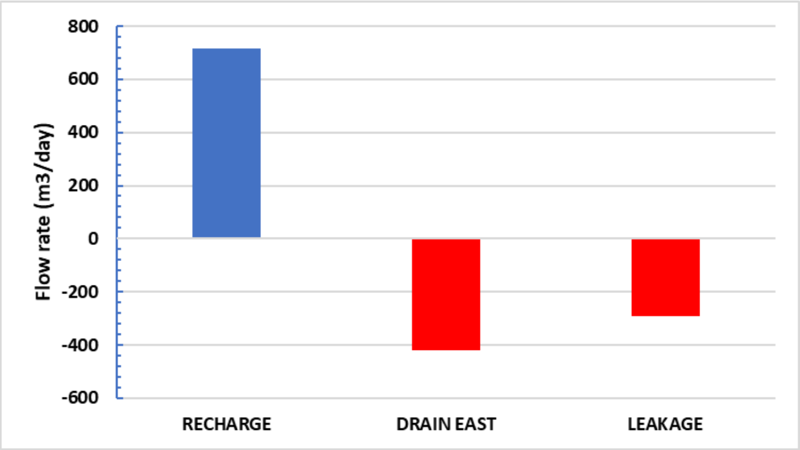

The spatial distribution of head is reported in Figure 89, where the drain line representing the sink in the central-east part is reported as well.

The terms of the budget obtained in the steady state are then commented in next section.

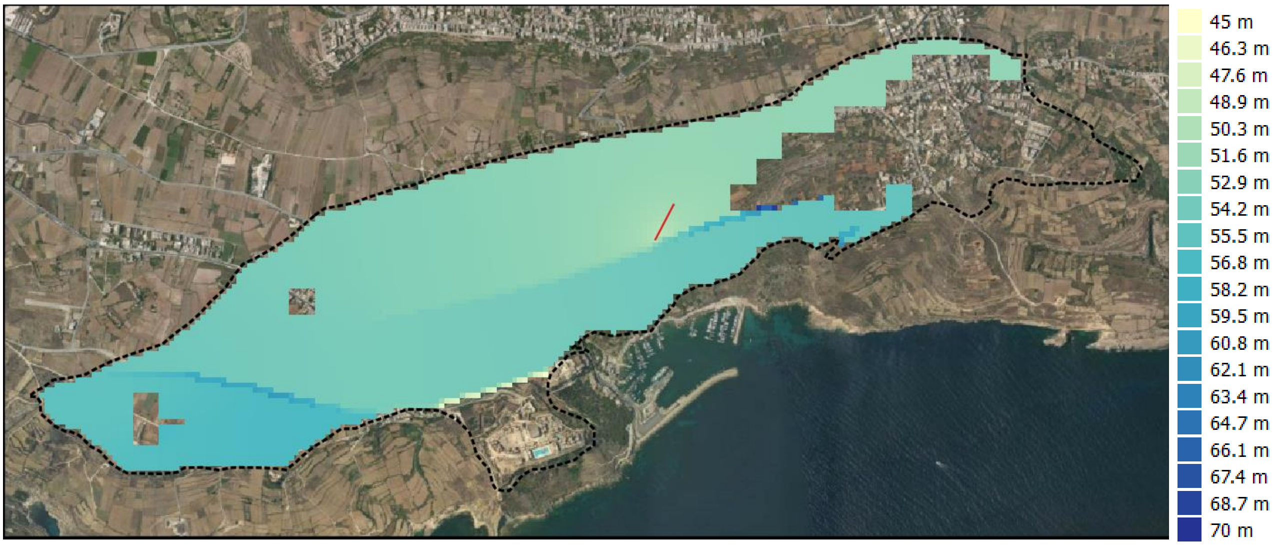

Figure 89. Spatial distribution of simulated head in the aquifer. In red the central drain line is represented.

Insights derived from the calibration process

The calibration procedure increased the model performance (measured using Model Evaluation indicators, see Table 37) but the model fit is not satisfactory, as shown by all the model-fit measures (see for instance Table 36). However, as for Gozo MSLA, the calibration results need to be evaluated from a qualitative point of view, due to the considerable lack of information, that implies a low conditioning of the model from real world information. In particular, the following findings can be argued from this model stage.

- The assumption of considering three types of different outflows distributed on the model domain, seems to be feasible for only 2 of them, namely the central-east drain and the vertical downward leakage through Blue Clay formation. As a matter of fact, the calibrated values of parameters lead to a water budget in which the west-side drain is not active at all. This result needs to be confirmed or rejected by collecting some information on the west-side part of the aquifer (Basin region).
- The importance of acquiring more information on the basin is also guided by the analysis of influencing observations arising from results of the DFBetas statistics (Figure 88): the most influencing observations (in terms of optimization problem) are all placed in the Basin (observations bh1481, bh1485).
- The simplified assumption of considering only one aquifer conductivity, KA (which is the sole feasible assumption due to the lack of prior information) needs to be removed and substituted by a zonation of conductivity, after acquisition of conductivity estimates. The calibration is indeed not so much affected by varying KA (see Table 35, for instance), since in the current setting the model is dominated by the geometry (elevation of top and bottom).
- Under these assumptions, the estimated vertical leakage is in line with the values estimated in former modelling studies (e.g. BRGM, 1991). In particular, considering an aquifer area of 2.75 km^2, the obtained leakage flux is equal to 1.07E-04 m/day, which is comparable with the one estimated by (BRGM, 1991), namely 1.70E-04 m/day.
- The water drained by the central-east source amounts at 421.96 m^3/day, which is a feasible value if compared with the geometric mean of the measurements done for some springs in Malta islands (BRGM, 1991), namely 332.41 m^3/day.

References

Anderson M., Woessner W., Hunt R. (2015). Applied groundwater modeling. Simulation of flow and advective transport. Second Edition. Elsevier.

ArcMap online manual (2019) - "Elevation Void Fill function". Link: http://desktop.arcgis.com/en/arcmap/latest/manage-data/raster-and-images/elevation-void-fill-function.htm. [last accessed: September 2019].

Aster, R., Borchers, B., and Thurber, C. (2005). Parameter estimation and inverse problems: Burlington, Mass., Elsevier Academic Press, 301 p

ASTM D5447 – 04, 2010. Standard guide for application of a groundwater flow model to a site-specific problem.

Bakalowicz M. and Mangion J. (2003). The limestone aquifers of Malta; their recharge conditions from isotope and chemical surveys. 49-54 in Hydrology of the Mediterranean and Semiarid Regions. Proceedings of an International Symposium. Montpelier. 2003. Publication no. 278, (Wallingford: IAHS).

Bakker, Mark, Schaars, Frans, Hughes, J.D., Langevin, C.D., and Dausman, A.M. (2013), Documentation of the seawater intrusion (SWI2) package for MODFLOW: U.S. Geological Survey Techniques and Methods, book 6, chap. A46, 47 p., http://pubs.usgs.gov/tm/6a46/

Bureau de Recherche Géologique et Minière - BRGM (1991). Study of the fresh-water resources of Malta.

Cassar J., Marocchi A., Santarelli M. L. & Muscat M (2008). Controlling crystallization damage by the use of salt inhibitors on Malta's limestone. Materiales de Construcción, Vol. 58, 289-293.

Celico P. (1986) - Prospezioni idrogeologiche. 1-2, Liguori editore, Napoli

Certes C, de Marsily G. (1991). Application of the pilot-points method to the identification of aquifer transmissivities: Advances in Water Resources

Civita M. (2005) - Idrogeologia applicata e ambientale. Casa Editrice Ambrosiana

Costain LTD (1958a). Report on Geological Investigation of the Mizieb Basin. Government of Malta - Water Supply, September 1958.

Costain LTD (1958b). Report on Geological Investigation of the Ghajnsielem/Qala Area and Fault. Government of Malta - Water Supply, September 1958.

Delang O. (2019). Vector Bender v0.2. QGIS Plugin. Link: https://github.com/olivierdalang/VectorBender

de Marsily, G., Lavedan, C., Boucher, M., and Fasanino, G. (1984). Interpretation of interference tests in a well field using geostatistical techniques to fit the permeability distribution in a reservoir model, in Verly, G., David, M., Journel, A.G., and Marechal, A., Geostatistics for natural resources characterization: NATO Advanced Study Institute, ser. C 182, p. 831–849

Doherty, J. (2015). Calibration and uncertainty analysis for complex environmental models - PEST: complete theory and what it means for modelling the real world. Watermark Numerical Computing, Brisbane, Australia

Doherty J. (2003). Groundwater model calibration using Pilot Points and Regularization. Ground Water

Doherty J., Fienen M., Hunt R. (2010). Approaches to highly parameterized inversion: Pilot-point theory, guidelines, and research directions: U.S. Geological Survey Scientific Investigations Report 2010–5168, https://pubs.usgs.gov/sir/2010/5168/pdf/sir20105168.pdf

Doherty J., Hunt R., Tonkin M. (2010). Approaches to highly parameterized inversion: A guide to using PEST for model-parameter and predictive-uncertainty analysis. U.S. Geological Survey Scientific Investigations Report 2010–5168, https://pubs.usgs.gov/sir/2010/5211/pdf/uncpest_sir2010-5211.pdf

Doherty J. (2007). Groundwater data utilities—Part A, Overview: Brisbane, Australia, Watermark Numerical Computing, 67 p

Doherty J. (2008). Guidelines for groundwater model calibration using regularized inversion: Brisbane, Australia, Watermark Numerical Computing, 41 p.

Harbaugh A.W. (2005). MODFLOW-2005, The U.S. Geological Survey modular ground-water model—the Ground-Water Flow Process: U.S. Geological Survey Techniques and Methods 6-A16.

Hill M.C. and Tiedeman C.R. (2007). Effective Groundwater Model Calibration: with Analysis of Data, Sensitivities, Predictions, and Uncertainty, John Wiley and Sons, New York.

Hunt R.J., Doherty J., Tonkin M.J. (2007). Are models too simple? Arguments for increased parameterization: Ground Water, v. 45, no. 3, p. 254–262, doi:10.1111/j.1745-6584.2007.00316.x

Lang D.M. (1960). Soils of Malta and Gozo. [Colonial Research Series Nº29]; London: HMSO.

LaVenue M., de Marsily G. (2001). Three-dimensional interference test interpretation in a fractured aquifer using the pilot-point inverse method. Water Resources Research

LaVenue A.M. and Pickens J.F. (1992). Application of a coupled adjoint sensitivity and Kriging approach to calibrate a groundwater flow model: Water Resources Research, v. 28, no. 6, p. 1543–1569, doi:10.1029/92WR00208

LaVenue A.M., RamaRao B.S., de Marsily G., Marietta M.G. (1995). Pilot-point methodology for automated calibration of an ensemble of conditionally simulated transmissivity fields—2, Application: Water Resources Research, v. 31, no. 3, p. 495–516, doi:10.1029/94WR02259

Malta Environment & Planning Authority (2013) - ERDF 156 data Developing National Environmental Monitoring Infrastructure and Capacity.

Menke W. (1984). Geophysical data analysis—Discrete inverse theory: New York, Academic Press Inc., 289 p

Muffels C.T. (2008). Application of the LSQR algorithm to the calibration of a regional groundwater flow model—Trout Lake Basin, Vilas County, Wisconsin: University of Wisconsin-Madison, Department of Geology and Geophysics, M.S. thesis, 106 p.

Oil Exploration Directorate, Office of the Prime Minister (1993). Geological Map of the Maltese Islands: Sheet 1 - Malta; Sheet 2 - Gozo and Comino.

Poeter E.P., Hill M.C., Lu D., Tiedeman C.R. and Mehl S. (2014). UCODE_2014, with new capabilities to define parameters unique to predictions, calculate weights using simulated values, estimate parameters with SVD, evaluate uncertainty with MCMC, and more: Integrated Groundwater Modeling Center Report Number GWMI 2014-02.

RamaRao B.S., LaVenue A.M., de Marsily G., Marietta M.G. (1995). Pilot point methodology for automated calibration of an ensemble of conditionally simulated transmissivity fields, Theory and computational experiments, Water Resources Research.

Sapiano M. (2015). MARSOL Project - Deliverable D10.1: Characterisation of the sea-level aquifer system in the Malta South Region, http://www.marsol.eu/ [last accessed: March 2019].

Stuart M. E., Maurice L., Heaton T. H. E., Sapiano M., Micallef Sultana M., Gooddy D. C. and Chilton P. J. (2010). Groundwater residence time and movement in the Maltese islands – a geochemical approach.

Tarantola A. (2005). Inverse problem theory and methods for model parameter estimation: Philadelphia, Pa., Society for Industrial and Applied Mathematics, 358 p

Thornthwaite C.W., Mather J. R. (1955). The Water Balance. Publications in Climatology, Laboratory of Climatology, Vol. 8, No. 1, 104 pp

Tikhonov A.N. and Arsenin V.I.A. (1977). Solution of ill-posed problems: New York, Halsted, 258 p.

Turc L. (1961). Water requirements assessment of irrigation, potential evapotranspiration: Simplified and updated climatic formula. Annales Agronomiques, 12, 13-49

USDA - Soil Survey Staff. (1999). Soil taxonomy: A basic system of soil classification for making and interpreting soil surveys. 2nd edition. Natural Resources Conservation Service. U.S. Department of Agriculture Handbook 436

Viaroli S., Mastrorillo L., Lotti F., Paolucci V., Mazza R. (2018) The groundwater budget: a tool for preliminary estimation of the hydraulic connection between neighboring aquifers. J Hydrol 556:72–86. https://doi.org/10.1016/j.jhydrol.2017.10.066

Appendix 1. Modelling journal

Malta Mean Sea Level Aquifer model

Modelling Stage	Sub-version	Main features	Main changes	Comments
MSLA_0	v1	Toy steady state model, to get confident with model domain, grid definition, packages compatibilities, etc. Grid size: 100x100 m, layer top is taken as the DEM, bottom uniformly at -100 m. No wells and faults included. Uniform K and recharge. Mizieb, Pwales and the northern portion of the island were included in the model with fictitious bottom elevations.		The model was used mainly to test the application of SWI package. Good response of the model has been observed, so that the usage of SWI was confirmed.
MSLA_1	v1	The grid was refined to 100x50 m cells; galleries, pumping stations and public boreholes were introduced; uniform average recharge was substituted by the detailed recharge distribution of the period of reference.	Adding of public abstraction and detailed recharge distribution.	Mizieb, Pwales and the northern portion of the island is still included in the model with approximate bottom elevations.
MSLA_1	v2	Target head observations from 1944 were introduced and a preliminary zone calibration was tested to check sensitivities.	Adding of observed heads.	Water balance indicates model stability. The model results being dominated by the sea boundary conditions, with little sensitivity of hydraulic conductivities.
MSLA_1	v3	Top and bottom surfaces are now passed as the values coming from Activity 1 (data analysis). Top is the surface	Inclusion of interpolated surface	The use of the more realistic surfaces gives convergence problems.

		elaborated by CGT which excludes the Rabat-Dingli Plateau. Bottom is set as (Top-150m). Cells where bottom > (-150m) are lowered so that bottom=-150m.	to represent Top and Bottom	Mizieb, Pwales and the northern portion of the island is still included in the model with realistic bottom elevations.
MSLA_2	v1	The northern portion of the Island, Mizieb and Pwales aquifers, are excluded from the MSLA model. Linearity test performed.	Model domain reduced	The convergence problems are solved, the model is slightly non-linear and numerical noise negligible.
MSLA_2	v2	Main 11 faults are introduced as HFB boundary condition with low conductivity.	Main faults introduced	The heads distribution and flow direction are strongly affected by the presence of faults
MSLA_2	v3	Private water abstraction was introduced based on the available data.	Agricultural wells introduced	
MSLA_2	v4-v15	Sensitivities and different calibration approaches were tested; v15 reports the use of Pilot Points of K calibration in conjunction with zones defined by the main faults. Calibration technique included the Tikhonov regularization based on the preferred values defined by the available K information. Faults properties were included as parameters in the calibration process. Linearity test performed.	Regularized calibration based on K distribution and faults properties	The reported calibrated version 15 represents a compromise between the good fit of data (whose quality and representativeness are unknown) and reliable parameters inferred by the available pumping tests. The model is slightly non-linear and numerical noise negligible.
MSLA_2	v16	Time setting of the steady state model are modified, including a second stress period (first SP = 250 years; second SP = 20 years); in the first SP pumping is not present, in order to reproduce natural conditions.	Time discretization	The applied changes were necessary to run SWI2 package

MSLA_2	v17	SWI2 was set and included in the model run in order to reproduce the freshwater-seawater interface	SWI2 inputs and run	Results were exported for the first and second SP

Mizieb/Pwales Aquifer

Modelling Stage	Sub-version	Main features	Main changes	Comments
MP_0	v1	Toy steady state model, to define model domain and preliminary boundary conditions. Grid size: 25x25 m, layer top is taken as the DEM, bottom is from the reconstructed Blue Clay top. Uniform average recharge. No wells and faults included. K zones geometry according to the geological map, K values according to assumptions.		The model is highly unstable, due to the bottom irregular geometry and to the big number of dry cells. Flooded cells are also present.
MP_1	v1	Grid refined to 12.5x50 m. No-flow boundary conditions introduced to limit the domain at South and West. Private wells with supposed discharges introduced. Boundary conditions modified in order to obtain reliable heads elevations and wet cells in places where wells are present (previously dry). The three sinkholes reported in Constain (1957) are introduced as GHB boundary conditions. The bottom surface is smoothed. Linearity test performed.	Wells and sinkholes are introduced, bottom smoothed	Little improvement in convergence, but budget discrepancy still not acceptable and numerical noise higher than 4-5 m.
MP_1	v2	Bottom surface smoothed again, faults with low conductivity are introduced as HFB bc. Linearity test	Bottom smoothed, faults introduced	Little improvement in convergence, but budget discrepancy still not acceptable and numerical noise higher

		performed.		than 4-5 m.
MP_2	v1	A 3 layers version is attempted in order to solve convergence problems. A second layer is added representing Blue Clay interrupted by sinkholes; a third layer is added representing Globigerina and LCL. Linearity test performed.	2 layers are added	Improvement in convergence, budget discrepancy is still too high (>1%), the model is highly nonlinear with high numerical noise. Surfaces would need drastic simplifications. The three layers version is abandoned.
MP_3	v1	The single layer version is modified. No-flow boundary conditions introduced to limit the domain at South and West are substituted by low K zones, as well as some portion of the faults, previously represented by HFB. Bottom is smoothed, especially in portions outside the Mizieb and Pwales aquifer. Linearity test performed.	No-flow cells and some HFB cells substituted by low K zones.	Improvement in convergence, budget discrepancy acceptable and numerical noise smaller than a few centimeters. Still dry cells are present where wells are supposed to find water, and portions of the domain are flooded. The "way out" represented by the sinkhole is not sufficient to reproduce a reliable potentiometric surface. Pwales does not give particular problems, being relatively simple (and with no data).
MP_3	v2	Sensitivities are evaluated, different hypothesis are tested concerning the northern fault; eventually it is replaced by a DRAIN bc.	Northern fault substituted by a drain bc.	Heads reach a level which is comparable with measurements available in Costain 1957, but most of the Mizieb aquifer is dry even where private wells are present. No information are available about the area at the North of Mizieb, but the resulting heads does not seem to be

				reliable (connection with the drain bc).
MP_3	v3	The Northern fault is modified introducing a thin zone at low K in addition to the DRAIN bc. In order to solve the wide area with dry cells, the existence of an additional fault is supposed. Linearity test performed.	Northern fault represented by low K zone + drain bc; an additional supposed fault is placed in Mizieb	Considering that water is supposed to be present in places where wells are drilled, the dry cells problem was solved. The hypothesis of a portion of the UCL characterized by a very low hydraulic conductivity would have solved the problem, but it was rejected. Considering the ground morphology and the available stratigraphic logs, a new hypothetical low permeability fault was added. Model convergence drastically improved, budget discrepancy reduced, and numerical noise remained smaller than a few centimeters.
MP_3	v4	Parameters including hydraulic conductivity, HFB conductance, Sinkholes conductance, Drain conductance were adjusted on the basis of qualitative information about local heads in Mizieb. Hydraulic conductivity in Pwales was left uniform. Water balance for the whole domain and for each aquifer was calculated through ZONEBUDGET.	Parameter are adjusted	Parameter are adjusted according to qualitative information. Model balance results seem to be reliable. Sinkholes represent a way out from Mizieb, as well as the drain. The only way out of Pwales is represented by the sea.
MP_3	v5	Inputs for SWI2 package are added and the model run.	SWI2 run	The present preliminary rough version of the MP model does not present any evidence of seawater intrusion, being the freshwater-seawater surface equal

				to the model bottom.

Gozo Mean Sea Level Aquifer model

Modelling Stage	**Sub-version**	**Main features**	**Main changes**	**Comments**
gz_0	v1	Toy model, to get confident with model domain, grid definition, packages compatibilities, etc. Grid size: 100mx100m, layer top is taken as the DEM, bottom uniformly at -100m. No faults included. Uniform Kx=13.5m/day. Here also Ghajnsielem perched aquifer is considered and included in the model.	-	The model was used mainly to test the application of SWI package. Good response of the model has been observed, so that the usage of SWI has been confirmed. Ghajnsielem is included, but bottom surface is not the real one.
gz_1	v1	Improvement of gz_0, by including 6 pumping wells wells	Adding WEL package	The model has a good response on pumping effect and no problem in convergence is recorded.
gz_1	v2	Top and bottom surfaces are know passed as the values coming from Activity 1 (data analysis). Top is the surface elaborated by CGT. Bottom is set as (Top-100m). Cells where bottom > (-100m) are lowered so that bottom=-100m. Setting an almost impermeable conditions for cells representing faults: Kx=8.64Ee-3 m/day = 1.0E-7 m/s .	Inclusion of interpolated surface to represent Top and Bottom	Good convergence also after changing the top surface. Ghajnsielem is still included, but bottom surface is not the real one.

gz_1	v3	Inclusion of SWI package to represent the saltwater interface.	SWI package included.	Not significance variations w.r.t. v2, a part the inclusion of SWI.
	v4	Application of Zone Budget to extract the water balance between the two aquifers.	Inclusion of Zone Budget analysis.	The zone budget shows how the perched aquifer is not isolated from the MSLA, which does not correspond to the reality. This suggests that a more realistic definition of layer surfaces is needed.
gz_2	v1	Inclusion of Top and Bottom surface for Ghajnsielem taken from data analysis (Activity 1). Zonation of Kx. Four different values: KA=13.5 m/day (LCL), KG=43.2 m/day (Globigerina), KBC=5.0E-03 m/day (Blue Clay) and KF=8.64Ee-3 m/day for faults in Ghajns.	Top and Bottom for Ghajns. Perched aquifer are now the realistic one	The new setting (closer to reality) represents the deep change in elevation between the two aquifers. This fact causes a bad response of the model in Ghajns. zone: head computed are too high.
	v2	Inclusion of Horizontal Flow Package to represent faults in Gozo MSLA.	HFB	This does not help solving the general problem of representing Ghajns. aquifer.
	v3	Sensitivity analysis (both manual and automatic). Used two bunches of observations: real (from EWA for Gozo MSLA and from Costain 1958 for Ghajns) and fake observations placed in Ghajns. that mimic the expected value of head.	Parametrization of Kx zoned-values. Inclusion of HOB package and application of UCODE	It is confirmed a well-defined spatial identification of parameters influence: the huge effect of KF and KBC on Ghajnsielem observation reflects on a minor scale the MSLA features. KF is always high correlated to KBC or KG (or both): this suggests that KF could be also fixed and taken out from the optimization process.

				For Ghajnsielem: • KBC and KF values are significantly most important than the conductivity of the aquifer itself (KG). • The most sensitive points are the one lying on the main depression of the aquifer (points W3, W4, W5) • KA does not affect the aquifer features, and this is coherent with the hydrogeological setting. For MSLA: • Observation W10802 confirms to be a probable outlier (as suggested by original data recording). • The high correlation of the three parameters KBC-KF-KG should be re-evaluated considering the above feature, since it seems to strongly influenced by the results driven by observation W10802. • The same argument applies for the influence of these three parameters on the MSLA (see CSS values): looking at DSS values it is clear that this influence is basically driven by W10802 only, while other observation are quite

				insensitive to these parameters.
gz_3	v1	Refining Ghajnsielem zone (a sort of telescopic refinement to get a 50m-cell size spaced in the center of Ghajnsielem aquifer).	Grid refinement for Ghajns. zone	Refinement does not solve the problems obtained at the previous stage. We always have (in Ghajnsielem) to manage the balance between insulation from MSLA (which causes too much high level of the water table) with the dry cells zones obtained with lower insulation (because of the increasing influence of the BC at the sea). The point is that, if insulated, we need to specify a sink for the model: this can be a series of zones in which springs or leakages are positioned. To be investigated. Next stage consists in separating Ghajnsielem from MSLA
gz_4	v1	Only Gozo MSLA is considered (Ghajnsielem perched aquifer taken out and substituted by inactive cells). Grid refined to 50mx50m. All the other settings are taken from gz_3, with data processed to be compliant with the new 50mx50m grid. Kx is almost everywhere equal to LCL, except where bottom of GL (= top of LCL) is under the sea level. Guess value for KX: LCL (zone 1) = 13.5 m/day GL (zone 2) = 1.35 m/day	Ghajnsielem aquifer not included anymore. RCH uniformly distributed on the domain.	The model works and it converges without problems.

	v2	Differently from what assumed before, the reference period is now 1941-1944. Therefore the pumping points (and rates) are now changed to represent the 2 water galleries active at that time.	Input of WEL package changed according to the new assumption.	The solution reflects the model changes in a coherent way.
	v3	Spatial weighting of natural recharge value (see report for details).	Inclusion of a spatially distributed input for RCH	No problem is recorded and the solution reflects coherently the change in recharge settings.
	v4	The same as v3, but without considering the contribution of perched aquifers (to test the importance of such term as stress of recharge)	RCH value is lowered by the leakage from perched aquifers	Not significant variations from version v3. This proves the importance of the other terms in the recharge rate calculation.
	v5	Ging back to v3 and inclusion of observations only for MSLA.	Update of HOB package definition.	Model converges smoothly, but a model misfit is recorded.
	v6	Inclusion of SWI package to estimate the fresh/seawater interface	Defining inputs for SWI and running with this package included.	The interface is always equal to bottom, it means that the bottom is to high
	v7	Bottom lower limit lowered to -200m to avoid problem recorded with SWI.	Reduction of bottom elevation	No problem in calculating the interface
	v8	Calibrated, also including SWI	Calibration using UCODE	Results of calibrated parameters are the following:

				KLC=5.528 m/day KGL=1.446 m/day Model fit is not satisfactory but due to the low number of targets and several data missing, the calibration is used as effective tool to inform the Modeler.

Ghajnsielem Perched Aquifer

Modelling Stage	**Sub-version**	**Main features**	**Main changes**	**Comments**
gh_0	v1	Toy model, to get confident with model domain, grid definition, packages compatibilities, etc. Grid size: 20mx20m, layer top is taken as the DEM, bottom as the bottom of UCL (revised wherever it outcrops the top). Uniform Kx=13.5m/day. Only RCH (with uniform recharge) and DRN package applied	-	The model was used mainly to test the definition of top and bottom, as well as to see if the inclusion of a drain can work. Good response of the model, but piezometry too high. It means that we have to include additional sink terms.
	v2	Including GHB to represent leakage from the aquifer	Activation of GHB to represent the leakage from the bottom	An initial guess value of
	v3	Including faults	K=8.64e-3 m/day on cells intersecting	No problem in convergence

			the faults	
	v4	Including spatially distributed recharge, as done for Gozo MSLA	Adding spatialized recharge.	Most reasonable results.
	v5	Parametrization and sensitivity study: parametrization of Kx for UCL and faults, as well as conductivities for DRN and GHB.	Inclusion of HOB package	Sensitivity analysis informs on parameters correlation, and influence of different observation points.
	v6	Calibration of KA, DREC, GHC	Run of UCODE automatic calibration.	Parameter estimation converged, but with not realistic values for KA
	v7	Calibration of DREC and GHC	Taking constant KA	Parameter estimation converged with realistic values for parameters and budget terms.

Appendix 2. Assumptions register

Malta MSLA Model

ID	Assumption Short name	Notes
1	Active domain	The active domain does not include the part the portion of the island at north of the Pwales fault. It is assumed that the two island areas are perfectly independent one each other.
2	Vertical discretization	It is assumed that the hydrodynamics in the aquifer can be effectively simulated by assuming only one layer, representing the coupling of LCL and GL.
3	Top of the layer	It corresponds to the top of GL, derived by the new stratigraphy and geological surfaces obtained in Activity 1.
4	Bottom of the layer	MSLA does not present a physical bottom. It is assumed that the bottom corresponds to the top elevation reduced by 150 m. Wherever this quota exceeds -150m, this is reduced at -150m (namely an upper limit of -150m has been imposed).
5	Galleries	Water galleries are represented as WELL boundary condition, with an overall discharge equal to the one of the closest pumping station.
6	Private wells	Private wells are given a supposed pumping rate, assigned according to the existing data.
7	Dams	Local infiltration though dams was roughly calculated considering the average capacity of measured dams and assuming a water refill of 5 times per year.
8	Rabat-Dingli Plateau	Recharge of the perched aquifer was independently re-calculated and compared with BRGM results of a lumped recharge-discharge model. Results are comparable. Leakage from the perched aquifer towards the MSLA was then taken from the BRGM output. It was assumed that the leakage preferentially happens through sinkholes, reallocating the leakage amount accordingly.

ID	***Assumption Short name***	***Notes***
1	Active domain	The cells are active all over the model domain. Physical limits represented by the Blue Clay outcrops are reproduced as low permeability zones.
2	Vertical discretization	It is assumed that the hydrodynamics in the aquifer can be effectively simulated by assuming only one layer, representing UCL.
3	Bottom of the layer	Mizieb and Pwales present a physical bottom. The bottom surface have been reconstructed from the available information and subsequently smoothed in order to facilitate numerical convergence.
4	Bottom leakage (sinkholes and northern fault)	In Mizieb, the only possible natural way out of water from the aquifer is where the lower heads are located, i.e, in the middle of the aquifer. This condition has been simulated adding GHB bc to represent the sinkholes, with a vertical gradient that naturally goes from the aquifer to the sea. A drain was also added along the breccia fault, being another possible natural way out.
5	Additional fault	In order to reduce the dry area in Mizieb aquifer (that would have been incoherent with the existence of agricultural wells), an additional fault was supposed. This assumption is needed if the hypothesis of UCL with very low hydraulic conductivity is rejected, as well as the hypothesis that the wells do not tap the aquifer but are rainwater cisterns.
6	Private wells	Private wells are given a supposed pumping rate, assigned according to the existing data.

ID	*Assumption Short name*	*Notes*
1	Active domain	The active domain does not include the part of MSLA on the south-east part, after the barrier created by the Qala fault. Geologically, this portion of LCL is still part of the aquifer, but from a hydrodynamic point of view the storage capacity is very low, due to the small (estimated) thickness of the saturated zone.
2	Vertical discretization	It is assumed that the hydrodynamics in the aquifer can be effectively simulated by assuming only one layer, representing the coupling of LCL and GL.
3	Top of the layer	It corresponds to the top of GL, derived by the new stratigraphy and geological surfaces obtained in Activity 1.
4	Bottom of the layer	Initially calculated as the top elevation reduced by 150m. Wherever this quota exceeds -150m, this is reduced at -150m (namely an upper limit of -150m has been imposed). This situation occurs basically on the whole aquifer domain, so that the obtained bottom is (almost everywhere) equals to -150m. This setting has been furtherly variated lowering the bottom limit at -200m, due to problem in getting convergence after applying SWI package.
5	Hydrodynamic parameters	No data on transmissivity or hydraulic conductivity are available. The guess values chosen for the two conductivity zones are taken from the geometric mean computed by estimates given for Malta MSLA.
6	Recharge	The spatial distribution of natural recharge has been computed, but using raw data taken from Malta MSLA.
7	Observations	Only 10 piezometric observations are available, with only 1 reading for each of these. Such information is taken as representative of the average annual piezometry, but this is (in principle) far from the reality. Furthermore, no estimate for measurement error is given.

Ghajnsielem model

ID	Assumption Short name	Notes
1	Active domain	The definition of active domain is done such that only the (isolated) Ghajnsielem aquifer is considered.
2	Vertical discretization	It is assumed that the hydrodynamics in the aquifer can be effectively simulated by assuming only one layer, representing the UCL.
3	Top of the layer	It corresponds to the top surface.
4	Bottom of the layer	Corresponds to the bottom of the UCL formation, derived by the new stratigraphy and geological surfaces obtained in Activity 1. Bottom elevation reduced to (top-15m) wherever this quota exceeds the top surface
5	Faults	Simulated applying a conductivity of 8.64e-3 m/day.
6	Recharge	The spatially distributed recharge computed for Gozo MSLA is here used, since this computation was done for the entire island.
7	Outflow	No specification of outflow is available for conceptual models. Therefore, three different outflows are assumed: (i) vertical leakage through the BC, modeled with GHB condition; (ii) springs from the west-side border of the aquifer, discharging to the sea; (iii) spring in the central-east part of the aquifer, where BC outcrops. The last two outflows are represented by DRN package.
8	Observations	18 observation points are taken from Costain (1958). These values have only one reading referring to the middle of dry season (July 1957), while the model is set up considering an annual-average.

Appendix 3. Calibration outputs

Parameter Sensitivities

Parameter name	Group	Parameter final value (m/s)	Composite sensitivity
kppp1	kp	7.67E-05	1.77E-03
kppp2	kp	1.93E-05	1.18E-03
kppp3	kp	1.11E-04	9.68E-04
kppp4	kp	1.11E-04	2.31E-03
kppp5	kp	1.39E-04	1.53E-03
kppp6	kp	5.71E-06	4.00E-03
kppp7	kp	1.60E-05	4.91E-03
kppp8	kp	2.82E-05	1.73E-03
kppp9	kp	1.44E-05	4.54E-03
kppp10	kp	1.88E-04	1.37E-03
kppp11	kp	2.27E-05	1.18E-03
kppp12	kp	1.53E-04	1.86E-03
kppp13	kp	2.69E-05	2.08E-03
kppp14	kp	3.16E-04	9.99E-04
kppp15	kp	6.18E-05	1.78E-03
kppp16	kp	4.74E-04	1.38E-03
kppp17	kp	8.16E-05	1.11E-03
kppp18	kp	1.00E-03	1.45E-03
kppp19	kp	8.35E-04	9.67E-04
kppp20	kp	1.02E-05	2.67E-03
kppp21	kp	5.53E-05	2.55E-03
kppp22	kp	4.41E-05	1.01E-03
kppp23	kp	1.45E-05	2.06E-03
kppp24	kp	3.43E-05	1.64E-03
kppp25	kp	2.00E-05	1.41E-03
kppp26	kp	2.28E-04	1.16E-03
kppp27	kp	8.44E-04	3.34E-03
kppp28	kp	1.01E-05	4.12E-03
kppp29	kp	1.26E-04	2.77E-03
kppp30	kp	1.22E-04	1.81E-03
kppp31	kp	6.65E-04	1.06E-03
kppp32	kp	2.61E-05	1.77E-03
kppp33	kp	1.20E-04	1.15E-03
kppp34	kp	7.63E-05	5.07E-03
kppp35	kp	3.54E-04	1.61E-03
kppp36	kp	1.54E-04	1.64E-03

kppp37	kp	2.83E-04	1.72E-03	kppp57	kp	2.43E-05	2.11E-03
kppp38	kp	1.60E-04	9.64E-04	kppp58	kp	1.02E-05	3.89E-03
kppp39	kp	3.83E-05	2.24E-03	kppp59	kp	2.72E-04	1.49E-03
kppp40	kp	1.59E-04	1.11E-03	kppp60	kp	1.54E-05	1.68E-03
kppp41	kp	5.60E-04	1.85E-03	kppp61	kp	2.11E-06	5.79E-03
kppp42	kp	7.87E-04	1.70E-03	kppp62	kp	3.64E-04	2.74E-03
kppp43	kp	1.07E-05	4.98E-03	kppp63	kp	2.02E-04	1.58E-03
kppp44	kp	1.21E-04	2.52E-03	kppp64	kp	1.46E-04	1.28E-03
kppp45	kp	2.72E-06	4.48E-03	kppp65	kp	1.30E-04	9.86E-04
kppp46	kp	4.85E-05	2.10E-03	kppp66	kp	1.67E-05	1.30E-03
kppp47	kp	5.75E-06	2.26E-03	kppp67	kp	3.35E-05	4.51E-03
kppp48	kp	5.37E-05	2.29E-03	kppp68	kp	1.16E-05	3.23E-03
kppp49	kp	5.20E-05	3.40E-03	kppp69	kp	2.76E-05	2.21E-03
kppp50	kp	1.23E-04	1.32E-03	kppp70	kp	3.79E-04	3.59E-03
kppp51	kp	5.06E-06	2.60E-03	kppp71	kp	4.21E-05	1.02E-02
kppp52	kp	5.04E-06	5.21E-03	kppp72	kp	3.33E-05	1.00E-02
kppp53	kp	6.77E-05	3.73E-03	kppp73	kp	7.35E-06	7.30E-03
kppp54	kp	1.09E-05	2.89E-03	kppp74	kp	6.62E-06	4.26E-03
kppp55	kp	3.69E-05	1.47E-03	kppp75	kp	7.50E-06	3.79E-03
kppp56	kp	4.13E-05	1.93E-03	kppp76	kp	5.40E-05	2.02E-03

kppp77	kp	1.31E-04	1.52E-03	kppp97	kp	1.03E-04	1.35E-03
kppp78	kp	1.22E-05	9.80E-04	kppp98	kp	3.51E-04	2.16E-03
kppp79	kp	4.82E-04	1.83E-03	kppp99	kp	2.92E-04	2.90E-03
kppp80	kp	7.79E-06	2.08E-03	kppp100	kp	9.08E-04	1.48E-03
kppp81	kp	1.99E-05	1.02E-03	kppp101	kp	4.39E-05	1.32E-03
kppp82	kp	5.08E-05	1.50E-03	kppp102	kp	9.12E-05	1.09E-03
kppp83	kp	1.36E-04	2.83E-03	kppp103	kp	1.98E-04	1.07E-03
kppp84	kp	3.43E-04	3.42E-03	kppp104	kp	3.49E-05	2.14E-03
kppp85	kp	1.13E-04	1.15E-03	kppp105	kp	4.94E-04	3.12E-03
kppp86	kp	4.72E-05	1.03E-03	kppp106	kp	2.08E-05	1.80E-03
kppp87	kp	1.54E-05	1.31E-03	kppp107	kp	1.56E-05	3.06E-03
kppp88	kp	9.62E-06	1.22E-03	kppp108	kp	8.74E-05	4.13E-03
kppp89	kp	3.50E-04	2.90E-03	kppp109	kp	5.83E-05	4.38E-03
kppp90	kp	2.09E-05	1.46E-03	kppp110	kp	2.72E-05	3.73E-03
kppp91	kp	1.09E-04	9.84E-04	kppp111	kp	5.53E-05	1.82E-03
kppp92	kp	1.43E-04	9.14E-04	kppp112	kp	3.02E-04	1.43E-03
kppp93	kp	8.35E-05	1.08E-03	kppp113	kp	1.00E-05	2.63E-03
kppp94	kp	4.39E-05	9.54E-04	kppp114	kp	2.36E-04	2.20E-03
kppp95	kp	5.61E-05	1.90E-03	kppp115	kp	6.75E-05	1.29E-03
kppp96	kp	1.38E-05	1.97E-03	kppp116	kp	2.95E-05	3.59E-03

kppp117	kp	3.62E-04	2.60E-03	kppp137	kp	1.11E-05	1.67E-03
kppp118	kp	2.05E-05	4.44E-03	kppp138	kp	1.17E-05	1.08E-03
kppp119	kp	3.76E-05	3.39E-03	kppp139	kp	7.27E-05	1.46E-03
kppp120	kp	9.42E-05	1.18E-03	kppp140	kp	6.65E-05	3.83E-03
kppp121	kp	1.61E-04	9.55E-04	kppp141	kp	4.12E-05	9.70E-03
kppp122	kp	4.63E-05	1.30E-03	kppp142	kp	2.51E-05	1.15E-03
kppp123	kp	3.37E-05	1.81E-03	kppp143	kp	6.07E-05	1.03E-03
kppp124	kp	7.49E-05	4.89E-03	kppp144	kp	2.88E-05	4.29E-03
kppp125	kp	9.14E-05	3.38E-03	kppp145	kp	3.04E-05	1.37E-03
kppp126	kp	8.73E-06	6.46E-03	kppp146	kp	9.63E-05	2.02E-03
kppp127	kp	2.37E-04	1.15E-03	kppp147	kp	7.24E-06	4.41E-03
kppp128	kp	6.57E-06	2.37E-03	kppp148	kp	2.70E-04	1.83E-03
kppp129	kp	2.38E-04	5.35E-03	kppp149	kp	7.12E-05	1.94E-03
kppp130	kp	3.52E-05	1.77E-03	kppp150	kp	1.28E-04	1.60E-03
kppp131	kp	1.41E-05	3.61E-03	kppp151	kp	4.80E-04	1.66E-03
kppp132	kp	4.93E-06	1.26E-03	kppp152	kp	4.49E-04	1.52E-03
kppp133	kp	1.41E-05	1.28E-03	kppp153	kp	7.45E-05	2.61E-03
kppp134	kp	8.05E-06	1.96E-03	kppp154	kp	4.48E-04	1.49E-03
kppp135	kp	4.89E-04	2.58E-03	kppp155	kp	2.42E-05	1.18E-03
kppp136	kp	1.01E-04	2.33E-03	kppp156	kp	1.02E-05	3.80E-03

kppp157	kp	3.58E-04	1.94E-03	kppp177	kp	1.02E-04	2.30E-03
kppp158	kp	3.52E-05	9.59E-04	kppp178	kp	7.08E-06	1.39E-03
kppp159	kp	4.96E-04	2.39E-03	kppp179	kp	3.93E-05	2.44E-03
kppp160	kp	2.81E-05	3.54E-03	kppp180	kp	9.26E-05	3.29E-03
kppp161	kp	8.54E-05	3.23E-03	kppp181	kp	3.38E-04	1.75E-03
kppp162	kp	9.73E-05	1.13E-03	kppp182	kp	1.59E-05	3.02E-03
kppp163	kp	1.74E-04	9.10E-04	kppp183	kp	2.58E-04	9.64E-04
kppp164	kp	1.00E-03	1.93E-03	kppp184	kp	1.91E-05	2.25E-03
kppp165	kp	1.00E-03	1.12E-03	kppp185	kp	2.44E-04	1.03E-03
kppp166	kp	9.90E-04	1.02E-03				
kppp167	kp	9.20E-04	1.06E-03				
kppp168	kp	3.94E-05	3.43E-03				
kppp169	kp	6.34E-05	1.01E-03				
kppp170	kp	1.18E-04	4.57E-03				
kppp171	kp	6.72E-05	1.02E-03				
kppp172	kp	7.63E-05	1.29E-03				
kppp173	kp	1.36E-05	2.52E-03				
kppp174	kp	1.00E-03	1.33E-03				
kppp175	kp	7.92E-05	1.44E-03				
kppp176	kp	1.03E-04	1.01E-03				

Residuals

Name	Group	Measured	Modelled	Residual	Weight
o1	head1	1.8	1.912676	-0.11268	1
o2	head1	2.9	2.487464	0.412536	1
o3	head1	3	2.612104	0.387896	1
o4	head1	4.6	4.557529	4.25E-02	1
o5	head1	2	1.894637	0.105363	1
o6	head1	2.3	1.985373	0.314627	1
o7	head1	1.3	1.299098	9.02E-04	1
o8	head1	1	1.145995	-0.146	1
o9	head1	1.9	1.726149	0.173851	1
o10	head1	3.4	3.116279	0.283721	1.2
o11	head1	2.9	2.644798	0.255202	1
o12	head1	3.3	3.303211	-3.21E-03	1
o13	head1	2.2	2.286206	-8.62E-02	1
o14	head1	0.1	0.252953	-0.15295	1
o15	head1	2.1	2.648309	-0.54831	1
o16	head1	3.2	3.159764	4.02E-02	1
o17	head1	3.3	3.119274	0.180726	1
o18	head1	0.9	0.926936	-2.69E-02	1
o19	head1	1.7	1.475865	0.224135	1
o20	head1	3.1	3.340107	-0.24011	1
o21	head1	2.7	2.989797	-0.2898	1
o22	head1	2.6	2.633333	-3.33E-02	1
o23	head1	1.8	1.663834	0.136166	1
o24	head1	2.8	2.683496	0.116504	1
o25	head1	2.5	2.836064	-0.33606	1
o26	head1	2.4	3.046237	-0.64624	1
o27	head1	3.2	3.235688	-3.57E-02	1
o28	head1	2.6	2.812039	-0.21204	1
o29	head1	3.9	3.844797	5.52E-02	1
o30	head1	4.1	4.093371	6.63E-03	1
o31	head1	3.6	3.628576	-2.86E-02	1
o32	head1	1.5	1.70781	-0.20781	1
o33	head1	2.1	2.055468	4.45E-02	1
o34	head1	1.4	1.470879	-7.09E-02	1
o35	head1	3.6	3.474148	0.125852	1
o36	head1	2.7	2.705907	-5.91E-03	1
o37	head1	1.9	1.931884	-3.19E-02	1

o38	head1	1.2	1.210336	-1.03E-02	1	i1k12	regul_kp1	-3.91813	-3.81442	-0.10371	0.209013
o39	head1	3.2	3.041673	0.158327	1	i1k13	regul_kp1	-3.98758	-4.57006	0.582486	0.209013
o40	head1	1.4	1.430145	-3.01E-02	1	i1k14	regul_kp1	-3.42447	-3.50083	7.64E-02	0.209013
o41	head1	4.3	4.336118	-3.61E-02	1	i1k15	regul_kp1	-3.97752	-4.20932	0.231807	0.209013
o42	head1	3.3	3.312576	-1.26E-02	1	i1k16	regul_kp1	-3.77105	-3.32423	-0.44682	0.209013
o43	head1	0.2	0.355475	-0.15548	1	i1k17	regul_kp1	-3.71938	-4.08822	0.368839	0.209013
o44	head1	0.4	0.393045	6.96E-03	1	i1k18	regul_kp1	-3.97138	-3	-0.97138	0.209013
o45	head1	3.4	3.355186	4.48E-02	1	i1k19	regul_kp1	-3.92892	-3.07823	-0.85069	0.209013
o46	head1	0.4	0.454346	-5.43E-02	1	i1k20	regul_kp1	-4.04549	-4.99144	0.945946	0.209013
i1k1	regul_kp1	-4.36564	-4.11507	-0.25057	0.209013	i1k21	regul_kp1	-4.44123	-4.25765	-0.18358	0.209013
i1k2	regul_kp1	-4.4263	-4.71376	0.287462	0.209013	i1k22	regul_kp1	-3.65432	-4.35533	0.701008	0.209013
i1k3	regul_kp1	-3.85395	-3.95594	0.101998	0.209013	i1k23	regul_kp1	-3.53632	-4.83809	1.301769	0.209013
i1k4	regul_kp1	-4.28987	-3.95315	-0.33672	0.209013	i1k24	regul_kp1	-3.91368	-4.46529	0.551616	0.209013
i1k5	regul_kp1	-4.11761	-3.85846	-0.25915	0.209013	i1k25	regul_kp1	-3.5856	-4.69933	1.11373	0.209013
i1k6	regul_kp1	-5.12196	-5.2431	0.121142	0.209013	i1k26	regul_kp1	-3.85554	-3.64256	-0.21298	0.209013
i1k7	regul_kp1	-4.36543	-4.79657	0.431134	0.209013	i1k27	regul_kp1	-3.9288	-3.07386	-0.85495	0.209013
i1k8	regul_kp1	-4.01619	-4.55037	0.534187	0.209013	i1k28	regul_kp1	-5.0153	-4.99674	-1.86E-02	0.209013
i1k9	regul_kp1	-4.4797	-4.84298	0.363275	0.209013	i1k29	regul_kp1	-3.85327	-3.8999	4.66E-02	0.209013
i1k10	regul_kp1	-3.66994	-3.72622	5.63E-02	0.209013	i1k30	regul_kp1	-3.97967	-3.91482	-6.49E-02	0.209013
i1k11	regul_kp1	-4.46845	-4.64409	0.175635	0.209013	i1k31	regul_kp1	-3.91249	-3.1769	-0.73559	0.209013

i1k32	regul_kp1	-4.73101	-4.58298	-0.14803	0.209013	i1k52	regul_kp1	-5.38939	-5.29795	-9.14E-02	0.209013
i1k33	regul_kp1	-3.84858	-3.92011	7.15E-02	0.209013	i1k53	regul_kp1	-4.17362	-4.16947	-4.15E-03	0.209013
i1k34	regul_kp1	-3.95404	-4.11769	0.163652	0.209013	i1k54	regul_kp1	-4.77572	-4.96091	0.185189	0.209013
i1k35	regul_kp1	-4.51822	-3.45066	-1.06756	0.209013	i1k55	regul_kp1	-4.23853	-4.43245	0.193921	0.209013
i1k36	regul_kp1	-3.98094	-3.81301	-0.16793	0.209013	i1k56	regul_kp1	-4.2474	-4.38364	0.13624	0.209013
i1k37	regul_kp1	-3.85288	-3.548	-0.30488	0.209013	i1k57	regul_kp1	-4.89311	-4.6143	-0.27881	0.209013
i1k38	regul_kp1	-3.8991	-3.79664	-0.10247	0.209013	i1k58	regul_kp1	-4.91775	-4.98961	7.19E-02	0.209013
i1k39	regul_kp1	-3.99008	-4.41713	0.427052	0.209013	i1k59	regul_kp1	-4.44249	-3.5653	-0.87719	0.209013
i1k40	regul_kp1	-3.98593	-3.79955	-0.18639	0.209013	i1k60	regul_kp1	-4.77953	-4.8114	3.19E-02	0.209013
i1k41	regul_kp1	-3.84794	-3.25198	-0.59596	0.209013	i1k61	regul_kp1	-4.20606	-5.67508	1.469018	0.209013
i1k42	regul_kp1	-3.91557	-3.10429	-0.81128	0.209013	i1k62	regul_kp1	-4.46192	-3.43937	-1.02255	0.209013
i1k43	regul_kp1	-4.41872	-4.97037	0.551648	0.209013	i1k63	regul_kp1	-3.78079	-3.69493	-8.59E-02	0.209013
i1k44	regul_kp1	-4.65269	-3.91741	-0.73528	0.209013	i1k64	regul_kp1	-3.92402	-3.83659	-8.74E-02	0.209013
i1k45	regul_kp1	-4.35318	-5.56562	1.212439	0.209013	i1k65	regul_kp1	-3.88582	-3.88749	1.67E-03	0.209013
i1k46	regul_kp1	-4.08722	-4.31426	0.227042	0.209013	i1k66	regul_kp1	-4.81519	-4.77683	-3.84E-02	0.209013
i1k47	regul_kp1	-5.22492	-5.23997	1.51E-02	0.209013	i1k67	regul_kp1	-4.67686	-4.47488	-0.20197	0.209013
i1k48	regul_kp1	-4.66153	-4.26995	-0.39158	0.209013	i1k68	regul_kp1	-4.71165	-4.93388	0.222238	0.209013
i1k49	regul_kp1	-4.76694	-4.28426	-0.48268	0.209013	i1k69	regul_kp1	-4.36509	-4.55867	0.193579	0.209013
i1k50	regul_kp1	-4.01218	-3.91105	-0.10112	0.209013	i1k70	regul_kp1	-4.63486	-3.42126	-1.2136	0.209013
i1k51	regul_kp1	-3.96047	-5.29583	1.335356	0.209013	i1k71	regul_kp1	-5.02348	-4.37559	-0.64789	0.209013

i1k72	regul_kp1	-4.74518	-4.47752	-0.26766	0.209013	i1k92	regul_kp1	-3.8282	-3.84441	1.62E-02	0.209013
i1k73	regul_kp1	-4.95156	-5.13364	0.182072	0.209013	i1k93	regul_kp1	-4.11651	-4.07837	-3.81E-02	0.209013
i1k74	regul_kp1	-4.67325	-5.17885	0.505602	0.209013	i1k94	regul_kp1	-4.27977	-4.35704	7.73E-02	0.209013
i1k75	regul_kp1	-4.51138	-5.12513	0.613756	0.209013	i1k95	regul_kp1	-4.41102	-4.25115	-0.15987	0.209013
i1k76	regul_kp1	-4.26072	-4.26722	6.50E-03	0.209013	i1k96	regul_kp1	-3.97402	-4.85965	0.885622	0.209013
i1k77	regul_kp1	-4.0969	-3.88166	-0.21524	0.209013	i1k97	regul_kp1	-4.48619	-3.989	-0.49719	0.209013
i1k78	regul_kp1	-4.93754	-4.91522	-2.23E-02	0.209013	i1k98	regul_kp1	-4.28638	-3.45501	-0.83137	0.209013
i1k79	regul_kp1	-4.58704	-3.31656	-1.27047	0.209013	i1k99	regul_kp1	-4.08815	-3.5343	-0.55385	0.209013
i1k80	regul_kp1	-4.96936	-5.10847	0.139105	0.209013	i1k100	regul_kp1	-3.85023	-3.04214	-0.80809	0.209013
i1k81	regul_kp1	-4.83429	-4.70206	-0.13223	0.209013	i1k101	regul_kp1	-4.08899	-4.35731	0.268321	0.209013
i1k82	regul_kp1	-4.38311	-4.29428	-8.88E-02	0.209013	i1k102	regul_kp1	-3.84524	-4.04022	0.194986	0.209013
i1k83	regul_kp1	-4.19078	-3.86748	-0.32329	0.209013	i1k103	regul_kp1	-3.75126	-3.70404	-4.72E-02	0.209013
i1k84	regul_kp1	-4.14794	-3.46524	-0.6827	0.209013	i1k104	regul_kp1	-3.69353	-4.45756	0.764034	0.209013
i1k85	regul_kp1	-3.90205	-3.94678	4.47E-02	0.209013	i1k105	regul_kp1	-3.95476	-3.30659	-0.64818	0.209013
i1k86	regul_kp1	-4.64112	-4.32583	-0.31529	0.209013	i1k106	regul_kp1	-4.31424	-4.68255	0.368306	0.209013
i1k87	regul_kp1	-4.79739	-4.81274	1.53E-02	0.209013	i1k107	regul_kp1	-4.19727	-4.80779	0.610522	0.209013
i1k88	regul_kp1	-4.72883	-5.01679	0.287964	0.209013	i1k108	regul_kp1	-4.01024	-4.05833	4.81E-02	0.209013
i1k89	regul_kp1	-4.30954	-3.45623	-0.8533	0.209013	i1k109	regul_kp1	-4.13399	-4.23426	0.100277	0.209013
i1k90	regul_kp1	-4.24018	-4.68086	0.440684	0.209013	i1k110	regul_kp1	-4.17533	-4.56558	0.390248	0.209013
i1k91	regul_kp1	-3.93219	-3.96334	3.11E-02	0.209013	i1k111	regul_kp1	-3.91808	-4.2569	0.338828	0.209013

i1k112	regul_kp1	-3.43857	-3.52034	8.18E-02	0.209013	i1k132	regul_kp1	-5.07383	-5.30732	0.233488	0.209013
i1k113	regul_kp1	-3.59688	-5	1.403116	0.209013	i1k133	regul_kp1	-4.47938	-4.85225	0.372862	0.209013
i1k114	regul_kp1	-4.11708	-3.62699	-0.49009	0.209013	i1k134	regul_kp1	-4.62374	-5.09406	0.470317	0.209013
i1k115	regul_kp1	-4.29981	-4.17079	-0.12902	0.209013	i1k135	regul_kp1	-4.45165	-3.31071	-1.14095	0.209013
i1k116	regul_kp1	-4.08503	-4.53011	0.445084	0.209013	i1k136	regul_kp1	-4.24423	-3.99394	-0.25029	0.209013
i1k117	regul_kp1	-3.99817	-3.44142	-0.55675	0.209013	i1k137	regul_kp1	-4.67924	-4.95386	0.274617	0.209013
i1k118	regul_kp1	-4.01693	-4.68892	0.671991	0.209013	i1k138	regul_kp1	-4.79161	-4.93346	0.14185	0.209013
i1k119	regul_kp1	-4.12595	-4.4251	0.299151	0.209013	i1k139	regul_kp1	-4.47818	-4.13834	-0.33984	0.209013
i1k120	regul_kp1	-3.9346	-4.02598	9.14E-02	0.209013	i1k140	regul_kp1	-4.30403	-4.17742	-0.12661	0.209013
i1k121	regul_kp1	-3.98677	-3.7935	-0.19327	0.209013	i1k141	regul_kp1	-4.0258	-4.38532	0.359524	0.209013
i1k122	regul_kp1	-3.92244	-4.33411	0.411662	0.209013	i1k142	regul_kp1	-4.5166	-4.60065	8.41E-02	0.209013
i1k123	regul_kp1	-4.87866	-4.4718	-0.40686	0.209013	i1k143	regul_kp1	-4.39172	-4.21691	-0.17481	0.209013
i1k124	regul_kp1	-3.96114	-4.12559	0.164451	0.209013	i1k144	regul_kp1	-4.13023	-4.54114	0.410917	0.209013
i1k125	regul_kp1	-3.96207	-4.03902	7.70E-02	0.209013	i1k145	regul_kp1	-4.35112	-4.51681	0.165688	0.209013
i1k126	regul_kp1	-4.87719	-5.05884	0.181654	0.209013	i1k146	regul_kp1	-3.91888	-4.01649	9.76E-02	0.209013
i1k127	regul_kp1	-3.49326	-3.62437	0.131114	0.209013	i1k147	regul_kp1	-4.0758	-5.14035	1.064544	0.209013
i1k128	regul_kp1	-5.16745	-5.18228	1.48E-02	0.209013	i1k148	regul_kp1	-3.96618	-3.56875	-0.39744	0.209013
i1k129	regul_kp1	-4.81988	-3.62384	-1.19603	0.209013	i1k149	regul_kp1	-4.03718	-4.14761	0.110429	0.209013
i1k130	regul_kp1	-4.84069	-4.45375	-0.38693	0.209013	i1k150	regul_kp1	-3.95894	-3.89326	-6.57E-02	0.209013
i1k131	regul_kp1	-4.9646	-4.85142	-0.11318	0.209013	i1k151	regul_kp1	-4.34126	-3.31894	-1.02233	0.209013

i1k152	regul_kp1	-3.89746	-3.3478	-0.54967	0.209013
i1k153	regul_kp1	-3.90055	-4.12802	0.227468	0.209013
i1k154	regul_kp1	-3.84685	-3.34827	-0.49857	0.209013
i1k155	regul_kp1	-3.95764	-4.61558	0.657932	0.209013
i1k156	regul_kp1	-4.00599	-4.99037	0.98438	0.209013
i1k157	regul_kp1	-4.11502	-3.44559	-0.66942	0.209013
i1k158	regul_kp1	-4.38584	-4.45325	6.74E-02	0.209013
i1k159	regul_kp1	-3.97236	-3.30422	-0.66814	0.209013
i1k160	regul_kp1	-4.10444	-4.55156	0.447122	0.209013
i1k161	regul_kp1	-4.27657	-4.06837	-0.2082	0.209013
i1k162	regul_kp1	-3.83539	-4.01205	0.176663	0.209013
i1k163	regul_kp1	-3.91249	-3.75985	-0.15264	0.209013
i1k164	regul_kp1	-3.98428	-3	-0.98428	0.209013
i1k165	regul_kp1	-3.88717	-3	-0.88717	0.209013
i1k166	regul_kp1	-3.91649	-3.00436	-0.91213	0.209013
i1k167	regul_kp1	-3.87194	-3.03622	-0.83573	0.209013
i1k168	regul_kp1	-3.98327	-4.40439	0.421127	0.209013
i1k169	regul_kp1	-3.82688	-4.1978	0.370921	0.209013
i1k170	regul_kp1	-4.24811	-3.92716	-0.32096	0.209013
i1k171	regul_kp1	-3.55885	-4.17231	0.613463	0.209013
i1k172	regul_kp1	-3.64619	-4.11728	0.471083	0.209013
i1k173	regul_kp1	-4.52549	-4.86698	0.341493	0.209013
i1k174	regul_kp1	-3.91189	-3	-0.91189	0.209013
i1k175	regul_kp1	-4.15032	-4.10131	-4.90E-02	0.209013
i1k176	regul_kp1	-3.9689	-3.98567	1.68E-02	0.209013
i1k177	regul_kp1	-4.03976	-3.99253	-4.72E-02	0.209013
i1k178	regul_kp1	-3.82899	-5.15013	1.32114	0.209013
i1k179	regul_kp1	-3.95236	-4.40562	0.453261	0.209013
i1k180	regul_kp1	-3.92275	-4.03327	0.110517	0.209013
i1k181	regul_kp1	-3.97776	-3.47136	-0.50641	0.209013
i1k182	regul_kp1	-3.96434	-4.79943	0.835085	0.209013
i1k183	regul_kp1	-3.4487	-3.58788	0.139176	0.209013
i1k184	regul_kp1	-3.45029	-4.71918	1.268894	0.209013
i1k185	regul_kp1	-3.43685	-3.61225	0.175401	0.209013

Appendix 4: Data Pre-Processing

This appendix briefly describes the pre-processing of the geographical data performed after delivering Deliverable D1.3, according to a continuous process of data acquisition, exploration and exploitation.

1. DTM rectification and geological data spatial adjustment

Since during the conceptual model development, several different geospatial data were collected (from different sources, see deliverable "D1.3 - Report on data assessment, gap-analysis and conceptual models"), issues concerning the correct geospatial placement of the data were detected. Generally, the different groups of geospatial data (eg. DEM and orthophoto, or geological data such as formation boundaries and linear structure) were scattered in several directions of about 30m from each other, aside from taking into account the simplified (respect reality) shape of some vector data and even after proper reprojection from the Maltese national geographic reference system to the used one (Figure 1).

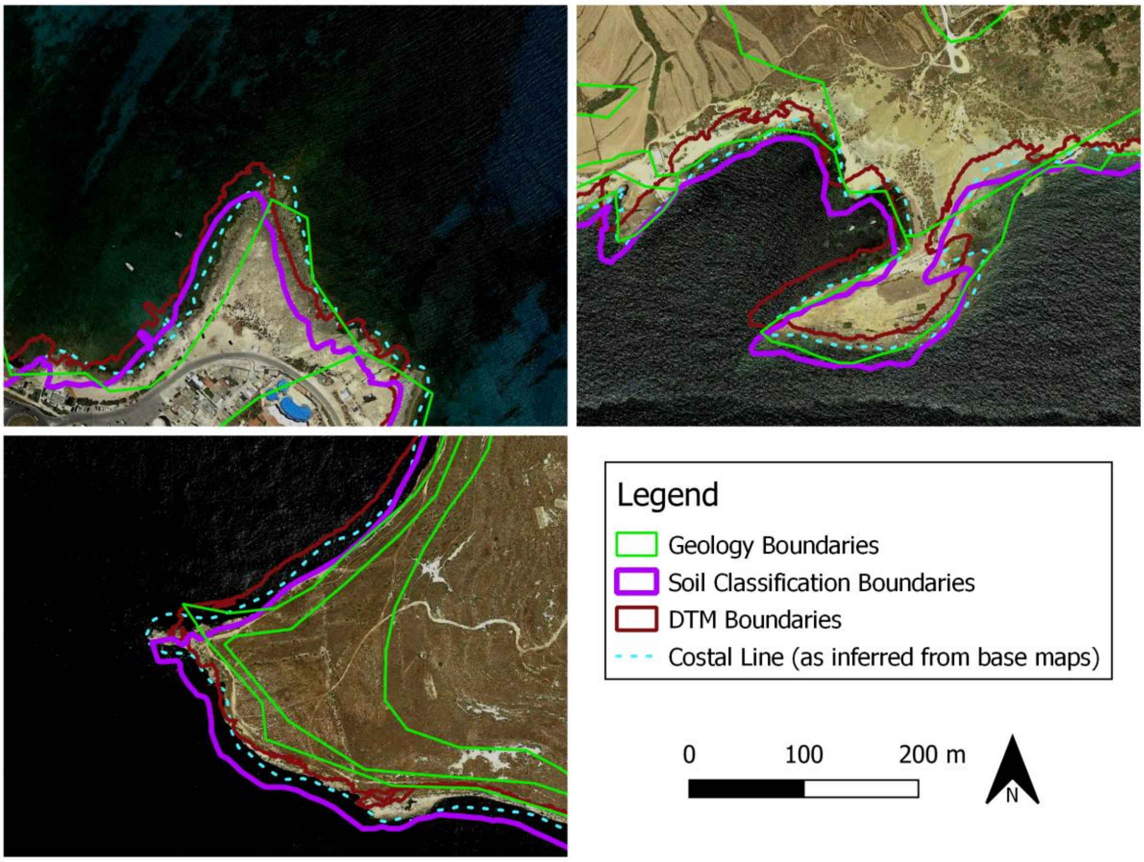

Figure 1. Examples of non-overlapping between three different data sets and a base map (from Google satellite data) used as reference.

To correct this non-overlapping issue, all the geospatial data acquired were rectified/adjusted using the Google satellite image as common reference and re-projected on a common reference system (WGS84/UTM zone 33N, EPSG: 32633).

The following paragraphs briefly describes the spatial corrections applied to the different data.

1.1 Raster file - DTM and orthophoto

The high resolution Digital Terrain Model (DTM) and orthophoto of Maltese islands were the two most important raster files rectified. A correct DTM, in particular, was required to be perfectly overlapped on the geological map in order to extract the elevation of the geological boundaries used to interpolate the surface of geological formations.

Produced by the same source (Malta Environment & Planning Authority, 2013) the DTM and orthophoto were overlapping correctly on each other, but not on the reference base map nor on the other vector data (Figure 1).

Both rasters were therefore rectified at the same time, but an extra initial step was required by the DTM in order to obtain a complete surface.

1.1.1 Step 1 - No-Data reconstruction

The original DTM raster has several areas where missing data are present (Figure 2).

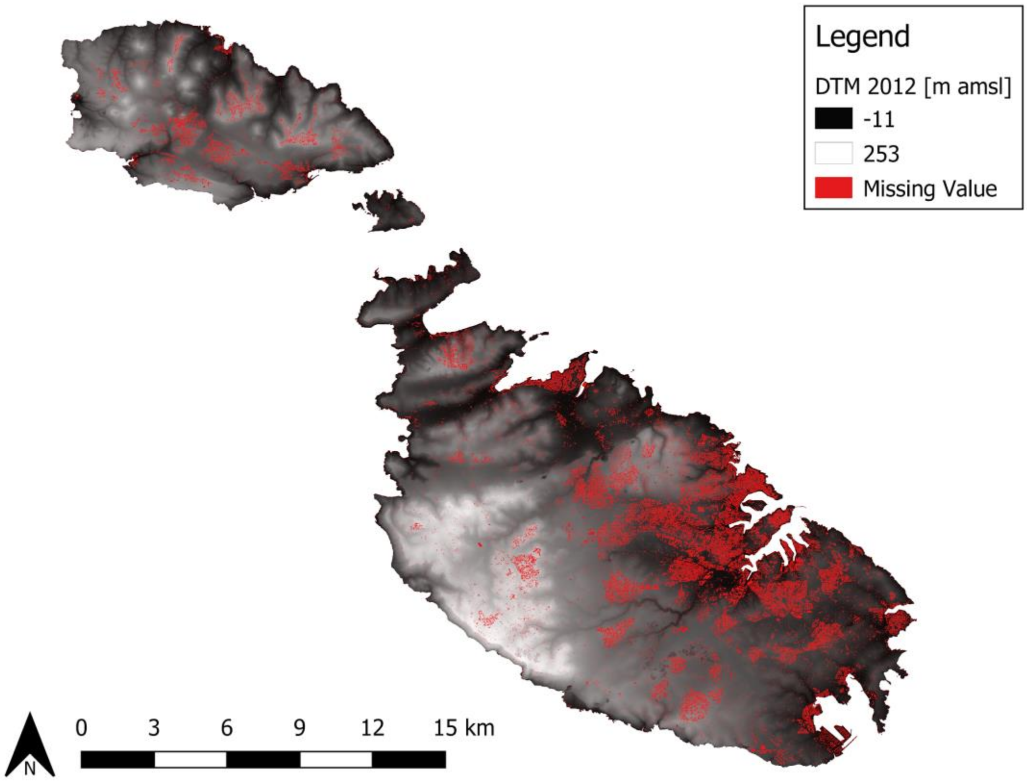

Figure 2. DTM missing values distribution.

These areas correspond mostly to the urban areas where the buildings elevation alter the real terrain elevation and therefore is not to be considered on the DTM.

Since, for the scope of this work a complete (without missing data on the land surface) terrain surface of the Maltese islands was required, the missing values of the DTM were filled by interpolation.

Several interpolation algorithms were tested (Table 1), and after a trial-and-error procedure the “Elevation void fill” algorithm (ESRI - ArcGIS) was selected as the most fitted to interpolate the missing DTM data.

The input parameters were set as follows (see ArcMap on line manual, 2019 for further details):

- Short range IDW radius = -1 (mean no maximum search radius is set)
- Max void width = 400 (m)

<table>
<tr><th colspan="2">Function</th><th>GIS Library</th><th>Method</th></tr>
<tr><td colspan="2">Elevation void fill</td><td>ArcGIS</td><td>Based on the Plane Fitting-IDW void fill method. First, small voids are filled by the average of the eight neighboring cells, then the plane fitting method is applied. If the plane fitting method gives poor results, the IDW method is applied</td></tr>
<tr><td colspan="2">r.fillnuls</td><td>GRASS</td><td>No-data area are interpolated from a buffer of neighboring cells using regularized spline interpolation or cubic or linear spline interpolation with Tykhonov regularization</td></tr>
<tr><td rowspan="3">Close gaps algorithm</td><td>Standard</td><td rowspan="3">SAGA</td><td>Nearest Neighbors</td></tr>
<tr><td>Spline</td><td>Spline</td></tr>
<tr><td>Stepwise resampling</td><td>Stepwise resampling</td></tr>
<tr><td colspan="2">Fill no data</td><td>GDAL</td><td>IDW followed by a smoothing</td></tr>
</table>

Table 1. Algorithms tested during the trial-and-error.

After the filling of the no-data value, a mask generated from the original DTM and corresponding to the island surfaces was used to clip away the no-data wrongly filled outside the coastal line.

1.1.2 Step - 2 Rectification

To rectify the filled DTM, 947 Ground Control Points (GCP) were used (Figure 3). Initially the GCPs were distributed along the coastal line, where common morphological features are easier to identify on the DTM and on the coastal line inferred from the base map. Then several other points where placed in the central area of the islands using as reference the orthophoto (Malta Environment & Planning Authority, 2013; perfectly overlapped on the DEM) and the google satellite base map used as reference.

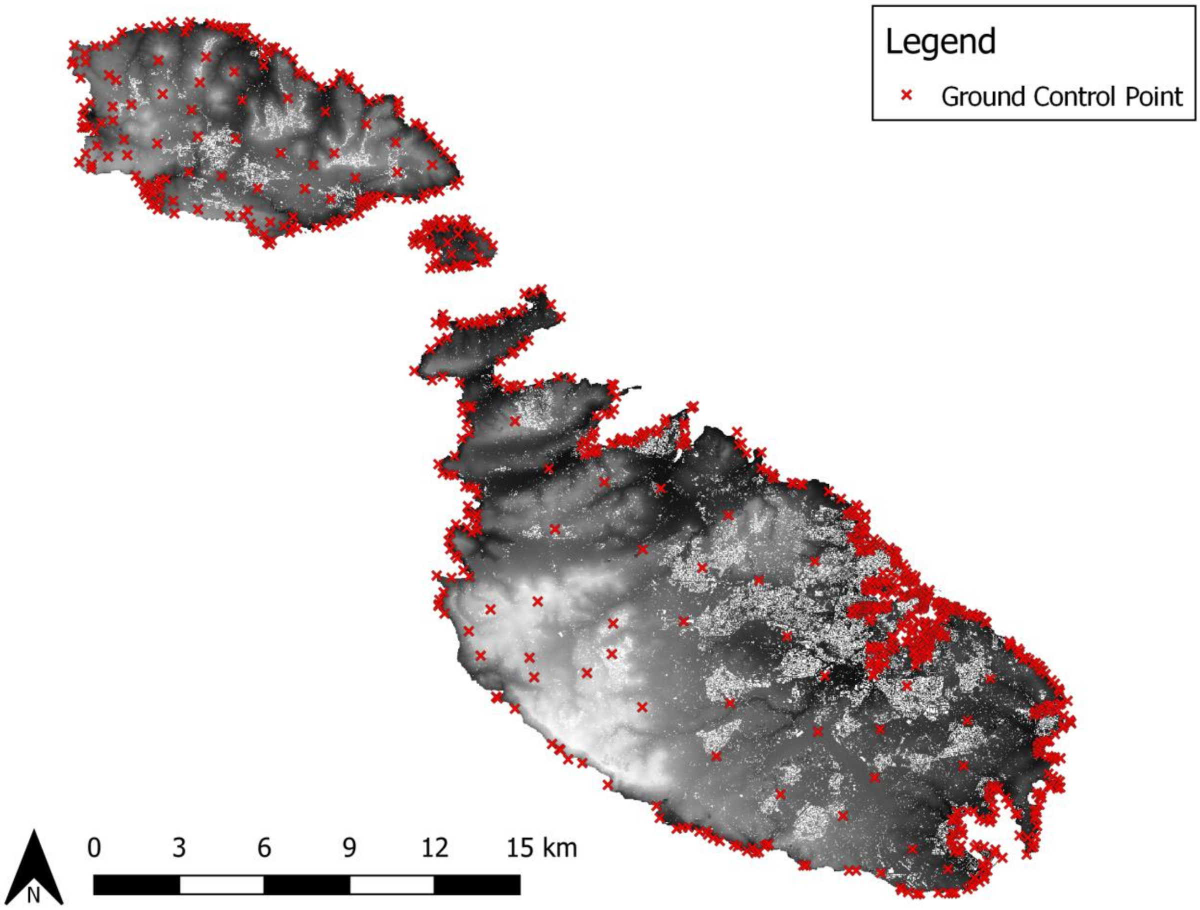

Figure 3. GCP used to rectify the DTM on the base maps.

The following parameters were used for the interpolation:

- Transformation type = polynomial 3
- Resampling = linear
- Resolution = 1 (m)

1.2 Vectors - spatial adjustment

Geospatial vector data were adjusted using the QGIS plugin called "vector bender" (v 0.2, Delang O. 2019), based on the "rubber sheet" method.

Since this method cause distortion within the geometries of a vector, it was used only when after an initial reprojection of the vector file a large discrepancy (> 10 m) between the reprojected file and the base map was noticed. Homogeneous vector files (eg. overlapping shapefiles) were adjusted using the same CGP in order to keep the correct spatial relationships within them (eg. overlapping of faults on geological formations boundaries).

2. Geological formations surfaces interpolation - Input Data

To interpolate the geological surfaces used in the numerical models of the studied aquifers, three main sources were analyzed:

A. the geological map (Oil Exploration Directorate, Office of the Prime Minister, 1993);

B. the cross-sections performed at the conceptual model stage;

C. the borehole log data provided by EWA or found in literature.

To compute all these different sources, several different GIS procedures were applied (as explained in Section 2.1 and Section 2.2) aiming to obtain spatially distributed points containing the absolute elevation of the geological formation boundaries.

2.1 Geological map formation boundaries (from geological map and cross-sections)

The boundaries of each geological formation were extracted from the spatially adjusted geological map as lines corresponding to the polygon boundaries. Aiming to get only boundaries representing a depositional geological contact, the line features overlapping faults or sea shores were excluded from the following steps (Figure 4).

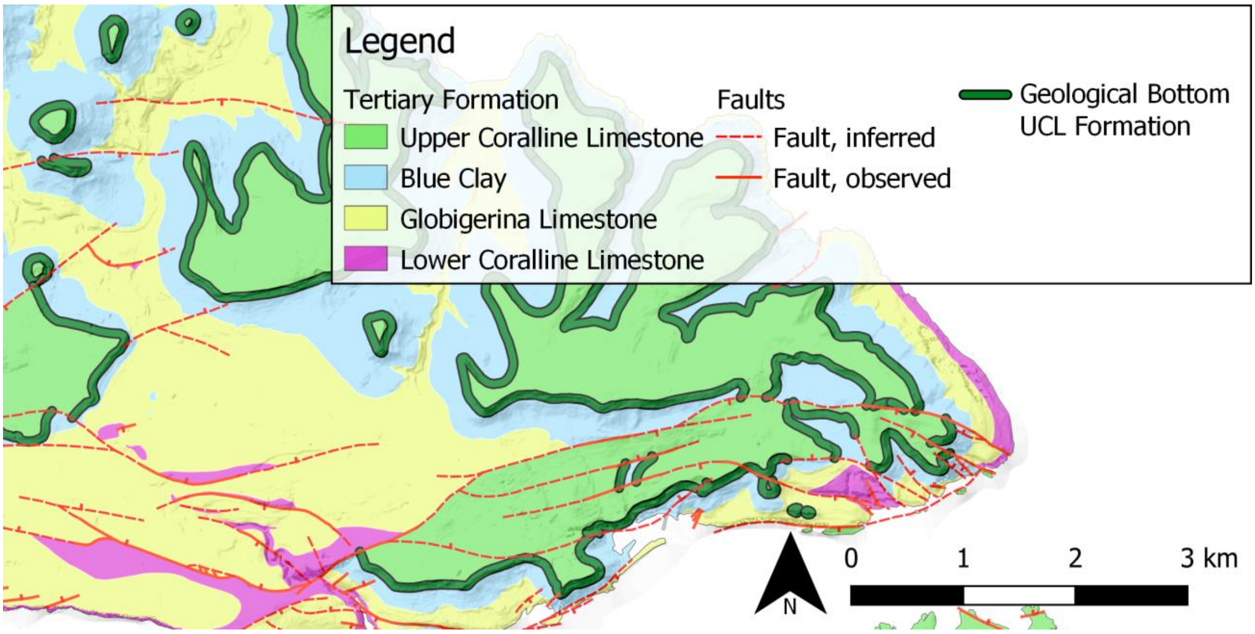

Figure 4. Example of geological boundaries used to interpolate the bottom boundary of the UCL formation (south east Gozo).

The resulting vertices were densified until reach a maximum distance from two connected vertices of the same line equal to 10 m (using the QGIS tool called "Densify by interval").

Once the vertices were densified, to each one was assigned an absolute elevation value obtained by the bathymetry DEM integrated raster (using the QGIS tool called "Drape").

Finally, all the vertices were extracted as point feature (Figure 5), containing as main attributes and geometric properties all the 3D spatial information (North, East and absolute elevation).

Figure 5. Example of 3D points extracted from geological boundaries used to interpolate the bottom boundary of the UCL formation (south east Gozo).

2.2 Cross-Sections formation boundaries

The 3D lines representing the beds of each geological member, digitalized from the cross-section performed (based on the geological map, see D1.3), were grouped by geological formation and imported on a GIS software (Figure 6).

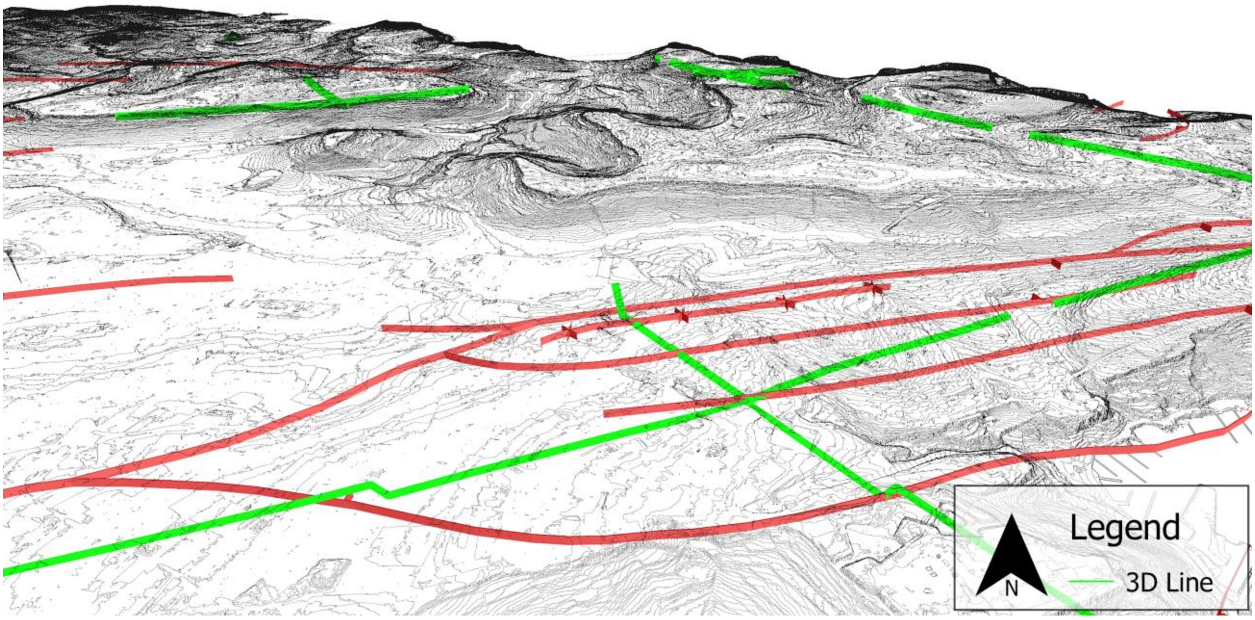

Figure 6. Example of 3D lines extracted for the UCL formation (south east Gozo).

When overlapping lines of the same geological formation were present, representing overlapping members of the same formation, the higher lines were deleted in order to keep the deepest line representing the formation bottom.

Finally, as for the geological boundaries, all the vertices were extracted as point feature, containing as main attributes and geometric properties all the 3D spatial information (North, East and absolute elevation).

2.3 Well log and borehole data

As final step, the information obtained by the geological map were integrated by well and borehole data provided by EWA or found in literature (Costain LTD 1958a and 1958b, Sapiano M. 2015b, BRMG 1991). A map and a list of the well and borehole data used are reported in the deliverable "D1.3 - Report on data assessment, gap-analysis and conceptual models" (Figure 2.2.1gg and Table 2.2.1a, respectively).

2.4 Inconsistencies in the input data

Several inconsistencies were detected during the control of the source data used for the interpolation. These inconsistencies were found both within a single data source and between different data sources (e.g. geological data and borehole data).

2.4.1 Geological data

By observing the absolute elevation of the points obtained for each geological formation, some discrepancies were detected.

These discrepancies are probably due to the following reasons:

A. the scale of the geological maps (1:25,000)

B. the not correct overlapping of the original DEM and the geological map vectors

C. the changes in morphology since the drawing of the geological map and the DEM productions

In order to obtain functional and corrects geological surfaces, the inconsistencies were removed by changing the geological boundaries.

2.4.2 Borehole data

Among the different sources and tables from where the data were gathered, some inconsistencies were detected. The inconsistencies are present between different sources and, sometimes, also within different parts of the same source. The main inconsistencies regarding the elevation (relative or absolute) of some geological boundaries (Table 2, Table 3 and Table 4), secondary inconsistencies are related to the difference in ground elevation between the tabled values and the DEM values (Table 5) and some inconsistencies are related to the points coordinates (Table 6).

Well Id	GL/LCL contact depth from surface		Difference [m]
	Appendix 2 [m]	Appendix 10 [m]	
10262	106.17	90.5	-15.67
10354	4.43	7.0	2.57
10362	31.00	33.5	2.50

10370	19.00	38.5	19.50
10377	38.00	42.3	4.30

Table 2. Inconsistencies within the BRMG report; the values express the depth from the surface of the boundary between the GL and the LCL formations. Only differences higher than 2 m are reported. Values for appendix 2 are calculated using the well depths reported in appendix 10 and the thickness of LCL reported in appendix 2, values for appendix 10 are directly reported from the document.

Well Id	GL/LCL contact depth from surface		Difference [m]
	MARSOL Deliverable 10.1 [m]	BRGM Appendix 10 [m]	
10370	19.0	38.5	19.5
10415	47.5	49.0	1.5

Table 3. Inconsistencies between the BRMG (Appendix 10) and the MARSOL (Deliverable 10.1-Table 2) reports; the values express the depth from the surface of the boundary between the GL and the LCL formations.

To solve the inconsistencies reported in Table 2 and Table 3 the values from the Appendix 10 of the BRGM report, were considered more consistent and preferred over the values form the Appendix 2 of the BRGM report and the values from the Deliverable 10.1 of the MARSOL report.

Well Id	GL/LCL contact		Difference [m]	Source selected for Interpolation
	EWA [m amsl]	BRGM [m amsl]		
10082	88.81	58.70	30.11	EWA
10083	94.57	105.10	-10.53	EWA
10084	15.76	5.10	10.66	EWA
10250	43.76	64.00	-20.24	BRMG
10262	-7.31	8.30	-15.61	BRMG
10271	-10.92	65.00	-75.92	BRMG
10278	23.43	60.00	-36.57	BRMG
10282	-61.17	67.00	-128.17	BRMG
10286	36.97	60.00	-23.03	EWA
10300	5.22	21.60	-16.38	BRMG
10318	32.94	-1.40	34.34	Average

10370	40.31	20.80	19.51	EWA
10405	87.45	77.00	10.45	BRGM
10410	7.09	42.10	-35.01	BRGM
10412	10.37	30.00	-19.63	EWA
10414	-35.00	35.00	-33.11	EWA
10419	-8.04	30.00	-38.04	BRGM

Table 4. Inconsistencies between the BRMG report and the data provided by EWA (Borehole Depths and Benchmarks.xlsx); the values express the elevation (m amsl) of the boundary between the GL and the LCL formations. Only differences higher than 10 m are reported.

In the case of the values reported in Table 4, the value to be used for the interpolation of the surface was chosen according to the data coming from the cross section and the geological map.

Well Id	Ground elevation [m amsl]		Difference [m]
	Literature data (BRMG, MARSOL, EWA)	DEM	
10031	54.25	49.77	4.48
10056	81.69	84.35	-2.66
10077	102.61	105.92	-3.31
10083	199.14	196.70	2.44
10084	59.05	56.61	2.44
10087	92.84	75.94	16.90
10092	123.84	126.15	-2.31
10093	75.98	71.44	4.54
10117	149.12	152.94	-3.82
10226	54.50	57.09	-2.59
10248	65.28	68.05	-2.77
10257	155.14	158.98	-3.84
10269	81.03	85.65	-4.62
10271	194.87	192.85	2.02
10281	55.45	57.78	-2.33

10287	145.12	147.16	-2.04
10295	91.00	93.05	-2.05
10312	43.18	41.02	2.16
10316	109.36	111.49	-2.13
10319	54.85	50.31	4.54
10327	83.80	86.96	-3.16
10332	13.76	17.87	-4.11
10343	38.80	36.22	2.58
10359	92.27	85.61	6.66
10363	112.00	118.96	-6.96
10365	99.01	92.13	6.88
10366	113.92	40.34	73.58
10370	59.31	55.28	4.03
10381	35.04	103.08	-68.04

Table 5. Inconsistencies between the literature elevation data (BRMG, MARSOL, EWA) and the used DEM; the values express the ground elevation (m amsl). Only differences higher than 2 m are reported.

Well Id	**Coordinates (Maltese National System) [m]**		**Source selected**
	EWA (Coordinates BH_PS.xlsx)	**EWA (Borehole Depths and Benchmark.xlsx)**	
10350	43956; 65940	53956; 65940	“Borehole Depths and Benchmark.xlsx”, since the coordinates from the other file place the well outside the island boundaries

Table 6. Inconsistencies within the boreholes coordinates provided by EWA.

3. Geological formations surfaces interpolation - Computing

Once all the available information was collected and homogenized as 3D points, several interpolators were assessed in order to choose the most effective.

3.1 Tested interpolator

The discarded interpolators (tested but not used) are reported in Table 7, together with some comments about their performances.

Method	Software/Code	Pros	Cons
IDW	QGIS 3.8	Simple and fast	High influence of the interpolation artifact on the result
Ord. Kriging	R, Gstat	Good semivariogram	Faults are not considered
Ord. Kriging with Faults	Isatis v11	Good semivariogram	Results are too far from the real data, inversion error is too high
TIN	QGIS 3.8	High faults definition	Rough changes when few data are present
TIN Plate - Spline	SAGA 2.1	Decent definition of faults, and smooth surfaces	Results are too far from the real data
Topo To Raster	ESRI ArcGIS 10.5	Good for surfaces	Faults smoothed too much
Diffusion Interpolation with Barriers	ESRI ArcGIS 10.5	Good results for local areas and good faults definitions	Too sensitive to the kernel “bandwith” parameter. Bandwith < 2km gives results very close to original data but limits the interpolated area (several empty areas are produced). Bandwith > 2 km extends the interpolation to the whole area but the smooths the faults and give less accurate results

Table 7. Interpolators tested.

The interpolator with the best case-specific performance, and therefore the choose one is reported in Table 8.

Method	Software/Code	Pros	Cons
Spline with Barriers	ESRI ArcGIS 10.5	High faults definition, close to the real data, local trends are used	A Trials-and-Error procedure is required, in order to add “dummy points” and keep the interpolation under control

Table 8 - Interpolator used.

3.2 Interpolation inputs

The “spline with barriers” interpolator requires, together with the points to interpolate, some linear vectors to be used as barriers with which compartilize the areas of interpolation.

Some of the main faults reported on the geological maps were, therefore, selected, extended and used as barriers (Figure 7).

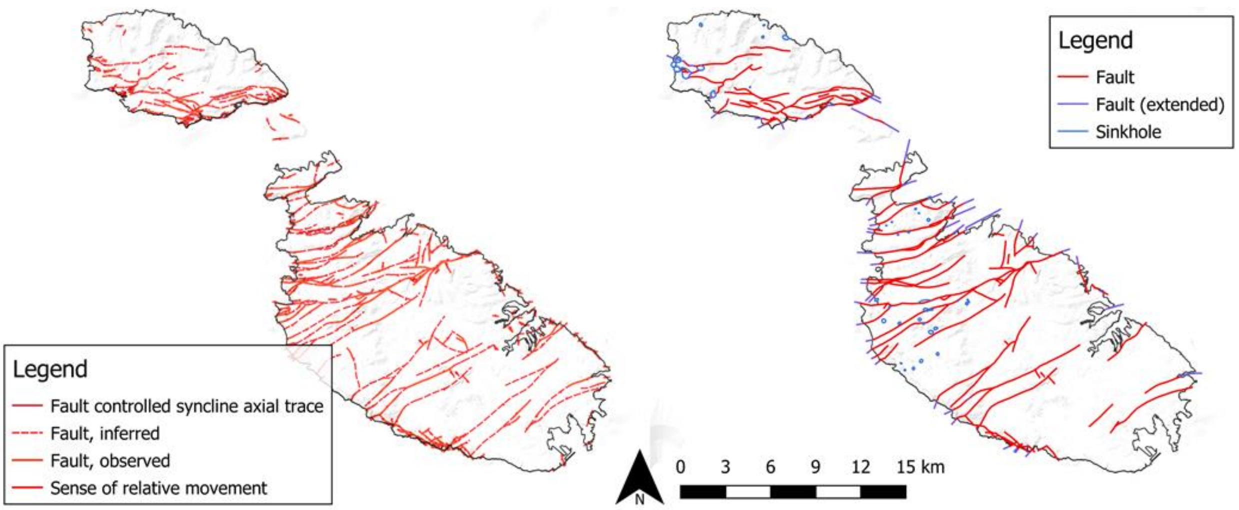

Figure 7. Interpolation area and faults mapped (left picture) and utilized as barrier faults (right picture).

Furthermore, also the boundary of the main sinkholes were included as barrier (Figure 8).

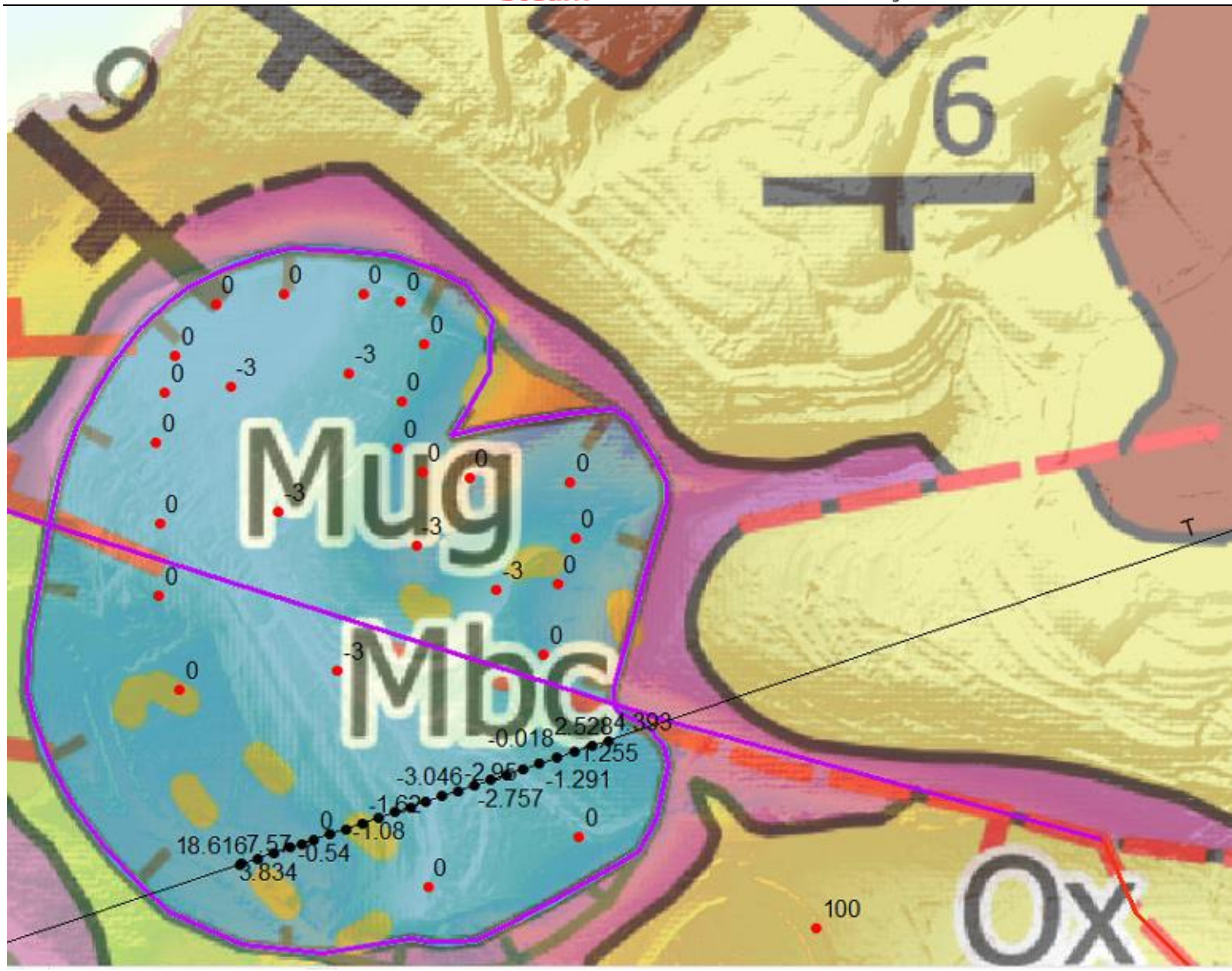

Figure 8. Example of sinkhole mapped boundary in north-western seaside of Gozo island, utilized as interpolation "barrier", together with cross sections (black dots) and dummies points (red dots) constraining the interpolation of sinkhole bottom.

As last important inputs, the cell size of the interpolation was set at 10*10 m and the cells were forced to be aligned with the DEM.

Following the initial interpolation, an iterative procedure took place (Figure 9) until the computation of a definitive surface: the interpolated surface was clipped according different masks representing the geological outcropping, the thickness of the geological formation represented by the interpolated surface was investigated (top minus bottom), eventual negative thicknesses were addressed by the use of dummy points to force the interpolation (according to the geological map).

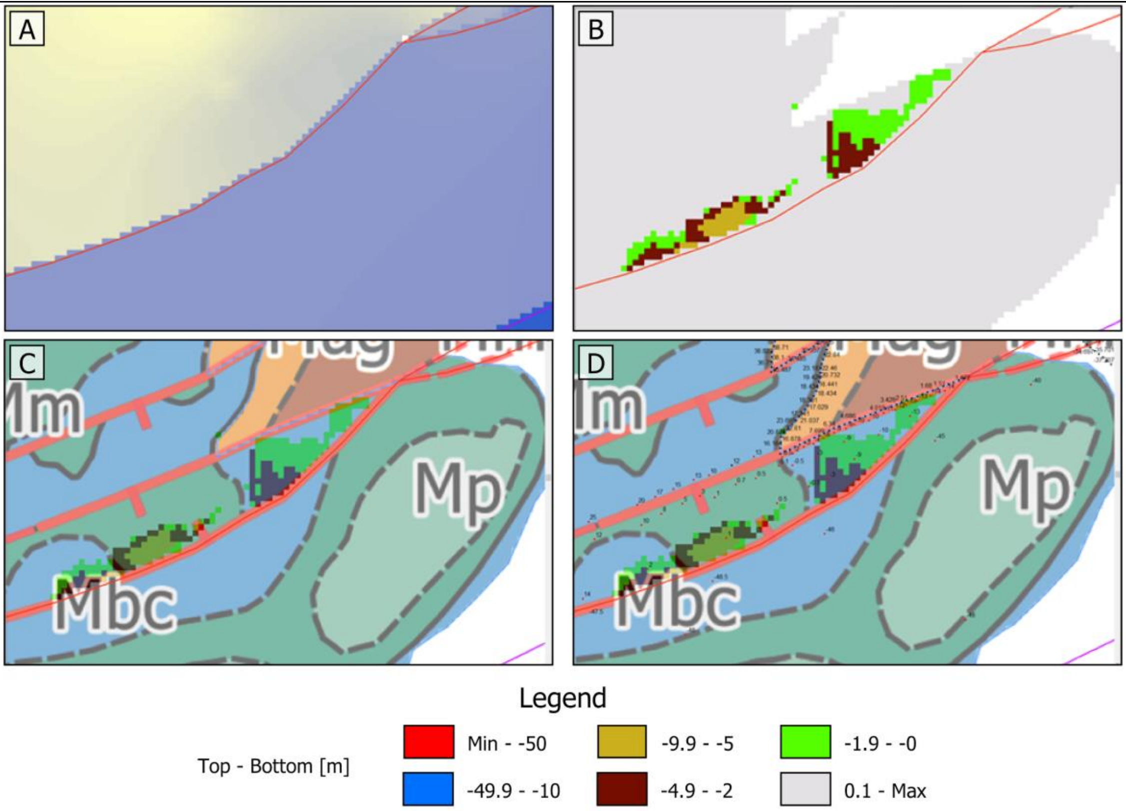

Figure 9. Surface control: A) interpolation; B) thickness calculation; C) geology check; D) extra dummy points added (red dots).

4. From the geological surfaces to the model one

The definitive geological surfaces were then clipped on the base of the geological map (Figure 10) in order to obtain several different parts.

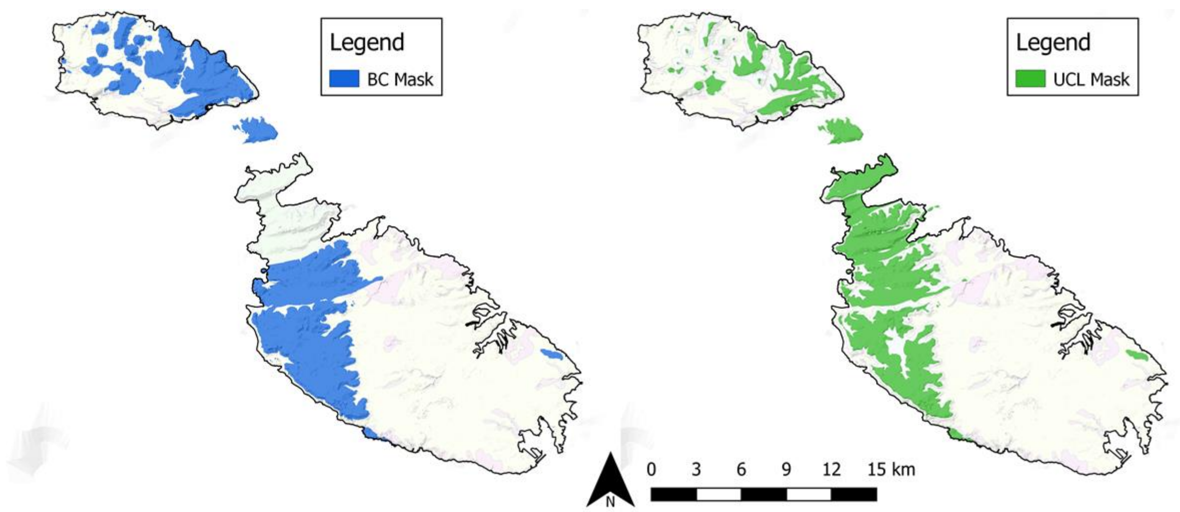

Figure 10. Masks used to clip the interpolated geological surfaces (for the Blue Clay and the Upper Coralline).

These parts were finally merged together to represent the model layer surfaces.

5. New data collection - future implementation

Successively to the model surface reconstruction, some new data were acquired during the 1st Interim Meeting with EWA (May 2019). These data included raster data of both Maltese and Gozo areas and borehole logs from Royal Engineers containing information on the geological and hydrological structure of some of the boreholes marked on the raster data (maps). All the maps were then georeferenced on the project referencing system of WGS84\33N and the data there contained (eg. boreholes, gallery and dams) were digitized creating vector layers of both points and lines (Figure 11).

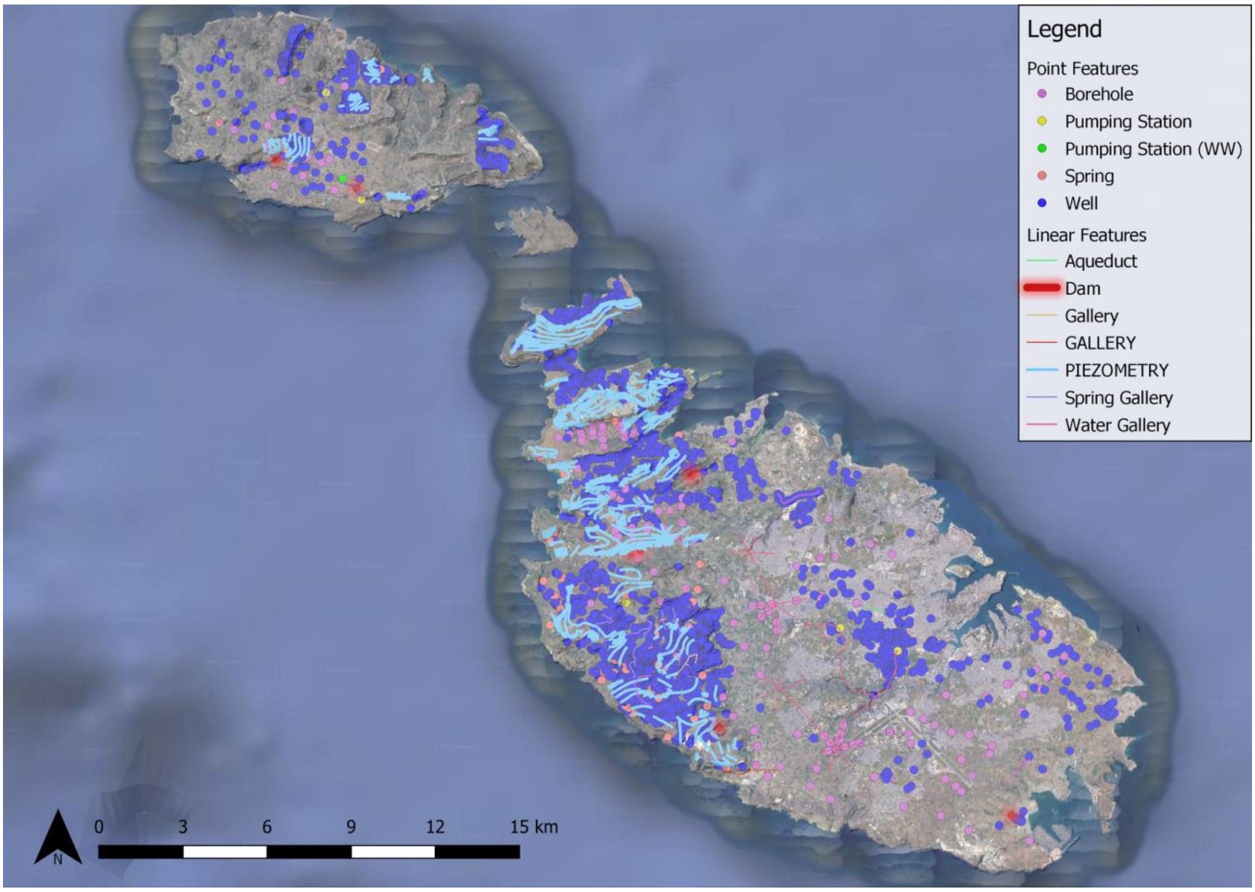

Figure 11 - Google satellite map of Maltese Island showing digitized points from the georeferenced map.

The borehole logs provided by Royal Engineers contain both hydrological and geological information on some of the boreholes on the map. When possible, this information was spatialized by means of the coordinated recorded on the logs or by joining the logs with the borehole points digitalize from the maps (using the borehole id as key value).

In total more than 70 and 100 points containing new hydrological (eg. head) and geological data, respectively, were found (Figure 12).

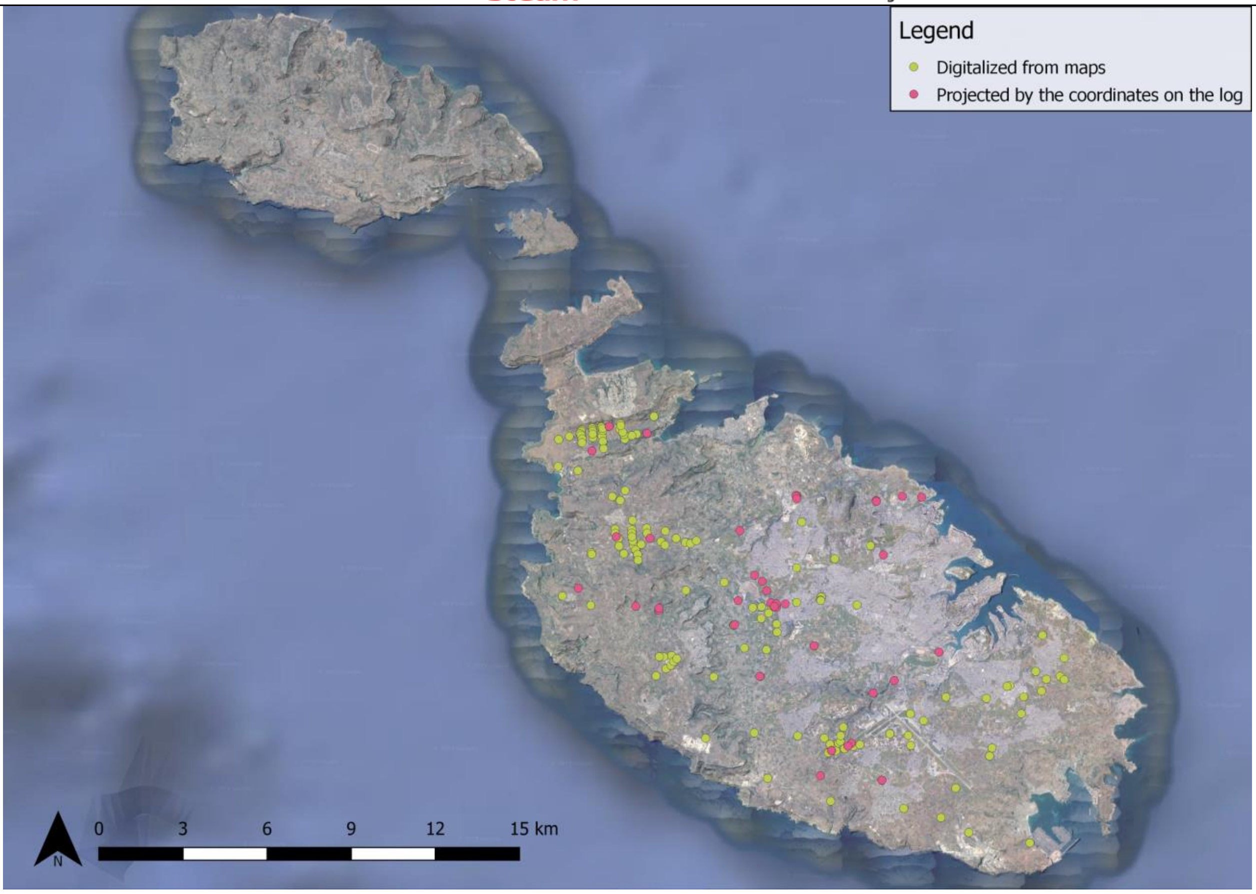

Figure 12 - Google satellite map of Maltese Island showing digitized points from the georeferenced map.

Unfortunately, no useful boreholes are present on Gozo.

This newly collected information is currently under review and they will be used to strengthen the solidity of the model surfaces in the next stage (transient modeling).